



HAL
open science

Vegetation and climate of north anatolian and north aegean region since 7 Ma according to pollen analysis

Demet Biltekin

► **To cite this version:**

Demet Biltekin. Vegetation and climate of north anatolian and north aegean region since 7 Ma according to pollen analysis. Earth Sciences. Université Claude Bernard - Lyon I; Istanbul teknik üniversitesi, 2010. English. NNT : 2010LYO10298 . tel-00720892

HAL Id: tel-00720892

<https://theses.hal.science/tel-00720892>

Submitted on 26 Jul 2012

HAL is a multi-disciplinary open access archive for the deposit and dissemination of scientific research documents, whether they are published or not. The documents may come from teaching and research institutions in France or abroad, or from public or private research centers.

L'archive ouverte pluridisciplinaire **HAL**, est destinée au dépôt et à la diffusion de documents scientifiques de niveau recherche, publiés ou non, émanant des établissements d'enseignement et de recherche français ou étrangers, des laboratoires publics ou privés.

THESE

en cotutelle

présentée

devant l'**UNIVERSITE CLAUDE BERNARD – LYON 1**

et l'**UNIVERSITE TECHNIQUE D'ISTANBUL**

pour l'obtention

du **DIPLOME DE DOCTORAT**

(arrêté du 7 Août 2006)

présentée et soutenue publiquement à Istanbul le 21 Décembre 2010

par

Demet BİLTEKİN

**Vegetation and climate of North Anatolian and North Aegean region
since 7 Ma according to pollen analysis**

Directeurs de thèse: Jean-Pierre SUC

Namık ÇAĞATAY

Jury :

Namık ÇAĞATAY, Professeur, Université Technique d'Istanbul, Directeur de thèse
Speranta-Maria POPESCU, Chercheur, Institut de Physique du Globe de Paris, Examineur
Mehmet SAKINÇ, Professeur, Université Technique d'Istanbul, Examineur
Jean-Pierre SUC, Directeur de Recherche émérite du CNRS, Directeur de thèse
Frédéric THEVENARD, Professeur, Université C. Bernard-Lyon1, Examineur
Namık YALÇIN, Professeur, Université d'Istanbul, Rapporteur

Rapporteurs absents :

Dimitar IVANOV, Chercheur, Académie des Sciences de Bulgarie, Rapporteur
Paul ROIRON, Maître de Conférence, Université Montpellier II, Rapporteur

ABSTRACT

Anatolia is an area inhabited today by relict thermophilous plants: *Liquidambar orientalis*, *Parrotia persica*, *Pterocarya fraxinifolia*, *Zelkova crenata* (Angiosperms) and *Cedrus* (Gymnosperm). These trees constitute forests relatively close to *Artemisia* steppes, being the two types of vegetation in competition during the climatic cycles along the last 2.6 million years. Thus, this makes the greatest interest for palynological investigations in the region. This study concerns a long marine section (DSDP Site 380 from the southwestern deep Black Sea: Late Miocene to Present) and onshore exposed sections (marine and lacustrine sediments) from the Late Miocene and/or Early Pliocene. The study area corresponds to the surroundings of the Marmara Sea (Enez, İntepe, Eceabat, Burhanlı, West Seddülbahir), southwestern Black Sea (DSDP Site 380), and northern Greece (Ptolemais Notio, Ptolemais Base, Prosilio, Trilophos and Lion of Amphipoli). The main target of this study is to reconstruct vegetation and climate during this time-interval in the region. The high-resolution pollen analysis of the 1,073.50 m long Black Sea Site 380 (to which I directly contributed for the interval 702.40 – 319.03 m) documents in great detail the evolution of vegetation and climate from the Late Miocene up to Present. Two vegetation types were alternately dominant for the last 7 million years: thermophilous forests and open vegetations including *Artemisia* steppes. At the early Messinian (before the Messinian Salinity Crisis), herbs prevailed in the Dardanelles area while mid- (*Tsuga*) and high-altitude (*Abies* and *Picea*) conifers were abundant with Cupressaceae close to the Olympe Mount (Prosilio). After the Messinian Salinity Crisis, North Aegean vegetation was mainly characterized by open plant ecosystems nearby forest assemblages with mesothermic trees (deciduous *Quercus*, *Carya*, *Zelkova*, etc.). In addition, strengthening of altitudinal conifers (*Cedrus*, *Tsuga*, *Abies* and *Picea*) may signify some uplift of the regional massifs. During the Late Miocene, most of the megathermic (tropical) and mega-mesothermic (subtropical) plants declined because of the climatic deterioration. However, some of them survived during the Late Pliocene, such as those which constituted coastal swamp forests (*Glyptostrobus*, *Engelhardia*, Sapotaceae, *Nyssa*) or composed deciduous mixed forests with mesothermic trees. Simultaneously, herbaceous assemblages (with Amaranthaceae-Chenopodiaceae, Poaceae, Asteraceae Asteroideae, Asteraceae Cichorioideae, etc.) became a prevalent vegetation component despite steppe elements (*Artemisia*, *Ephedra*, *Hippophae rhamnoides*) did not significantly develop. This suggests cooler and chiefly drier conditions during the Late Pliocene. At the Early Pleistocene (2.6 Ma), as a response to the onset of Arctic glaciations, megamesothermic elements rarefied despite some taxa persisted (Taxodiaceae: probably *Glyptostrobus*, *Engelhardia*, Sapotaceae, and *Nyssa*). In parallel, deciduous mixed forest assemblages composed of mesothermic trees (deciduous *Quercus*, *Betula*, *Alnus*, *Liquidambar*, *Fagus*, *Carpinus orientalis*, *Carpinus betulus*, *Tilia*, *Acer*, *Ulmus*, *Zelkova*, *Carya*, *Pterocarya*, etc.) almost disappeared too while steppe environments strongly enlarged. Then, *Artemisia* steppic phases developed during longer temporal intervals than mesophilous tree phases all along the glacial-interglacial cycles (first with a period of 41 kyrs, then 100 kyrs). This suggests shorter interglacials (warm and humid climate) than glacials (cool to cold and dry climate). From the beginning of the Ioanian Stage (1.8 Ma), herbaceous ecosystems (with Amaranthaceae-Chenopodiaceae, Poaceae, Asteraceae Asteroideae, Asteraceae Cichorioideae, etc.) and *Artemisia* steppes still continuously enlarged up today. Such an expansion of *Artemisia* steppes in the Ponto-Euxinian region was observed at the earliest Pliocene (DSDP Site 380) but their earliest settlement in Anatolia seems to have occurred in the Early Miocene (Aquitanian). The development of the *Artemisia* steppes in Anatolia might result from the uplift of the Tibetan Plateau. At last, relictuous plants such as *Carya*, *Carpinus orientalis*, *Pterocarya*, *Liquidambar orientalis*, *Zelkova* persisted up today for most of them. This story can be explained by some influence of the Asian monsoon which reinforced as a result from the uplifted Tibetan Plateau.

RESUME

L'Anatolie est un secteur aujourd'hui habité par des plantes thermophiles en situation de refuges. Sont concernées des Angiospermes (*Liquidambar orientalis*, *Parrotia persica*, *Pterocarya fraxinifolia*, *Zelkova crenata*) et une Gymnosperme (*Cedrus*), arbres de forêts contrastant avec la steppe à *Artemisia*, les deux types de végétation en forte compétition pendant les cycles climatiques des 2,6 derniers millions d'années. Ainsi, ceci confère-t-il le plus grand intérêt aux investigations palynologiques dans la région. Cette étude concerne un long enregistrement sédimentaire marin (Site profond DSDP 380 en Mer Noire sudoccidentale) et des affleurements à terre de dépôts marins ou lacustres du Miocène supérieur et(ou) du Pliocène inférieur. Le secteur étudié à terre porte sur les environs de la Mer de Marmara (Enez, Eceabat, Seddülbahir) et la Grèce septentrionale (Ptolemais Notio et Ptolemais Base, Prosilio, Trilophos et Lion d'Amphipoli). L'objectif principal de cette recherche est de reconstruire la végétation et le climat régionaux pendant ces intervalles de temps. L'enregistrement pollinique à haute résolution des 1.073,50 m du Site 380 (auquel j'ai contribué de façon significative à travers l'intervalle 702,4 – 319 m) documente en détail l'évolution de la végétation et du climat de la fin du Miocène à l'Actuel. Deux types de végétation y furent alternativement dominants au cours des 7 derniers millions d'années : les forêts de plantes thermophiles et les steppes à *Artemisia*. Au début du Messinien (avant la Crise de salinité messinienne), les herbes étaient dominantes dans la région des Dardanelles tandis que les conifères de moyenne (*Tsuga*) et haute altitude (*Abies* et *Picea*) abondaient avec les Cupressaceae près du Mont Olympe (Prosilio). Dans cette même région nord-égéenne, la végétation était après la Crise de salinité messinienne caractérisée principalement par des formations ouvertes à côté de groupements forestiers à arbres mésothermes (*Quercus* décidus, *Carya*, *Zelkova*, etc.). Par ailleurs, l'expansion des conifères altitudinaux (*Cedrus*, *Tsuga*, *Abies* et *Picea*) y est documentée et semble traduire un soulèvement des massifs environnants. A la fin du Miocène, la plupart des éléments mégathermes (tropicaux) et méga-mésothermies (subtropicaux) avaient régressé en raison des détériorations climatiques. Cependant, certains d'entre eux ont survécu pendant le Pliocène supérieur, notamment ceux qui constituaient des forêts littorales marécageuses (*Glyptostrobus*, *Engelhardia*, Sapotaceae, *Nyssa*) ou participaient à des forêts mixtes avec des arbres décidus mésothermes. Pendant ce temps, les formations ouvertes à herbes (Amaranthaceae-Chenopodiaceae, Poaceae, Asteraceae Asteroideae, Asteraceae Cichorioideae, etc.) sont devenues prédominantes dans la végétation sans que les éléments steppiques (*Artemisia*, *Ephedra*, *Hippophae rhamnoides*) soient très abondants. Ceci suggère un refroidissement au Pliocène supérieur et surtout l'installation de conditions plus sèches. Au début du Pléistocène (2,6 Ma), sous l'effet des premières glaciations arctiques, les éléments méga-mésothermes se sont très raréfiés malgré la persistance de quelques reliques (Taxodiaceae : probablement *Glyptostrobus*, *Engelhardia*, Sapotaceae, *Nyssa*). Simultanément, les forêts mixtes à éléments mésothermes (*Quercus* décidus, *Betula*, *Alnus*, *Liquidambar*, *Fagus*, *Carpinus orientalis*, *Carpinus betulus*, *Tilia*, *Acer*, *Ulmus*, *Zelkova*, *Carya*, *Pterocarya*, etc) ont aussi quasiment disparu tandis que les environnements steppiques se développaient fortement. Désormais, tout au long des cycles glaciaire-interglaciaire (d'abord de 41 ka de périodicité puis de 100 ka), les steppes à *Artemisia* occuperont plus d'espace temporel que les phases arborées. Ceci suggère des interglaciaires (chauds et humides) plus courts que les glaciaires (frais à froids et secs). Depuis le début de l'étage Ionien (1,8 Ma), les environnements à herbes (Amaranthaceae-Chenopodiaceae, Poaceae, Asteraceae Asteroideae, Asteraceae Cichorioideae, etc.) et les steppes à *Artemisia* n'ont cessé de s'étendre jusqu'à aujourd'hui. Cette expansion des steppes à *Artemisia* dans la région du Pont-Euxin a été observée au tout début du Pliocène (Site DSDP 380) mais leur premier enregistrement en Anatolie date de l'Aquitaniien (Miocène inférieur). Le développement de la steppe à *Artemisia* en Anatolie pourrait résulter du soulèvement du Plateau tibétain. Enfin le maintien dans cette région de plantes thermophiles reliques en situation de refuges (*Carya*, *Carpinus orientalis*, *Pterocarya*, *Liquidambar orientalis*, *Zelkova*), dont certaines jusqu'à nos jours, peut être expliqué par l'influence grandissante de la mousson asiatique dont le renforcement aurait aussi résulté du soulèvement du Plateau tibétain.

ACKNOWLEDGEMENTS

This PhD thesis study is the French-Turkish (Co-tutelle de thèse) enabled me chance for studying between the University of Claude Bernard-Lyon1 and the Istanbul Technical University. I would like to thank all people helped me during my PhD thesis study.

Firstly, I would like to thank my thesis directors: Prof. Dr. Jean-Pierre SUC (University of Claude Bernard-Lyon 1) and Prof. Dr. Namık ÇAĞATAY (Istanbul Technical University). They were of great help. Warm thanks to Prof. Dr. Jean-Pierre SUC who supported me in Palynology, thanks to him for his great experience on pollen grain taxonomy, on identifying pollen grains and for his endless patience during my thesis. He encouraged and helped me everytime during my stay in the University of Claude Bernard-Lyon 1. I also would like to thank to him for his efforts, advices and guidance during my thesis study. Warm thanks to Prof. Dr. Namık ÇAĞATAY who gave me opportunity to study Palynology and He introduced me to Prof. Dr. Jean-Pierre SUC. He always encouraged and helped me during my PhD thesis. I also would like to thank for his precious advices, his enthusiasm and his support during my thesis.

Many thanks to the members of my Comittee of Pilotage in the University of Claude Bernard-Lyon1: Speranta-Maria POPESCU, Marc PHILIPPE, Serge LEGENDRE and Gilles ESCARGUEL for their advices and collaboration.

Many thanks to member of my thesis Comittee in Istanbul Technical University: Prof. Dr. Naci GÖRÜR, Prof. Dr. Mehmet SAKINÇ, Prof. Dr. Ercan ÖZCAN and Prof. Dr. Namık YALÇIN of Istanbul University for their advices and contribution.

I would like to thank Dr. Speranta-Maria POPESCU for her helping and advising during my thesis and staying in the University of Claude Bernard-Lyon1.

I am very grateful towards the members of the Examination Board of my thesis who accepted to report on my manuscript (Prof. Dimiter IVANOV from Sofia, Prof. Paul ROIRON from Montpellier and Prof. Namık YALÇIN from Istanbul) and/or to discuss it at my oral defense (Prof. Frédéric THEVENARD, Dr. Speranta-Maria POPESCU, Prof. Naci GÖRÜR, Prof. Ercan ÖZCAN, Prof. Mehmet SAKINÇ and Prof. Namık YALÇIN).

Thanks to the technical support in the Laboratory PEPS of the University C. Bernard – Lyon 1 and thanks to the French Embassy by the financial support obtained (thesis in cotutelle) in Lyon.

Thanks to TÜBİTAK and EMCOL (Eastern Mediterranean Oceanography Center) for financial support in İstanbul during my PhD thesis.

Many thanks to Lysiane THENEVOD, Mathieu DALİBARD, Anissa SAFRA, and Simona BOROI, I shared with them microcope work in the lobaratory and also thanks to Philippe SORREL, Eric FAVRE, Sébastien JOANNIN, Florent DALESME and Gwénael JOUANNIC for all their friendship.

Many thanks to EMCOL staff: Ümmühan SANCAR, Umut Barış ÜLGEN, Emre DAMCI, Sena AKÇER ÖN, Dursun ACAR, Zeynep ERDEM and Ayşe KAPLAN for all their friendship during my PhD thesis.

Finally, I thank my family, they supported me through my education life. Especially my mother, she always believed in me and encouraged me to begin my PhD studies and supported every step in my thesis study.

TABLE OF CONTENTS

1. INTRODUCTION	1
<u>1.1 Aims of the Study</u>	8
2. PHYSIOGRAPHY, STRATIGRAPHY AND PALEO GEOGRAPHY OF THE STUDY AREAS	9
<u>2.1 Turkey</u>	9
<u>2.1.1 Present-day vegetation</u>	9
<u>2.1.2 Climate</u>	13
<u>2.1.2.1 Turkey</u>	13
<u>2.1.2.2 Greece and Macedonia</u>	16
<u>2.1.3 Stratigraphy of the study areas</u>	19
<u>2.1.4 Paleogeography</u>	23
3. METHOD	31
<u>3.1 Sampling and Chemical Processing</u>	32
<u>3.2 Identification of Pollen Grains</u>	33
4. CHRONOLOGY OF THE STUDIED SECTIONS	41
5. RESULTS	45
<u>5.1 DSDP Site 380</u>	45
<u>5.1.1 Lithology</u>	45
<u>5.1.2 High-resolution pollen record of DSDP 380</u>	51
<u>5.2 Gulf of Saros</u>	58
<u>5.2.1 Enez</u>	58
<u>5.3 Dardanelles Strait</u>	61
<u>5.3.1 İntepe</u>	61
<u>5.3.2 West of Seddülbahir</u>	65
<u>5.3.3 Eceabat</u>	67
<u>5.3.4 Burhanlı</u>	68
<u>5.4 Western Macedonia</u>	69
<u>5.4.1 Ptolemais notio</u>	69
<u>5.4.2 Ptolemais base</u>	71
<u>5.5 Northern Greece</u>	75
<u>5.5.1 Trilophos</u>	75
<u>5.5.2 Prosilio</u>	76
<u>5.5.3 Lion of Amphipoli</u>	78
6. DISCUSSION	81
<u>6.1 Flora and Floristic Refuges</u>	81
<u>6.2 Vegetation</u>	89
<u>6.2.1 The development of <i>Artemisia</i> steppes</u>	95
<u>6.3 Climate</u>	99
<u>6.3.1 Global climate context during the Miocene and Pliocene</u>	99
<u>6.3.2 Climatic evolution of the studied areas</u>	102
7. CONCLUSIONS	107
REFERENCES	111

ABBREVIATIONS

MSC	: Messinian Salinity Crisis
NAF	: North Anatolian Fault
Ma	: Million years
cP	: Continental Polar Air Mass
mP	: Marine Polar Air Mass
cT	: Continental Tropical Air Mass
mT	: Marine Tropical Air Mass
PJF	: Polar Front Jet
STJ	: Subtropical Jet
ITCZ	: Intertropical Convergence Zone

1. INTRODUCTION

Present flora and vegetation of the North Aegean region and Anatolia show peculiar characteristics that find their origin in the past (Zohary, 1973; Quézel and Médail, 2003). In fact, this area counts today a lot of relictous plants (such as *Platanus orientalis*, *Liquidambar orientalis*, *Pterocarya fraxinifolia*, *Zelkova crenata*, *Cedrus libani*) inhabiting separated places within more or less thermophilous residual forests (Fig. 1a, 1b). In addition, vegetation shows high contrasts between forest (Pontus Euxinus forests, mid- to high-altitude forests) and open landscapes (mediterranean assemblages, pre-steppic to steppic ecosystems). This plant assemblage constitutes the alone current testimony of the flora and primary vegetation which inhabited the Northern Mediterranean region during the last millions years. The geographical situation of the studied area makes the greatest interest of this region for palynological studies. Pollen analyses developed on a botanical background are very rare in Turkey if it is almost inexistent. There are some studies on Miocene and Pliocene in Anatolia (Nakoman, 1967; Benda, 1971; Akgün and Akyol, 1999), but (1) their very poor botanical interest because of a very limited pollen morphological approach, and (2) the highly questionable quantitative information that they are supposed to provide make them almost completely unusable. This study is the first investigation to have been developed in the region on a fine pollen morphology investigation resulting in reliable botanical comprehensive information. Pollen identification was performed after their accurate morphology examination by comparing Neogene pollen grains with their living relatives using databanks of modern pollen grains and modern-past pollen grains photographs (atlases, databases) with respected to botanical nomenclature. At present, the history of the flora, vegetation and climate of the Mediterranean region are very well-documented for the last 23 Myrs after the thesis of Jean-Pierre Suc (1980) and the about twenty theses that he supervised (e.g.: Bessedik, 1985; Zheng, 1986; Combourieu-Nebout, 1987; Drivaliari, 1993; Fauquette, 1998; Bachiri Taoufiq, 2000; Popescu, 2001; Jiménez-Moreno, 2005; Joannin, 2007; Favre, 2007).

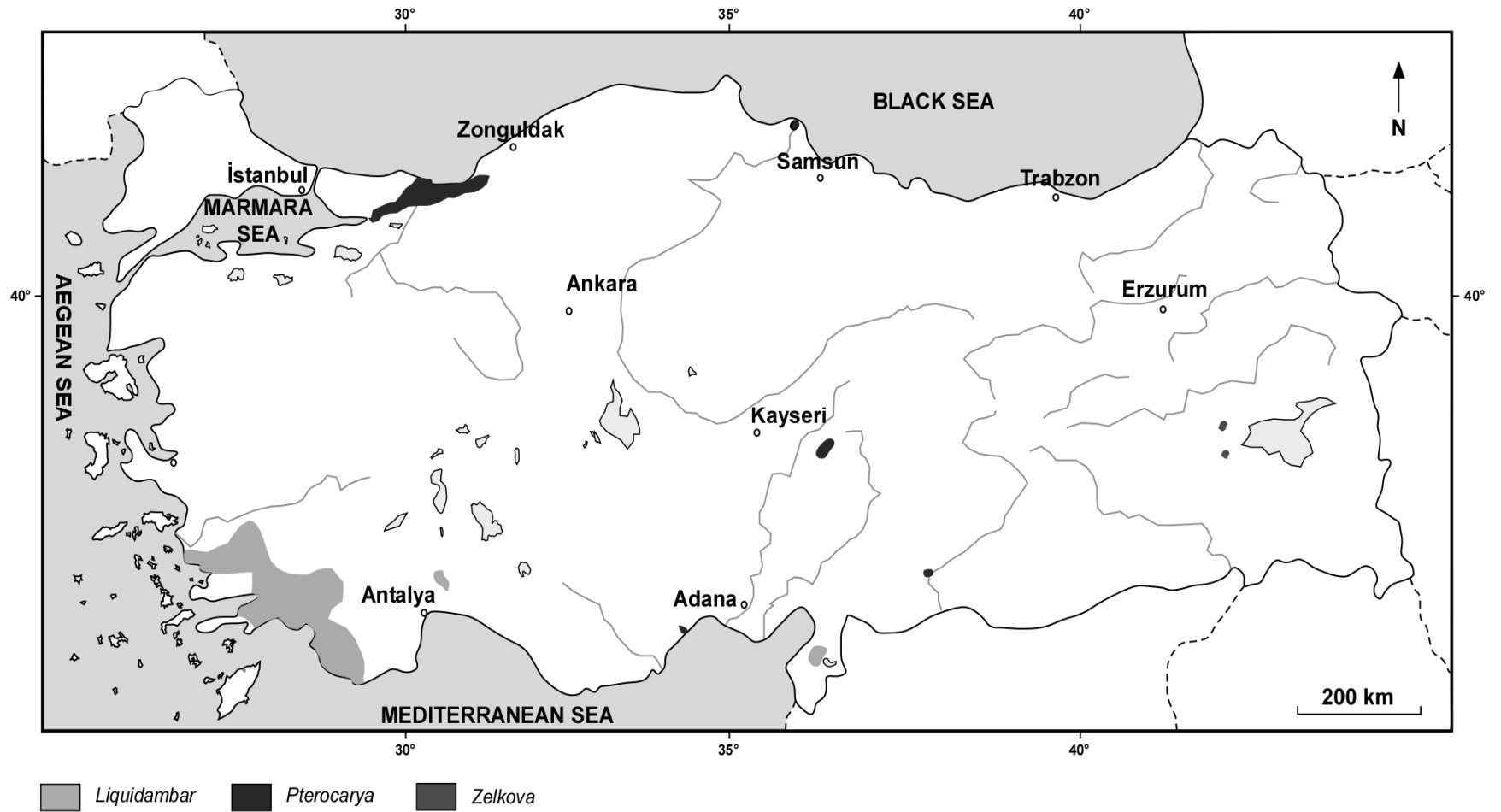


Figure 1A : Distribution of *Liquidambar*, *Pterocarya* and *Zelkova*.

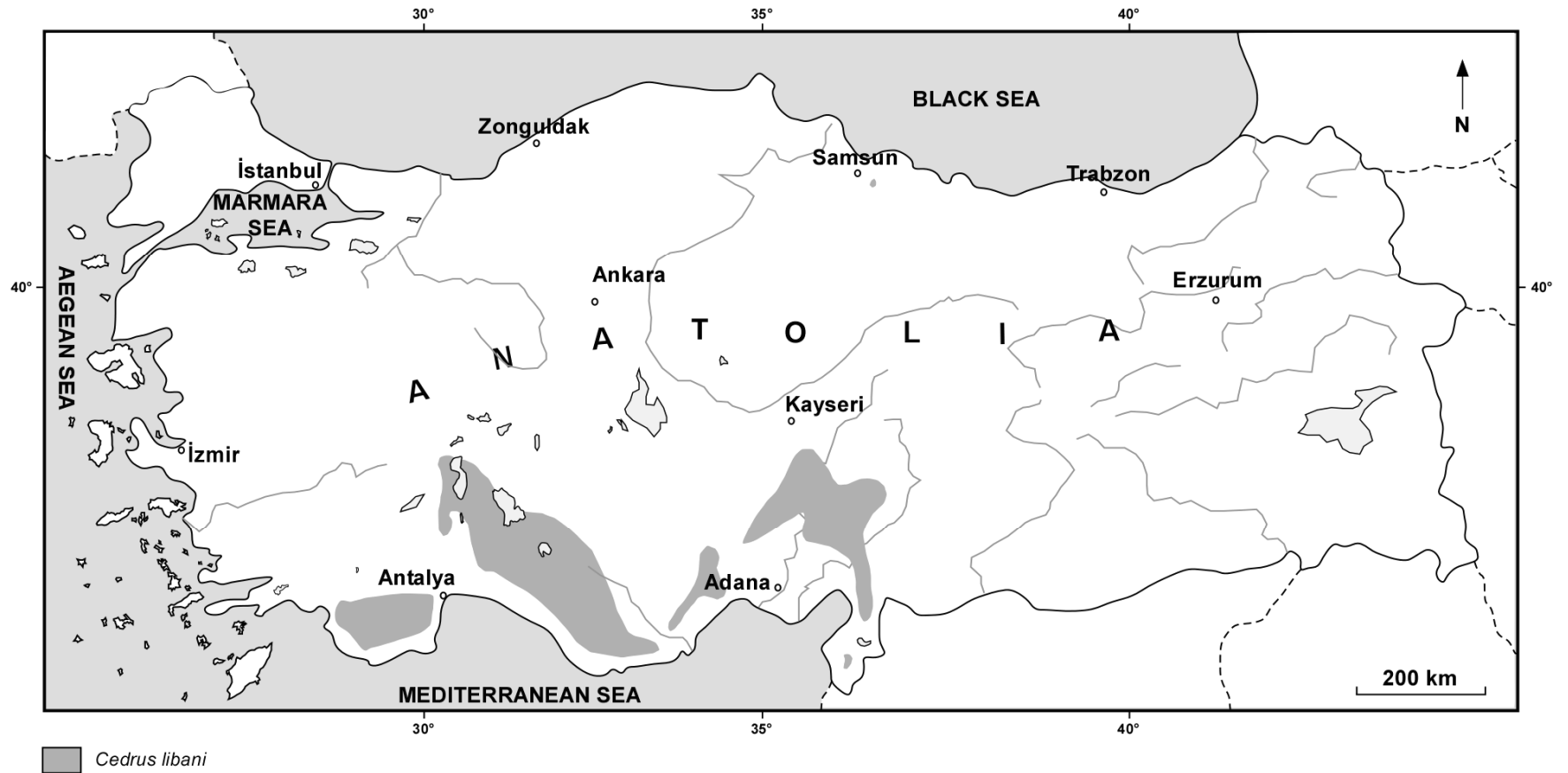


Figure 1B : Distribution of *Cedrus libani*.

Suc, J-P. (1980) studied different areas from the North-western Mediterranean region. He demonstrated that the modern Mediterranean vegetation took root in the Late Pliocene¹. Two important events occurred at 3.4 and 2.6 Ma. The former was the establishment of the modern Mediterranean vegetation and the latter the first evidence of the vegetation response in the Mediterranean region to the earliest glacial in the Northern Hemisphere. The previous vegetation was impacted by glacial-interglacial fluctuations and finally, by human activity.

Jiménez-Moreno, G. (2005) documented Early to Late Miocene vegetation and climate dynamics from the South-eastern Europe to the North-eastern Mediterranean. There was a progressive rarefaction of the most thermophilous trees and shortening of the broad-leaved evergreen forest. On the contrary, there were a development in mesothermic (mainly deciduous) elements, altitudinal trees and herbs during the Middle and Late Miocene. This can be related to enlargement of the East Antarctic Ice Sheet (EAIS) and regional uplift.

Popescu, S. (2001) carried out high resolution pollen analysis on the Lupoia section (SW Romania). Pollen records enabled the reconstruction of the early Pliocene vegetation of southwestern Romania. Repeated changes in vegetation occurred with clay-lignites alternation. While altitudinal trees corresponded a decrease in temperature, thermophilous trees developed under humid conditions.

Popescu *et al.*, (2006) studied pollen records of the western Dacic Basin. The Early Zanclean sediments of Dacic Basin was provided by pollen records and eccentricity curve. According to this, thermophilous plants increased during the lowest eccentricity minima (in 400 kyrs cycles). On the contrary, altitudinal elements are enriched during the highest eccentricity maxima.

Popescu, S. (2006) studied to investigate paleovegetation during the Late Miocene-Early Pliocene from high-resolution pollen analysis in DSDP Site 380. According to this study, the Late Miocene vegetation was characterized by delta environment. During Early Pliocene, two vegetation types were defined by thermophilous plants and dry steppes.

¹ Here, we follow the chronostratigraphic nomenclature recently adopted by IUGS (Gibbard *et al.*, 2009) where Pliocene is constituted by two stages, Zanclean (5.332 – 3.6 Ma) and Piacenzian (3.6 – 2.588 Ma), Gelasian becoming the first stage of Pleistocene (i.e. Quaternary).

In order to be sure to well appreciate the contrast between forest and steppe vegetation, the investigated region has been defined a little larger than the Anatolia region and includes also the surroundings of the Marmara Sea, a part of the southwestern Black Sea shorelines and of northern Greece (Fig. 1.2).

The region was subject to intense paleogeographic changes controlled by regional tectonics extremely active since 6 Ma and by the partly coexisting desiccation of the Mediterranean and Black seas (5.6-5.33 Ma) (Armijo *et al.*, 1999; Görür *et al.*, 1997, 2000; Gillet, 2004; Clauzon *et al.*, 2005; Melinte *et al.*, 2009). The North Anatolian Fault (NAF) extends from Karlıova to the Gulf of Saros along the Black Sea mountains of North Anatolia (Fig. 1.3). It seems to have originated during the Late-Middle Miocene when the Anatolian plate separated. The westward motion of the Anatolia plate with respect to Eurasia and African plates induced great geodynamic changes in the Eastern Mediterranean. This gave rise to the Aegean extensional regime and deformation of Anatolia (Şengör, 1979).

Today, relictous plants are distributed in the eastern Mediterranean region. Such an evolution was forced by the successive coolings in the Antarctic area first (at 14 Ma then 5.8 Ma), then especially the repeated Arctic coolings (since 3.6 Ma) that controlled the glacial-interglacial cycles since 2.6 Ma. Simultaneously, the environments in the South Mediterranean, already characterized by open vegetations since the earliest Miocene (probably because of the neighborhood of the pre-existing Sahara Desert), were enriched in *Artemisia* steppe element probably originating from the Anatolian Plateau (*Artemisia*) (Popescu, 2006) that repeatedly invaded the entire Mediterranean realm at each Arctic glaciation. Some testimonies of these relictous floras and thermophilous vegetations exist both to the West (mountains of South Morocco, Canary Islands) and to the East (Anatolia, southern Caucasus) (Quézel and Médail, 2003).

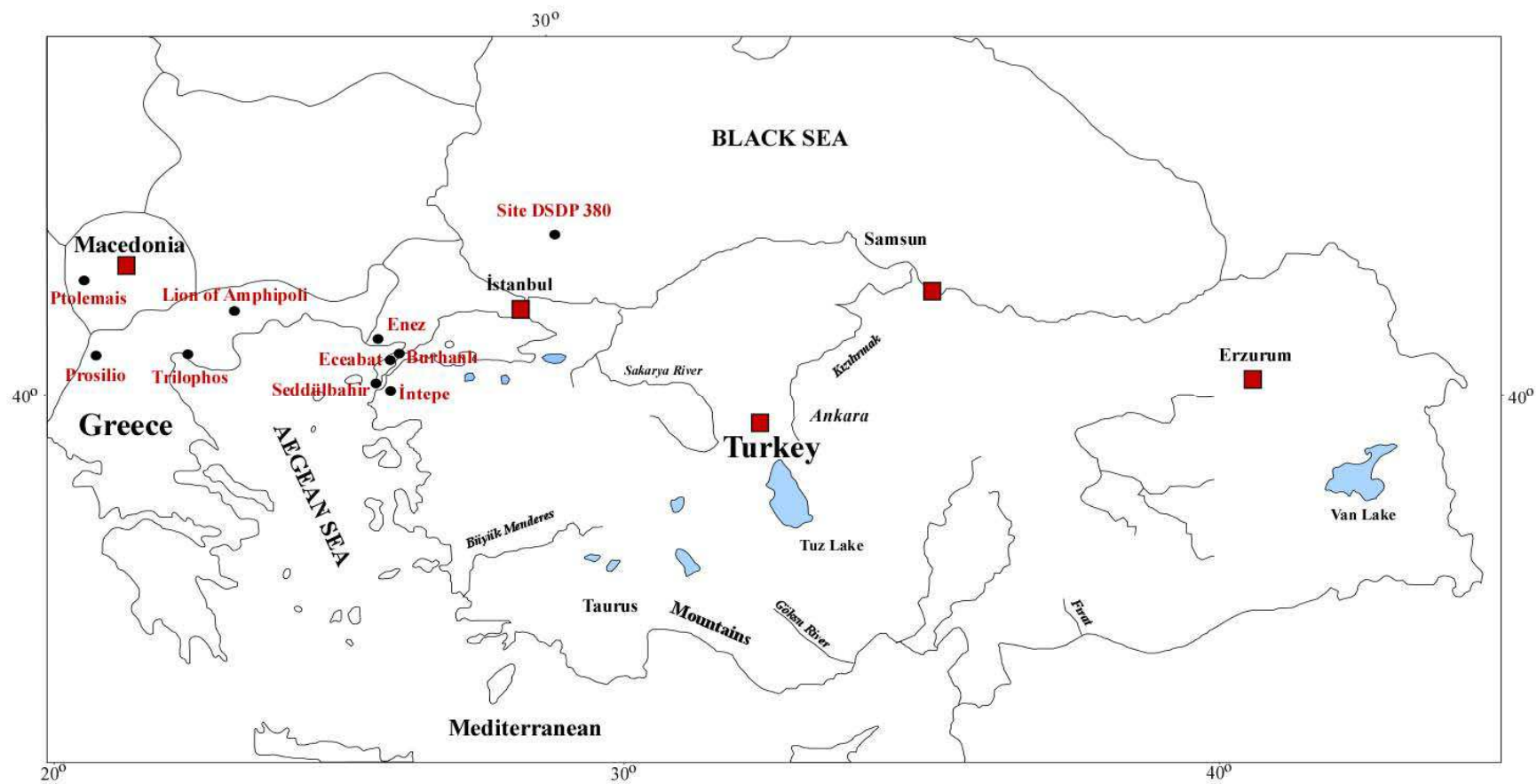


Figure 1.2 : Map showing the studied pollen localities (black dots).

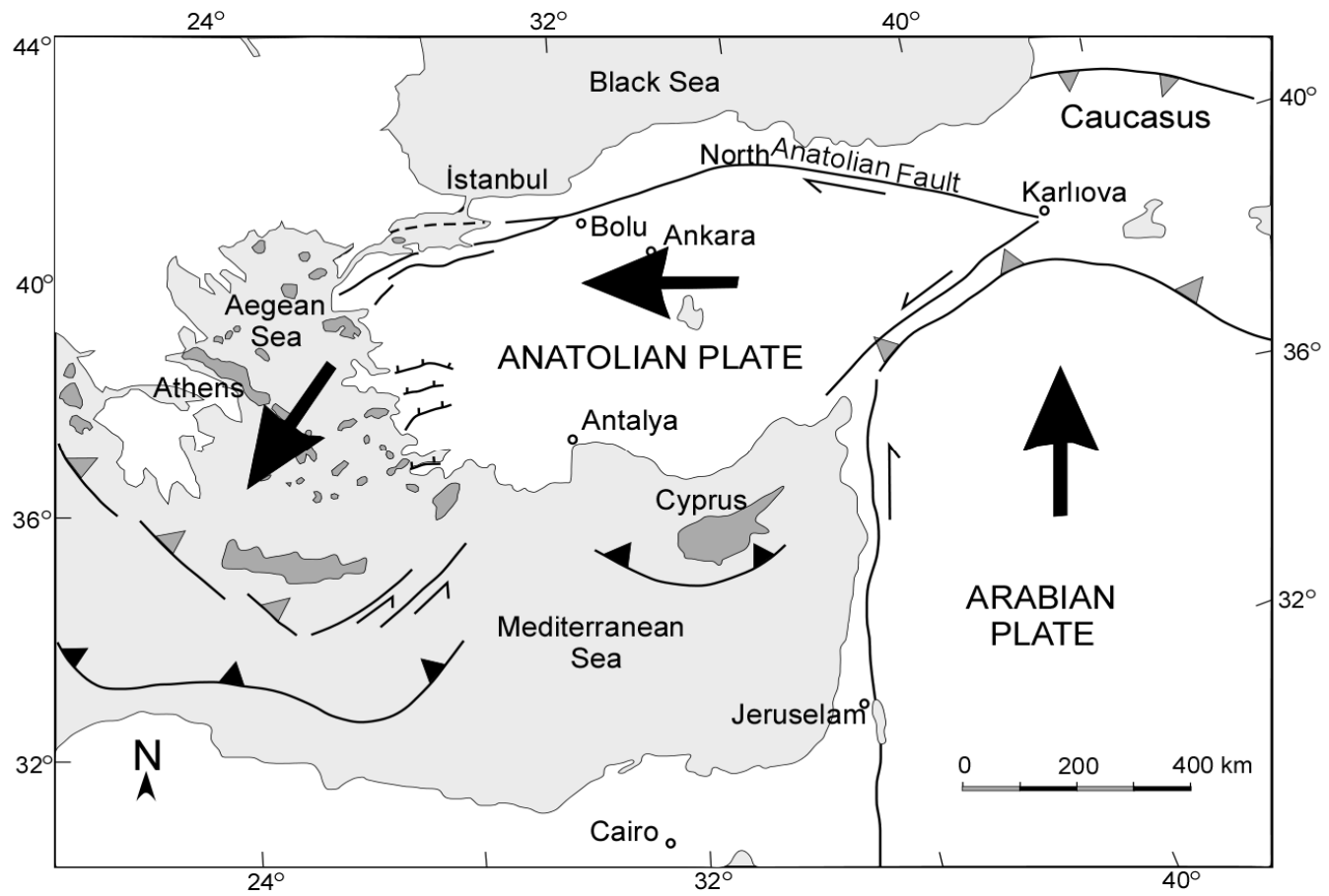


Figure 1.3 : Map showing the main tectonic elements of eastern Mediterranean regions (modified from McKenzie, 1972; Şengör *et al.*, 1985; Okay *et al.*, 1999).

1.1 Aims of the Study

Anatolia is one of the most important refuge area. The geographic position of Turkey also makes concerned area significant for palynological investigations. There are some pollen studies both Miocene and Pliocene in Turkey. However, they have lack of accurate botanical identification and therefore they are questionable. Hence, this thesis work is the first study based on the pollen botanical nomenclature which improve significantly floristic and vegetation interpretations. In this study, 436 samples from both marine (in the western Black Sea, DSDP Site 380) and outcrops sediments in the NW Turkey (Enez, İntepe, Eceabat, Burhanlı and West Seddülbahir), Northern Greece (Prosilio, Trilophos and Lion of Amphipoli) and Western Macedonia (Ptolemais Notio and Ptolemais Base) which covers time-intervals between the Late Miocene-Early Pleistocene are analysed palynologically. On the whole, samples are rich in terms of pollen grains. Some samples are barren in pollen grains. Because of this, these samples are not taken into account in the synthetic and detailed pollen diagrams. The targets of this thesis using the pollen analysis of sediments, their identification being botanically driven are:

- (1) to document the history of the flora and vegetation of Anatolia, then to compare with the Western Mediterranean region which is already well-known,
- (2) the reconstruction of the vegetation through the studied time-window using pollen records,
- (3) to follow-up on the tropical and subtropical thermophilous plants (distribution, abundance, etc.) during the Late Cenozoic,
- (4) to determine global climatic changes (coolings, warmings, glacial-interglacial cycles),
- (5) to assess the role possibly played by the Asian monsoon effect in the persistence of floral refuges in the studied regions, and
- (6) to determine the relative influence of regional geodynamics.

2. PHYSIOGRAPHY, STRATIGRAPHY AND PALEOGEOGRAPHY OF THE STUDY AREAS

2.1 Turkey

2.1.1 Present-day vegetation

In spite of its diversity and complexity, the present-day vegetation of Anatolia may be summarized as follows, relating both to the Mediterranean, Irano-Touranian, European and Euxino-Hyrcanian phytogeographic regions (Fig. 2.1). On the whole, the Mediterranean realm concerns the West and South coastal areas, with a variable width (100 to 300 km), but it sporadically appears along the North shoreline and also in some encased valleys within the Pontic Ranges. It is mainly controlled by climate (Akman & Ketenoglu, 1986). Several bioclimates and altitudinal vegetation belts have been defined according to rainfall and altitude (Quézel & Médail, 2003). The thermo-Mediterranean belt is constituted by assemblages with *Olea europea* and *Pistacia lentiscus* where *Ceratonia* is scarce, and also by coniferous forests with *Pinus brutia* occupying large areas. Some riparian forests are noteworthy, as they show *Alnus* associated with *Liquidambar orientalis* and *Platanus orientalis*. Basically, the meso-Mediterranean belt should be characterized by sclerophyllous oaks, but *Quercus ilex* is actually very rare being only present from Samsun to Trabzon. *Quercus calliprinos* is obviously the most frequent sclerophyllous oak while *Q. aucheri* is recorded along the Lycian shoreline. Here, deciduous oaks (*Quercus cerris*, *Q. trojana*, *Q. ithaburensis*, etc.) have been almost everywhere replaced by cultivations. On contrary, *Pinus brutia* occupies an important place which is not yet completely understood (Boydak, 2006). The supra-Mediterranean belt is theoretically inhabited by deciduous associations. This is right in the northern region where *Quercus pubescens*, *Q. cerris*, *Q. petraea* subsp. *iberica* take up a significant place, often with *Carpinus orientalis* and *Ostrya carpinifolia*.

Contrarily, westward and southward, as also on the Amanos Mountains, this vegetation belt is practically invaded by *Pinus brutia*, whereas deciduous trees are

very scarce and restricted to residual localities. *Pinus nigra* subsp. *pallasiana* already appears in its uppermost part. The Mediterranean montane belt is actually the altitudinal coniferous belt with abundant specimens of *Pinus pallasiana* and also *Cedrus libani* occupying significant areas on the Taurus and Anti-Taurus massifs, in association with *Abies cilicica* westward Antalya in spite of distinct ecological requirements. These forests, generally very deteriorated, are often replaced by pre-steppic associations with arborescent *Juniperus* (*J. excelsa*, *J. foetidissima*). The oro-Mediterranean belt (Quézel, 1973) is invaded by meadows and steppes where prickly cushion-shaped xerophytes are abundant, a belt already influenced by the Irano-Touranian conditions. The Irano-Touranian phytogeographic region encompasses the Anatolian Plateau, mostly eastward the Centro-Anatolian Ridge, and westward areas characterized by annual precipitations lower than 200 mm. Man greatly disturbed this region because of repeated attempts in development since antiquity (Akman & Quézel, 1996). The area is occupied by a very rich steppe vegetation where *Artemisia* is relatively subsidiary, at least to the West. Pre-steppic structures with trees appear only over reliefs where precipitations are higher and man activity less apparent. *Quercus pubescens* subsp. *anatolica* is widely present, very often in a state of grazed shoots in the northwestern part of the region. Westward, *Pinus pallasiana* and *Juniperus excelsa* are prevalent while Irano-Touranian oaks (*Q. libani*, *Q. brantii*, *Q. infectoria* subsp. *boissieri*) grow to the East.

The European phytogeographic region is secondary in Anatolia. Only some deciduous hilly structures with *Quercus* and *Carpinus betulus* may belong to it. Some other European associations are more obvious within the montane vegetation belt, from the Kaz Mount to the area of Kastamonu, where beautiful forests develop including *Fagus orientalis* (often difficult to distinguish from *F. sylvatica*) and firs (*Abies equi-troyani*, *A. bornmuelleriana*).

The Euxino-Hyrcanian phytogeographic region, characterized by high precipitations and the lack of any summer drought, develops all along the Black Sea shoreline. Here, wonderful hilly forests still exist, dominated by deciduous elements (*Quercus hartwissiana*, *Q. macranthera*, *Carpinus betulus*, *Castanea sativa*, with *Fagus orientalis* and *Rhododendron ponticum* in some places, even *Rh. flavum*).

Some alluvial associations and riparian forests show *Alnus*, *Fraxinus*, and *Pterocarya* in some localities (see below).

The montane belt is mainly occupied by *Fagus orientalis* and *Rhododendron ponticum*, with locally *Abies nordmannian*, and Eastward *Picea orientalis*. *Pinus sylvestris* is present from place to place in marginal areas, especially to the South. The subalpine and alpine belts are mainly developed to the East where Caucasus influences infer within a very diversified flora (*Juniperus communis* and *J. sabina* coexist with several Ericaceae). *Buxus sempervirens (colchica)*, often associated with *Taxus baccata*, abound on the rare calcareous spaces in the region. Back to the Euxinian zone, a transition area has been identified between the Mediterranean and Irano-Touranian phytogeographic regions, the so-called Pre-Pontic region (Quézel *et al.*, 1980), the vegetation of which is dominated by *Abies* spp., *Pinus nigra* subsp. *pallasiana*, and *P. sylvestris*.

May Anatolia be considered as a present-day refuge area of a thermophilous flora?

Some warm-temperate Eurasian taxa (such as *Liquidambar*, *Pterocarya*, *Cedrus*) have already emerged from this brief overview of the Anatolian vegetation (Quézel, 1995), currently recorded in the European Late Cenozoic pollen records as it will be emphasized below. According also to Browicz (1982-1994), few taxa are still present in Anatolia (*Liquidambar*, *Pterocarya*, *Zelkova*) and in the Hyrcanian zone (*Parrotia*). *Zelkova crenata* is today recorded only in two very restricted riparian localities in easternmost Anatolia close to the Van Lake, although it is still well-developed in Abkhazia, Small Caucasus, and mainly in the Hyrcanian region. In addition, this genus is still present in residual stations of Crete (*Z. abelicea*) and Sicily (*Z. sicula*) (Quézel, 1995).

Liquidambar orientalis is concentrated in some more or less important areas (Fig. 2.1): the vastest of which concerns the alluvial and riparian forests of the southwesternmost part of Anatolia (mainly the area of Köyceğiz – Marmaris), another one of significantly less extent locates northeastward Antalya (Köseler area; Akman *et al.*, 1993), the third one along the Oronte River close to Hatay is today questionable because it seems that it was not recently re-visited. The strong reducing of the two last localities is attested by ancient documents indicating that *Liquidambar* was abundant during the Hellenic time and intensely used for producing styrax (Amigues, 2007).

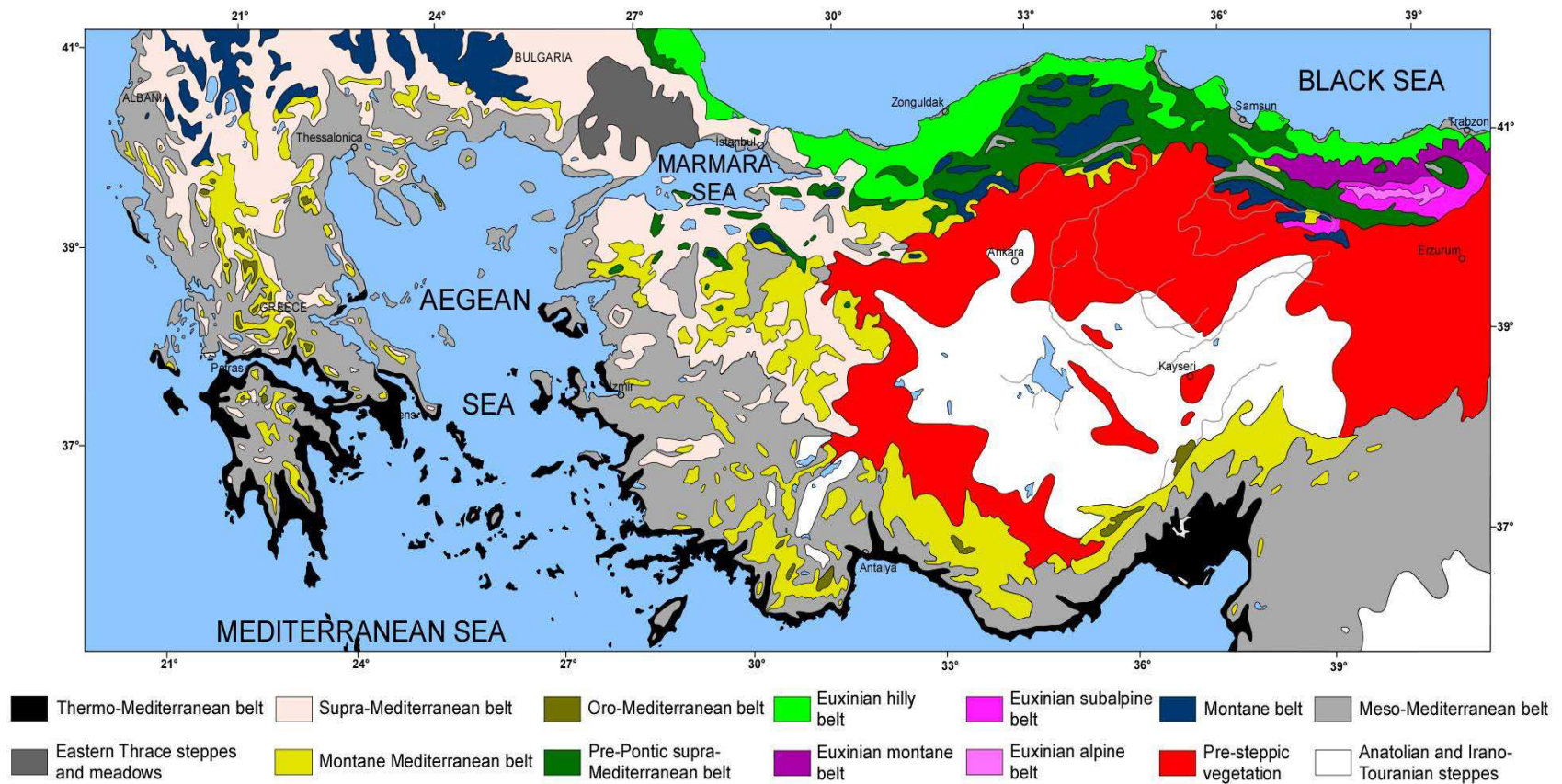


Figure 2.1 : The present-day vegetation map of Turkey and Greece (Quézel and Barbero, 1985).

Pterocarya is still present in alluvial forests along the Black and Marmara seas, being relatively abundant in the latter (Fig. 2.1). It is also recorded in some localities near the Iskenderun Gulf where precise information is missing (Fig. 2.1). However, the tree is frequent out of Anatolia in the above-mentioned regions where *Zelkova* is living. *Cedrus* benefits from better conditions (Quézel and Médail, 2003): it abounds on the Taurus and Anti-Taurus massifs, although it is declining. Few reduced localities persist on the back slope of the Pontic Ranges (Erbaa region; Fig. 4), the indigenous status of which is supported by pollen data (Bottema, 1986). Some other plants should be added to the above discussed Anatolian relicts, such as *Diospyros lotus*, *Ilex colchica*, *Rhododendron* spp., even *Quercus pontica* and *Osmanthus decorus* which grows today along the Black Sea shoreline (Quézel, 1986). Anatolia can undoubtedly be considered as a present-day refuge area of warm-temperate plants, however with less importance than the Hyrcanian region. Present-day vegetation of Greece is divided into different vegetation types (Fig. 2.1). They are:

- 1) Thermo-Mediterranean belt,
- 2) Meso-Mediterranean belt,
- 3) Supra-Mediterranean belt,
- 4) Montane Mediterranean belt,
- 5) Oro-Mediterranean belt,
- 6) Montane belt,

2.1.2 Climate

2.1.2.1 Turkey

The location and geographical characteristics of Turkey give a variety of climates, landscapes and plant diversity. Turkey is located in large Mediterranean geographical area. The climate is characterized by Mediterranean macro climate. Eastern Mediterranean region is influenced by three main atmospheric systems (Fig. 2.2): the main middle to high latitude westerlies to the north and northwest, the mid-latitude subtropical high-pressure systems extending from the Atlantic across the Sahara and the monsoon climates of Indian subcontinent and East Africa (Akcar and Schlüchter, 2005).

Marine tropical air masses (mT) bring hot and humid air from the tropical north Atlantic. Continental tropical airstreams (cT) convey from the northern African and Arabian deserts. It passes over the Mediterranean Sea, and they can obtain moisture and then condensate over the southern coasts of Anatolia. Marine polar air masses (mP) carry the humid and cold air from the polar north Atlantic. They have significant influence when they progress over the Mediterranean Sea. Continental polar air masses (cT) bring the dry and cold air from Siberia. They can acquire moisture and condensate on the northern coasts of Turkey (over the Black Sea) (Fig. 2.2). The climatic conditions are warm-temperate in Turkey (Erinç, 1959). It is now usually known that the climate variability in the middle- and high-latitude continental Northern Hemisphere mainly controlled by the Arctic Oscillation and North Atlantic Oscillation (AO/NAO) at interannual and interdecadal timescales (Thompson and Wallace, 2001). This changing patterns also affect the climate of Turkey and its surrounding fields (Cullen and deMenocal, 2000; Karaca *et al.*, 2000; Türkeş and Erlat, 2003; Karabörk *et al.*, 2005; Kahya and Cengiz, 2007). The secondary cyclogenesis in eastern Mediterranean enables a physical linkage between the NAO (known as a key provider of precipitation to the Middle East region) (Cullen and deMenocal, 2000) and climatic surface variables in Turkey (Kahya and Cengiz, 2007). Turkey's climate is modified by its topographic relief that result in great regional differences in the amount of mean annual precipitation and by rapid transitions from rainy areas to dry ones. Most abundant precipitation (>1000 mm) occurs in Black Sea coast in the north and on the western Taurus Mountains in the southwest.

The Eastern Black Sea and the Western Mediterranean coasts are the wettest areas of the country in winter, with a mean rainfall total of more than 650 mm (Türkeş, 1996). Approximately half of the country has less than 50 mm mean rainfall in summer, with a minimum of less than 5 mm along the Turkey–Syria border. Mean annual rainfall total is about 300 mm over continental central Anatolia. Besides, along the Western Black Sea, Eastern Black Sea, and Western Mediterranean coasts are more than 1,000 mm. The highest mean annual rainfall total was recorded on the Eastern Black Sea coast (2,304 mm). Over the continental Mediterranean region, mean annual rainfall increases from south (with about 400 mm) to north (with about 800 mm).

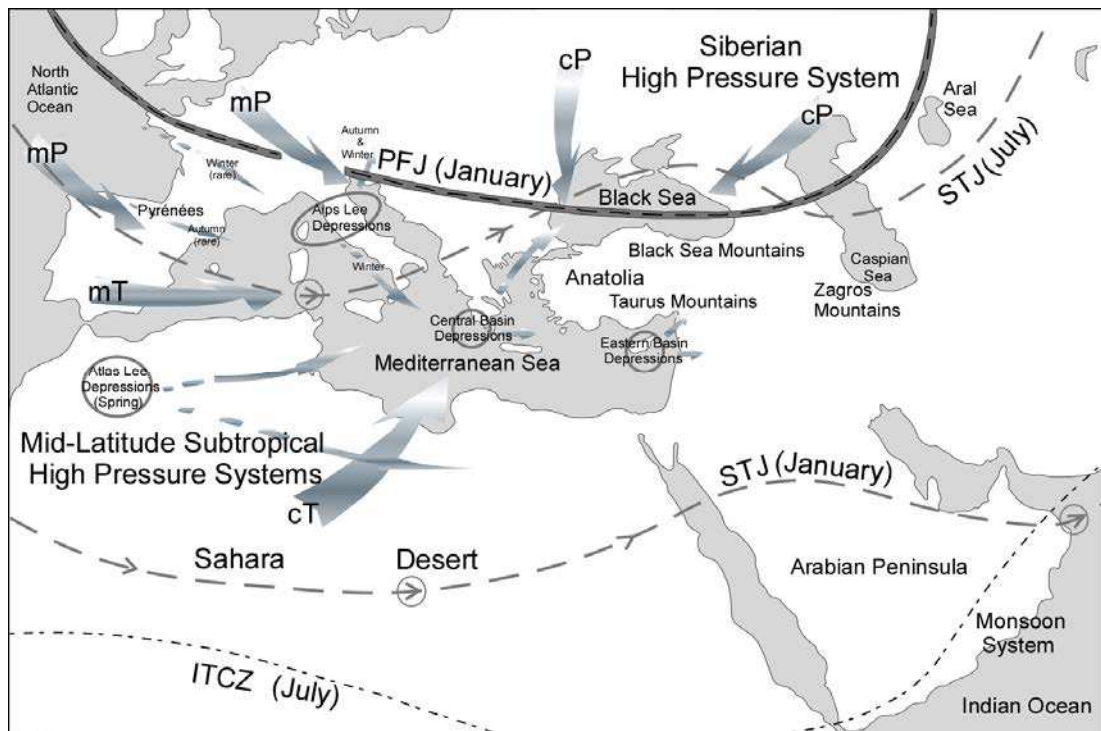


Figure 2.2 : Atmospheric air masses affecting the Eastern Mediterranean region (cP: Continental Polar Air Mass; mP: Marine Polar Air Mass; cT: Continental Tropical Air Mass; mT: Marine Tropical Air Mass, PFJ: Polar Front Jet; STJ: Subtropical Jet; ITCZ: Intertropical Convergence Zone (modified from Wigley and Farmer, 1982).

The annual rainfall is more than 500 mm over a considerable part of the continental eastern Anatolia region, and it increases over mountains. According to climatic differences of the regions in Turkey due to the existence of irregular topography, four macroclimate types are determined (Erinç, 1996). These macroclimate types are as follows hereafter (Fig. 2.3):

1) I - Steppe Climate:

In this climate type, semi-arid conditions dominate. Rainfall pattern resembles the coasts of Mediterranean. It is divided into two types:

- a) **Ia – Anatolian steppe climate:** The summers are hot (20-25°C) and the winters are cold (0-3°C).
- b) **Ib – Southeastern Anatolian steppe climate:** While the summers are considerably hot (>30°C), the winters are cold (0-5°C). High evaporation is observed (annually 1000-2000 mm).

2) II – Black Sea Climate: All seasons are rainy. It is composed of three types according to rainfall and temperature:

a) IIa – Eastern Black Sea climate: it has high rainfall. Winters are temperate.

b) IIb – Central Black Sea climate: with an average rainfall.

c) IIc – Western Black Sea climate: less amount of rainfall, winters and summers have less temperature.

3) III – Mediterranean Climate: Although high annual precipitation, it is observed a severe summer aridity. This climate type is divided into two types according to temperature: IIIa and IIIb

a) IIIa – Mediterranean climate: very high summer temperature. In the winters, small amount of snow.

b) IIIb – Marmara region climate: very cold winters, low evaporation.

4) Eastern Anatolian Climate: very cold winters, it is divided into two types:

a) IVa – All seasons with precipitation: it represents a continental climate regime.

b) IVb – Arid summer type: high precipitation in winter and spring; little precipitation and high evaporation during summer and autumn.

2.1.2.2 Greece and Macedonia

The climate in Greece is a Mediterranean type climate with dry and hot summers (Mariolopoulos, 1938). Between October and March exist cold and rainy period, from April to September, warm and dry period exist. The coldest months are January and February with average minimum temperature ranging between 5-10 degrees Celsius. Rainfall is high on the west coast, about 1000 mm (Mariolopoulos, 1925).

The main factors controlling the climatic conditions in Greece are the atmospheric circulation, the latitude, the altitude and generally, the orography, the Mediterranean sea surface temperature (SST) distribution, the land-sea interactions (distance from the sea) and smaller-scale processes (Lolis *et al.* 1999). In Greece, there are five climatic regions. These regions are :

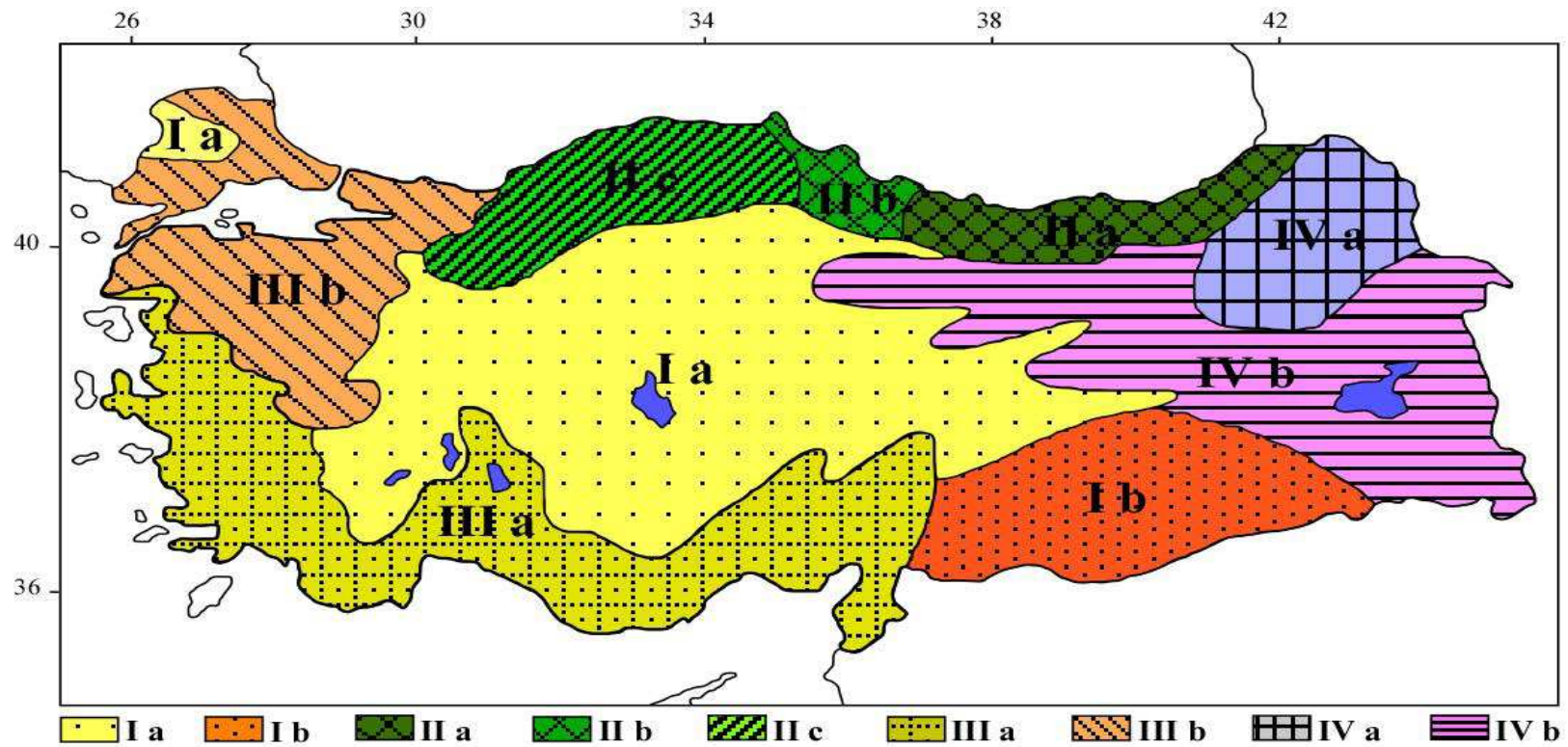


Figure 2.3 : Macroclimate types of Turkey. Ia: Anatolian steppe climate; Ib: Southeastern Anatolian steppe climate; IIb: Central Black Sea climate; IIc: Western Black Sea climate; IIIa: Mediterranean climate; IIIb: Marmara climate; IVa: All seasons with precipitation type; IVb: Arid summer type (modified from Erinç, 1996).

- 1) in the western coast of Greece and the islands of Ionian Sea which take high amounts of precipitation. The maximum precipitation observed in autumn and a minimum precipitation occurs during the summer. The annual temperature range is small in this region,
- 2) in the Aegean region (the islands of the Aegean Sea and the west coast of southern Greece) exist low winter temperatures, high summer temperatures and low precipitation. The annual precipitation is on average,
- 3) in the northern and the central part of Greece is characterized by long duration storms, short drought periods, low temperatures during winter and large annual temperature range,
- 4) in Crete and the southern Greece characterize the Mediterranean desert type climate with low annual precipitation and droughts of long duration,
- 5) in the Pindous Mountain range which divides Greece into western and eastern regions, and the mountains of northern, central and southern Greece. The climate in this region is the typical climate of mountain areas with high annual precipitation and strong gradients of precipitation and temperature with elevation (Loukas *et al.*, 2001).

The frontal depressions approaching Greece (from January to April) are rain producers along the western coast of Greece and in the central Aegean Sea. During winter, in the Atlantic near the Gibraltar Strait depressions originate. High rainfall is limited to the islands and the coastal areas of Ionian Sea with some influence in Thessaly (central Greece). The frontal depressions approaching Greece from the west, they cause southwest winds over the Ionian and Aegean Seas forcing the maritime air eastwards (Xoplaki *et al.*, 2000). During summer, the high pressure belts of the subtropics drifts northwards. In Macedonia, the climate is characterized by the submediterranean to a continental and mountainous climate. However, the Mediterranean climate basically influences. An Average daily temperature exist in Skopje, ranging from 32° to -3° (Kendrovski, 2006). Continental climate occurs in the central part of Macedonia. The average annual temperature is 12°C and summer temperature is 19°C (April-September).

During winter, an average temperature is 5°C between October and March (Hristovski *et al.*, 2007). In addition, in winter, there is little wind and rain. In

addition during this season, a slight lowering of pressure over central eastern Europe brings low-pressure zone over the Mediterranean. The cyclonic depressions in the winter months follow one another from west to east over the Mediterranean. Spring and Autumn are signed by heavy thunderstorm which cause rainfall. The dry season lasts two months in Macedonia (Ogilvie, 1920).

2.1.3 Stratigraphy of the study areas

The Marmara region mainly consists of the İstanbul and the Strandja zones to the north, the Sakarya zone and İzmir-Ankara Zone to the south. These zones are overlain by fore-arc Thrace Basin rocks formed during Eocene-Oligocene time. Today, these zones are separated from each other by the major structural elements (suture zones/transform faults). The northern shorelines of Marmara Sea are generally cliffy and shore type includes pocket beaches. Neogene rocks are widely distributed in the NE Aegean, around of the Sea of Marmara and Greece (Fig. 2.4). In the north-west Marmara shorelines, south of the North Anatolian Fault, from Gaziköy westward, along the Çanakkale shorelines, there exist Miocene micaceous quartz sandstones (Kirazlı and Gazhanedere formations) (Türkecan and Yurtsever, 2002).

Kirazlı Formation conformably overlies the Gazhanedere Formation, and consists of cross-bedded, yellow sandstones with rare mudstone and conglomeratic intercalations in the northern Gulf of Saros. The overlying Alçıtepe Formation is widely distributed in the Sea of Marmara and the Gulf of Saros regions (Sayar, 1987; Sümengen *et al.*, 1987; Siyako *et al.*, 1989; Görür *et al.*, 1997; Çağatay *et al.*, 1999; Sakınç *et al.*, 1999; Görür *et al.*, 2000).

Alçıtepe Formation lies conformably over the Kirazlı Formation (Sakınç *et al.*, 1999; Yalıtırak *et al.*, 2000). However, other workers claim unconformable relationship between the Kirazlı and Alçıtepe Formations (Armijo *et al.*, 1999; Melinte *et al.*, 2009). The nannofossil data show that the age of the Alçıtepe Formation is younger than the Messinian Salinity Crisis (Melinte *et al.*, 2009). The Alçıtepe Formation demonstrates different facies characteristics in the northern coast of the Gulf of Saros and Gelibolu and Biga peninsulas.

In Enez, (NW of the Gulf of Saros), the Alçıtepe Formation (Mastra-bearing limestone section) is 23-m thick and includes a rich and sandstone intercalations in the upper part . The formation is overlain unconformably by the alluvial fan deposits of the Conkbayırı Formation in the Gelibolu Peninsula. The Alçıtepe Formation contains mudstone and marl in the lower part, bioclastic and oolitic limestones with marl in the upper part in the Gelibolu and Biga peninsulas. It is overlain with an erosional unconformity by the Göztepe Formation (NN12 zone), composed of shallow marine siltstone and sandstone with ostrea banks and mollusc-rich sandy interbeds towards the upper part.

The DSDP 380 Black Sea core includes five stratigraphic units and fourteen sub-units identified by Ross (1978). Unit 1 consists of terrigenous sediments, including muds, sandy silts. Unit 2 includes aragonite, sideritic and calcitic siltstone, interbedded in muds. Unit 3 compose of seekride, including calcitic oozes and marls. Unit 4 includes calcitic, sideritic, aragonitic and dolomitic, interbedded in muds and Unit 5 consists of Black shales with dolomite and zeolitic silt intercalations (Fig. 2.5).

Neogene rocks in the Florina-Ptolemais-Servia (FPS) Basin (Upper Miocene-Lower Pliocene) is located in Greece. The lacustrine sediments in this basin are appeared in a series of open-pit lignite quarries. The age of the Ptolemais section is between 5.3 and 3.9 Ma (Van Vugt *et al.*, 1998; Steenbrink *et al.*, 2000). The Florina, Ptolemais and Servia sub-basins are located between 300 and 700m above the sea level. These sub-basins are surrounded by mountains (~2000 m) that consist of Mesozoic limestones, Upper Carboniferous granites and Paleozoic schists.

The Late Miocene-Early Pleistocene lake sediments contain lignites and alluvial deposits. The studied stratigraphic sections include four lithostratigraphic units: Komnina Formation, Ptolemais Formation, Proastio Formation and Perdika Formation. The Ptolemais Formation is ~110 m thick and includes alternation of lignites and lacustrine marls with fluvial sand, silts and some volcanic ash intercalations.

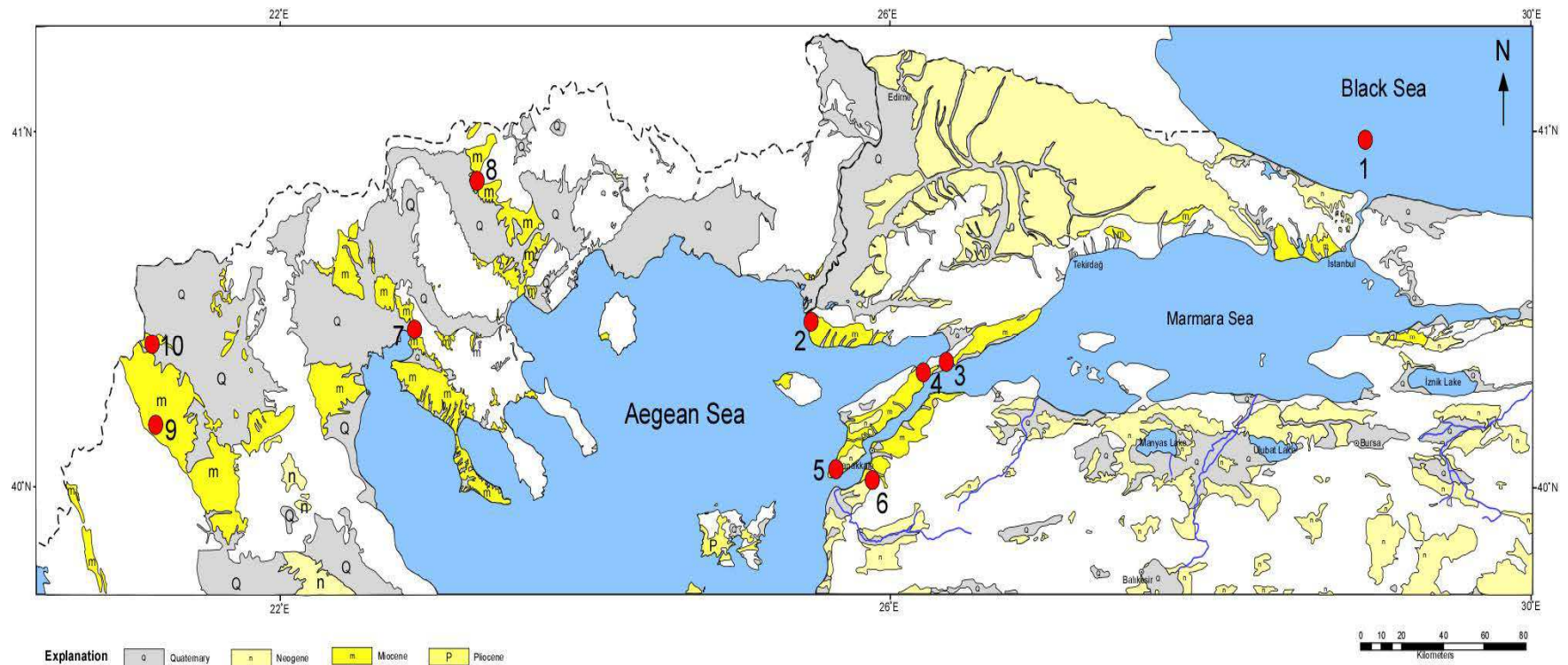


Figure 2.4 : Distribution of Neogene rocks in the Marmara regions and North Aegean (simplified from Türkecan and Yurtsever, 2002; Okay *et al.*, 1996 and Aldanmaz, 2002; Bornovas *et al.*, 1983) and numbers: 1; DSDP Site 380, 2; Enez, 3; Burhanlı, 4; Eceabat, 5; west Seddülbahir, 6; İntepe, 7; Trilophos, 8; Lion of Amphipoli, 9; Prosilio, 10; Ptolemais (Notio and Base).

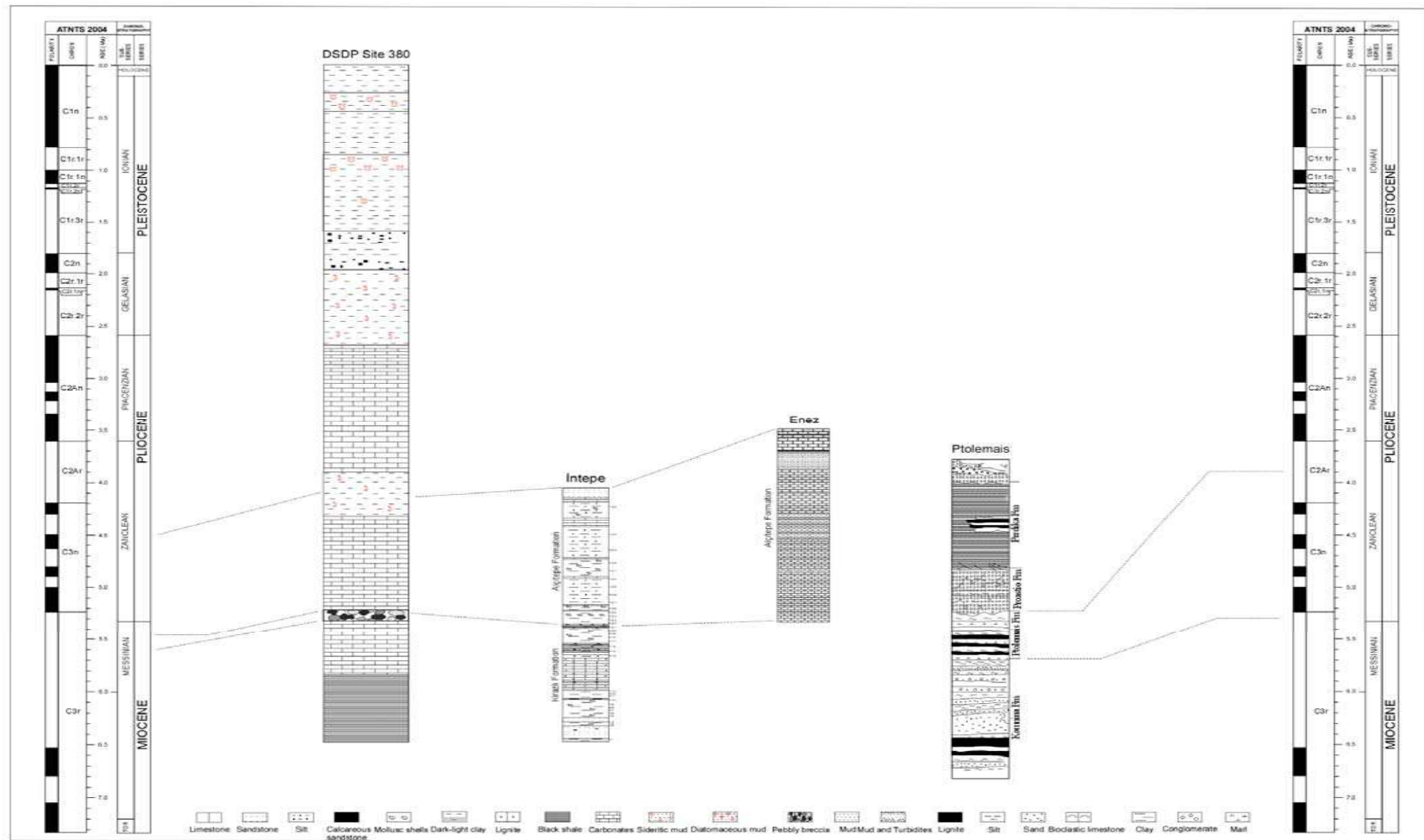


Figure 2.5 : Stratigraphy of studied sedimentary sections in DSDP Site 380, Intepe, Enez and Ptolemais.

The age of the Ptolemais Formation is Early Pliocene (MN 14 and 15) based on paleontological data, magneto- and cyclo-stratigraphy and $^{40}\text{Ar}/^{39}\text{Ar}$ dating (Van Vugt *et al.*, 1998; Steenbrink *et al.*, 1999). The Komnina Formation is approximately 300 m thick and overlays uncorformably the pre-Neogene basement. The formation contains alluvial sands, conglomerates, lacustrine marls and clays with some intercalated lignite seams (Steenbrink *et al.*, 2006).

The middle part of the Komnina Formation is dated as the Late Miocene based on the small mammals (de Bruijn *et al.*, 1999), magneto and cyclo-stratigraphy (Steenbrink *et al.*, 2000). The Prosilio section is located in 10 km SW of Servia. This section includes ~200 m of lacustrine and alluvial sediments (marls, lignites, clays, sands and conglomerates) (Steenbrink *et al.*, 2006).

2.1.4 Paleogeography

Paleogeography affects the climate, and thus also influence vegetation and fauna. During the Neogene, convergence between the Eurasian plate and African plate caused Tethys to close and form in it place the Mediterranean Sea and Paratethys (Meulenkamp and Sissingh, 2003). Paratethys realm includes a part of the Alps, Carpathians, Pannonian, Dacic and the Euxinian basin (Black Sea, Caspian Sea and Aral Sea today). In the Late Tortonian (Pannonian), larger portions of northern Peri-Tethys were emerged and extensive sedimentation started to break up in the western and central domains. During this time, alluvial deposits and lacustrine carbonates accumulated in the Ebro Basin (NE Iberia) (Meulenkamp *et al.*, 2000b).

In the central Europe, brackish to fluviolacustrine conditions existed in central Paratethys in the Late Tortonian. Mediterranean marine connection with intra-arc domains no longer existed. Ephemeral marine incursions in the outer Carpathian were restricted to Dacic basin. The sediments of the Late Tortonian (Middle Maeotian) includes nannoplankton assemblages indicating the lower part of NN11 zone (Fornaciari *et al.*, 1997; Marunteanu and Papaianopol, 1998). In addition, in the Late Tortonian Dacic basin became a part of the Eastern Paratethys. In the latest Early to earliest Middle Miocene, marine invasion occurred in the central part of Arabian Platform. However, sea regressed during the late Middle Miocene (Meulenkamp *et al.*, 2000b) (Fig. 2.6).

In the late Miocene (Late Messinian; Late Pannonian-Early Pontian), the Messinian Salinity Crisis affected the Mediterranean basins (Fig. 2.7). Evaporites were deposited in different depths (Popov *et al.*, 2006). According to the largely accepted hypothesis (CIESM, 2007; Clauzon *et al.*, 2001), sea level drop occurred in two steps separated by a flooding event. The first step (5.8 Ma), Mediterranean margins were impacted (sea-level fall of ca. 150 m). The second step occurred in an outstanding sea level fall of about 1500 m at 5.6 Ma and effected the whole basin (Clauzon *et al.*, 1996). The Paratethys had a strong influence on the Mediterranean region during the Messinian Salinity Crisis. Between the two low-stand phases, the Lago Mare event took place probably originating from the Paratethys (Cita *et al.*, 1978a).

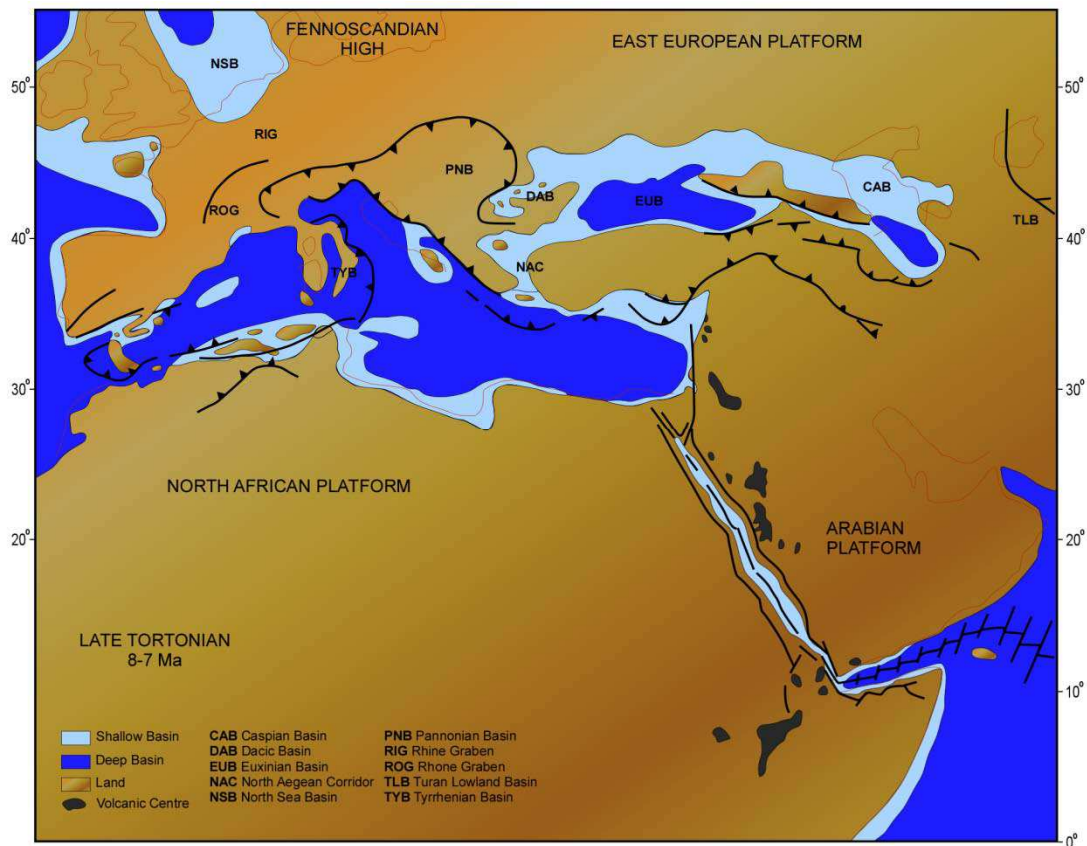


Figure 2.6 : Paleogeographic map of the Late Tortonian (8-7 Ma), indicating position of continental, shallow and deep basins. Thick black lines show fault zones (modified from Meulenkamp *et al.*, 2000b; Meulenkamp and Sissingh, 2003).

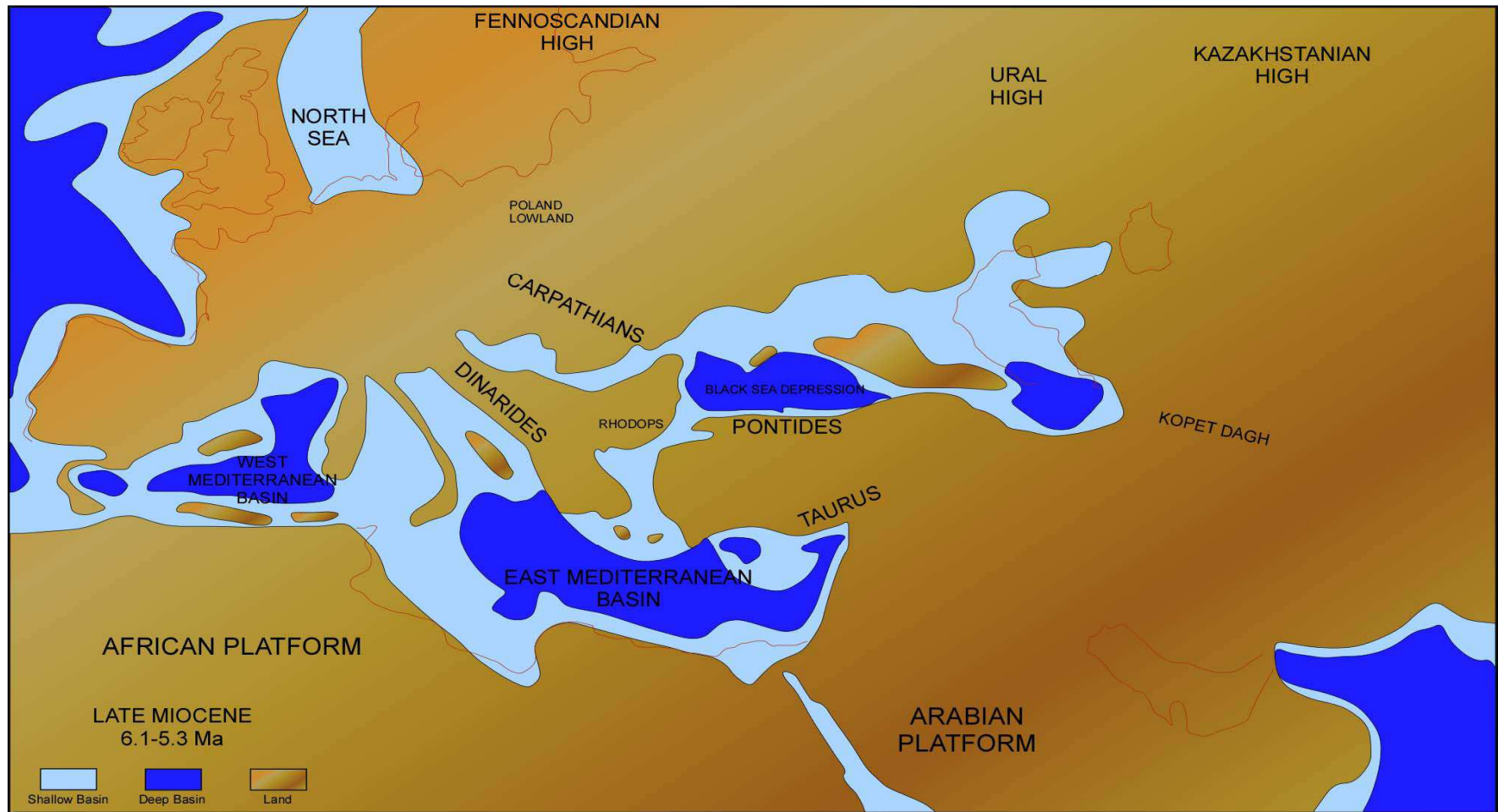


Figure 2.7 : Palinspastic paleogeographic map for Late Miocene (Late Messinian, Late Pannonian-Early Pontian) showing shallow and deep basins (modified from Popov *et al.*, 2006; Olteanu and Jipa, 2006).

The Lago Mare facies is characterised by common brackish shallow water fauna: *Congerina*, *Dreissena*, *Melanopsis* among molluscs; *Cyprideis pannonica* gr., *Loxococoncha*, *Tyrrhenocythere*, etc., among ostracods (Ruggieri, 1967; Cita and Colombo, 1979) and endemic Paratethyan dinocysts *Galeacysta etrusca* (Müller *et al.*, 1999; Bertini *et al.*, 1995; Bertini, 2002). In the Late Messinian (Early Pontian), Eastern Paratethys reached its maximum areal extent (Popov *et al.*, 2006) (Fig. 2.8). The eastern and northern margins of the early Pontian basin was caused by the transgression (Popov *et al.*, 2004). At the same time, paleogeographic changes were controlled by regional tectonics, and the desiccation of the Mediterranean and Black seas that were partly coeval during the Messinian took place (Armijo *et al.*, 1999; Görür *et al.*, 1997, 2000; Gillet, 2004; Clauzon *et al.*, 2005; Melinte *et al.*, 2009).

Significant paleogeographic changes occurred during the Late Miocene in the eastern Mediterranean. During the Messinian, the MSC effected on terrestrial and marine ecosystems (i.e., planktonic foraminifers, calcareous nannoplankton and dinoflagellates). The MSC has been observed all over the Mediterranean region including Aegean Sea. The rocks of Messinian-Early Zanclean age are widely distributed in northwestern Turkey. The Messinian erosional surface has been observed in the Mediterranean area and Eastern part of Black Sea (Clauzon *et al.*, 1996). Some localities indicate discontinuity occurred by weak erosion in İntepe (Çağatay *et al.*, 2007, Melinte *et al.*, 2009). During the Late Miocene, continental and marine sedimentation existed in northern Anatolia (Görür *et al.* 1997).

Marine sedimentation existed in the Black Sea area. Continental sedimentation developed in basins formed by the North Anatolian Fault which initiated during the Early-Late Miocene (Barka and Hancock, 1984; Barka, 1985, 1992). Mediterranean extensively dried up (Hsü, 1972, 1974; Adams *et al.*, 1977; Ryan and Cita, 1978) and also Black Sea desiccated (Gillet, 2004; Popescu, 2006) during the Messinian. Paleogeography of the studied region covering time-window from the Early Messinian to the Latest Messinian-Earliest Zanclean is shown in Figs. 2.8-2.9. Pollen records from the studied areas provide information about palaeoenvironments just before and just after the Messinian Salinity Crisis (Melinte *et al.*, 2009). Herbs were abundant before the Messinian Salinity Crisis in Burhanlı, Eceabat and İntepe sections.

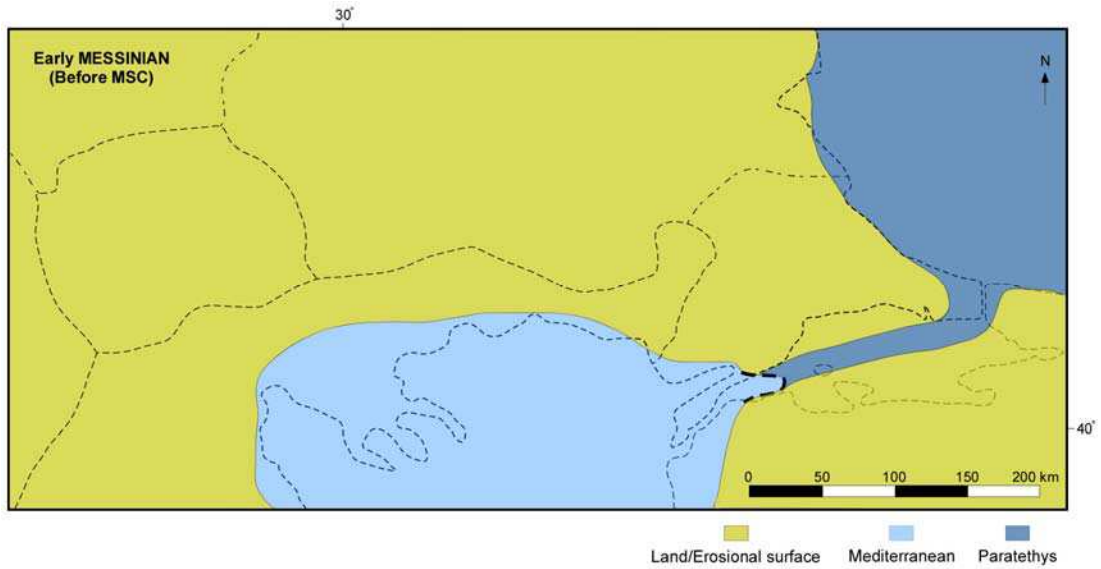


Figure 2.8 : The Paleogeographic map of Marmara region and Greece and Macedonia before the Messinian Salinity Crisis (Early Messinian) (modified from Görür *et al.*, 1997; Sakıncı *et al.*, 1999; Vasiliev *et al.*, 2004; Çağatay *et al.*, 2006; Melinte *et al.*, 2009; Krijgsman *et al.*, 2010).

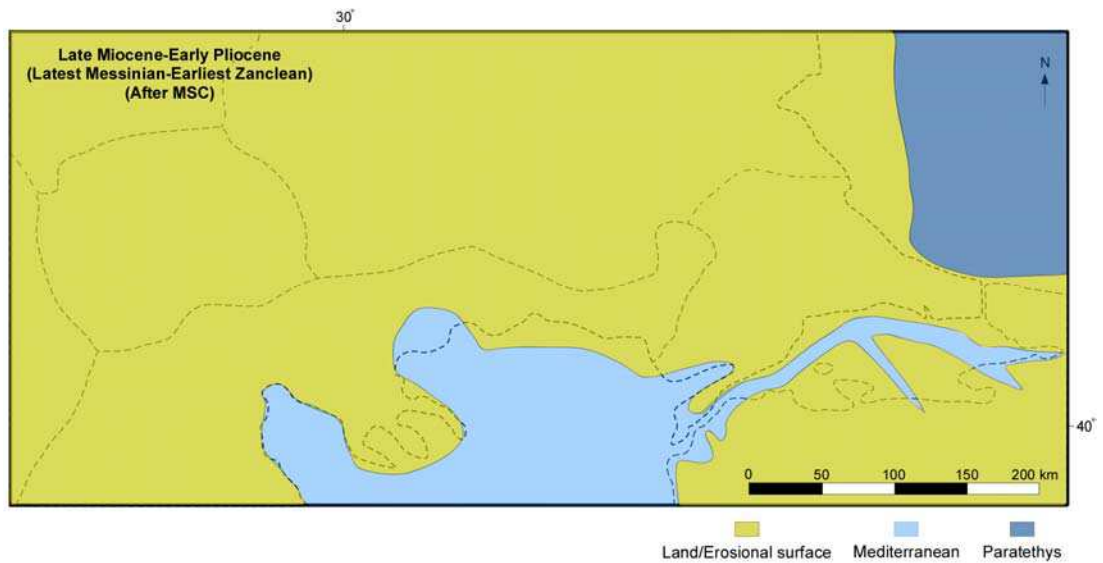


Figure 2.9 : The Paleogeographic map of Marmara region and Greece and Macedonia after the Messinian Salinity Crisis (Latest Messinian-Earliest Zanclean) (modified from Sakıncı and Yaltrak, 2005; Rögl and Steininger, 1983; Meulenkamp and Sissingh, 2003; Suc, J.-P., personal data).

Black Sea witnessed desiccation during the Messinian Salinity Crisis (Hsü and Giovanoli, 1979), as indicated by the 19 m thick "Pebbly Breccia" (containing blocks of stromatolitic dolomite) in DSDP Drill Hole 380 (Ross *et al.*, 1978). This presumably produced a shorter break in the pollen record. In addition, diatom data of the Black Sea hole suggests that Black Sea was very shallow at that time (Schrader, 1978). Deep dessicated basin evaporates were deposited during that time. At this time, subtropical and warm-temperate trees were abundant in the southwestern Black Sea (Popescu, 2006). Before the MSC, in northern Greece (Prosilio), meso-microthermic (mainly *Tsuga*) and microthermic trees (*Abies* and *Picea*) are abundant. This could be explained as by uplifting of the surrounding region.

The connections between the Mediterranean and Paratethys were enabled after the Messinian Salinity Crisis. During the Pliocene time interval, the Mediterranean Sea was inundated by marine waters due to the connection with Atlantic Ocean after the Messinian Salinity Crisis (Hsü and Bernoulli, 1978). Early Zanclean reflooding occurred within two steps: collapse (at 5.480 Ma) and widening (at 5.330 Ma) of the Gibraltar Strait (Clauzon *et al.*, 2007). During the Early Pliocene, northern margin of the Sea of Marmara Basin was uplifted and eroded, while the southern margin turned into continental areas (Görür, *et al.*, 1997). At the Latest Messinian-Earliest Zanclean (after MSC), altitudinal conifers (*Cedrus*, *Abies*, *Picea* and *Pinus*) indicate an augmentation in the north-western Aegean (i.e. İntepe and west Seddülbahir).

This could indicate uplifting of the region. Indeed, uplifting occurred during the Messinian due to propagation of the North Anatolian Fault (NAF) (Armijo *et al.*, 1999; Melinte *et al.*, 2009).

During the Middle Pliocene (Piacenzian)-Early Pleistocene (Gelasian), Iberian domain emerged. In these basins which located in south-eastern Iberia (Aguirre, 1998) and Atlantic coast, alluvial and shallow marine sediments deposited (Fig. 2.10). In the central Paratethys (intra-Carpathian domains) continental clastic accumulated in the Middle Pliocene-Early Pleistocene. Back-arc basin in the southwestern part were filled with Pliocene deposits (reaching thickness about 1000 m) (Meulenkamp *et al.*, 1996). In addition, widespread volcanism occurred in the Styrian and Danube basins, Great Hungarian plain, South Slovakian-North Hungarian volcanic domain and south-eastern Transylvania (Szabo *et al.*, 1992).

Nevertheless, the faunal composition of Dacic basin changed significantly (extinction of Limnocyprids and appearance of Unionids, Viviparids and Melanopsids) during the Pliocene (Meulenkamp *et al*, 2000b). Eastern Paratethys contained two major basins (Dacic-Euxinian basin system and the Caspian basin) since latest Miocene (Late Pontian). In the Caspian basin occurred a major regression with reduction of salinity in the Early Pliocene. The Akchagylian Sea was characterised by low salinity and euryhaline biotas (Meulenkamp *et al*, 2000b). Pollen assemblages and macroplant fossils (leaf remains) show that existence of a forested hinterland with similar to those of present-day taiga.

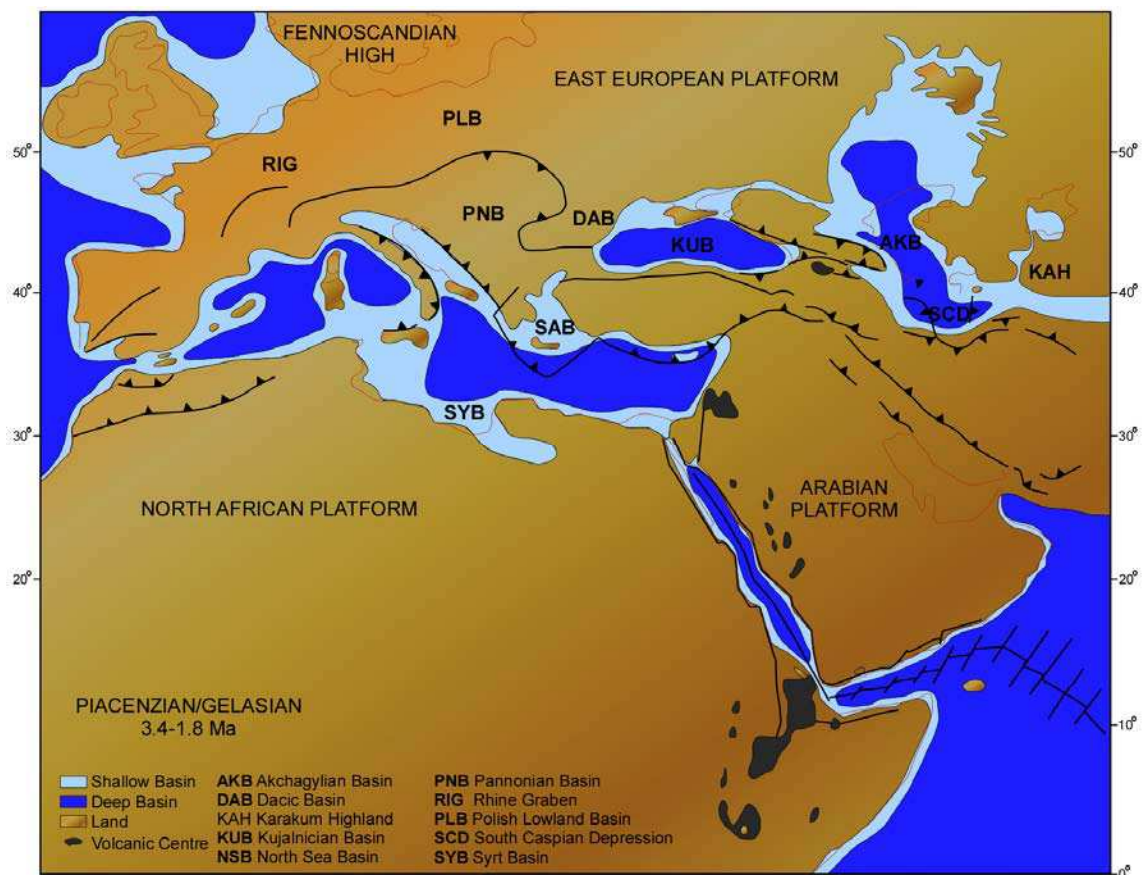


Figure 2.10 : Paleogeographic map of the Piacenzian-Gelasian (3.4-1.8 Ma), indicating position of continental, shallow and deep basins. Thick black lines show fault zones (modified from Meulenkamp *et al*, 2000b; Meulenkamp and Sissingh, 2003).

They show climatic conditions changing from cool and dry towards relatively warm and wet (broad-leaved forest zone; Neogene System, 1986). The connection between the Mediterranean and Paratethys during the Late Pliocene is also supported by its faunal assemblages in the sediments.

The faunal distribution of the sediments shows that the Marmara Basin was firstly invaded by Paratethys and then by the Mediterranean during the Late Pliocene. At the beginning of the Pleistocene (2.6 my ago), the climate got cooler and glacial-interglacial cycles appeared in the Northern Hemisphere. This is also well recorded in the pollen spectra. For instance, *Artemisia* steppe became important during the glacial periods (DSDP Site 380). At the interglacial periods, forest formations developed. Nevertheless, during glacial periods, the Sea of Marmara was isolated from the Mediterranean and became a brackish water environment and reconnected during the Quaternary interglacials including the Early Holocene (Stanley and Blampied, 1980; Smith *et al.*, 1995; Aksu *et al.*, 1999; Çağatay *et al.*, 2009).

3. METHOD

Palynology is the science of the present and fossil palynomorphs such as pollen, spores, dinoflagellate cysts and acritarchs. Because of the strong wall (exine) of the pollen grains, they can be well-preserved for a long time in the sediments. Pollen provide a high resolution and continuous record of climate. Palynology is especially a very good tool for assessing paleovegetation and paleoclimate history. In addition, palynological studies are used for biodiversity, biostratigraphy and characterisation of the past environmental changes.

Samples used in this study are located in the western Black Sea (DSDP Site 380), NW Turkey (İntepe, Burhanlı, Eceabat, West Seddülbahir, Enez) and Northern Greece (Prosilio, Trilophos, Lion of Amphipoli) and Western Macedonia (Ptolemais Notio and Ptolemais Base) (Fig. 1.2). Pollen grains are generally well preserved in the sediments. In this study, a total of 436 samples have been analysed (Table 3.1). 378 of these samples (Late Miocene-recent) are from the Black Sea DSDP borehole and the remaining 58 samples come from outcrops (Late Miocene-Early Pliocene).

The four samples (374.5, 376, 413 and 593 m) from Black Sea core, three samples (samples 1, 2 and 3) from Trilophos, three samples (samples 1, 3, 4, and 5) from Eceabat, five samples (samples 1, 2, 4, 5 and 6) from Burhanlı, two samples (samples 1 and 2) from Ptolemais Notio are barren (containing no or very low number of pollen grains).

The high-resolution long-term pollen record of DSDP Site 380 completely covers the last 7 million years. The top 0-308.46 m was analysed by S. Boroi, and the lower part 704.34-1019.85 m by S.-M. Popescu. In this thesis, the studied interval of the DSDP borehole covers the interval between 319.030 and 702.4 meters the middle part of the hole.

Table 3.1: Study locations and number of samples.

Studied locations	Number of analysed samples
DSDP 380 borehole	378
Enez	8
İntepe	8
Eceabat	5
Burhanlı	6
Seddülbahir	2
Prosilio	6
Ptolemais (Notio and Base)	16
Trilophos	5
Lion of Amphipoli	2
	Total: 436 samples

3.1 Sampling and Chemical Processing

Sampling intervals were taken differently. In DSDP 380 Site, samples were taken approximately at 0.5 m intervals. The outcrop samples have a one meter intervals. The sampling were done always with maximum precaution to avoid the contamination of samples. For the chemical treatment ca. 20 grams sediment was used. The samples were processed using the classical method of Cour (Cour, 1974).

The analysis was processed as indicated below:

1. Weighted ca. 20 grams sediment (depending on the sort of sediment),
2. Remove carbonate content of sediment using HCl acid (35%) for 12 hours,
3. Add water twice,
4. Eliminate silicates in the sediment using HF acid (70%) for 24 hours,
5. Add water twice,
6. $ZnCl_2$ (density>2) is used to separate palynomorphs in the sediments, and then samples are centrifuged at 1000 r.p.m. for 10 minutes,
7. Add HCl acid (35%) to dissolve minerals which are left during $ZnCl_2$ reaction,

8. Centrifuge at 2500 r. p. m. for 5 minutes,
9. Wash deposited samples 2 times to eliminate ZnCl₂ and HCl acid at 2500 r. p. m. for 10 minutes,
10. Sieve the remaining residue using 10 µm nylon sieve,
11. Centrifuge again to remove remaining water at 2000 r. p. m. for 10 minutes,
12. Add glycerol. The glycerol is added as much as final residue,
13. Calculate the volume of residue sediment with glycerol,
14. Mount samples on slide by placing the residue 50 µl, adding glycerol, covering it with the thin slide cover and sticking it with glue (histolaque).

3.2 Identification of Pollen Grains

The analysis on the microscope has been performed using two light-transmitted microscopes (alternately in İstanbul and Lyon), Zeiss and Leica with different oil-immersion objectives (x25, x40 and x100). The analysis consisted in identifying and counting pollen grains along several lines. Spores were not considered due to their poor presence in the sediments. The identification was done from end to end parallel to the longest edge of the slide. So, the same pollen grain could never be encountered twice in this way.

The pollen grains were counted until a minimum of 150 pollen grains excluding *Pinus*. Because *Pinus* is generally overrepresented owing to their prolific production and having ability of transportation in air and water. The botanical identification is made by the study of morphological characters of pollen grains, which are compared with the living relatives. Pollen identification benefited from many pollen photographs, atlases, and also Photopal website (<http://medias.obs-mip.fr/photopal>). All pollen data are available on the web from the “Cenozoic Pollen and Climatic values” database (CPC) (<http://cpc.mediasfrance.org>).



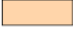









In this study, 107 different taxa were identified. During the analysis, several pollen species were photographed (in Figs. 3.1 and 3.2). However, some pollen grains could not be identified because of their poor preservation, and so they were defined as indeterminate in the pollen diagrams. All identified taxa and species are shown in Table 3.2. Complete pollen data are presented in the form of synthetic pollen diagrams (Suc, 1984) and detailed pollen diagrams. In this kind of detailed pollen diagrams, taxa are individually indicated with their percentage.

Table 3.2: Taxa identified in the study.

Megathermic trees	Mesoathermic trees		Herbs		Steppe
<i>Avicennia alba</i> Euphorbiaceae Rubiaceae Rutaceae	deciduous <i>Quercus</i> <i>Corylus</i> <i>Betula</i> <i>Alnus</i>	<i>Salix</i> <i>Tamarix</i> <i>Fraxinus</i> <i>Ilex</i>	Poaceae Caryophyllaceae Amaranthaceae-Chenopodiaceae Asteraceae Asteroideae Asteraceae Cichorioideae	Plumbaginaceae <i>Centaurea</i> Mercurialis Alismataceae <i>Scabiosa</i> <i>Viola</i> Saxifragaceae <i>Euphorbia</i> <i>Thalictrum</i> Solanaceae <i>Cannabis</i> Urticaceae <i>Clematis</i> Linaceae Campanulaceae Boraginaceae Oenotheraceae <i>Cistus</i> <i>Galium</i> <i>Knautia</i>	<i>Artemisia</i> <i>Ephedra</i> <i>Hippophae rhamnoides</i>
Mega-mesoathermic trees	<i>Carpinus orientalis</i> <i>Juglans</i> <i>Populus</i> <i>Juglans cf. cathayensis</i> <i>Rhus</i> <i>Fagus</i> <i>Pterocarya</i> <i>Ulmus</i> <i>Buxus sempervirens</i> <i>Liquidambar orientalis</i> <i>Carpinus betulus</i> <i>Platanus</i> <i>Hedera</i>	<i>Tilia</i> <i>Celtis</i> <i>Eucommia</i> <i>Lonicera</i>	<i>Plantago</i> Liliaceae <i>Geranium</i> <i>Sparganium</i> Ericaceae Cyperaceae <i>Potamogeton</i> Lamiaceae Thymillaceae <i>Typha</i> Brassicaceae Fabaceae <i>Rumex</i> <i>Polygonum</i> Apiaceae <i>Myriophyllum</i> <i>Convolvulus</i> <i>Erodium</i> Papavareceae		Mediterranean xerophytes
Taxodiaceae <i>Engelhardia</i> <i>Taxodium</i> type Platycarya Sapotaceae <i>Distylium</i> <i>Microtropis fallax</i> <i>Ginkgo</i> <i>Loropetalum</i> Arecaceae	<i>Nyssa</i> <i>Carya</i> Oleaceae <i>Vitis</i> <i>Castanea</i> type <i>Acer</i> <i>Zelkova</i>				<i>Quercus ilex</i> type <i>Olea</i> <i>Ligustrum</i> Myrtaceae <i>Phillyrea</i>
Microathermic trees					Non-significant
<i>Abies</i> <i>Picea</i>					Ranunculaceae Rosaceae
Meso-microathermic trees					Cathaya
<i>Cedrus</i> <i>Tsuga</i>					Pinus
					Cupressaceae

In synthetic pollen diagrams, different taxa are grouped into 12 different groups according to the ecological significance of their living relatives (Table 3.3). Thus, such diagrams allow comparison with the other pollen records obtained from the other localities, such as the European and Mediterranean regions.

Table 3.3: Groups used in synthetic pollen diagrams according to classification of Nix (1982).

Legend	Groups used in synthetic pollen diagrams
	Megathermic elements (Tropical trees)
	Mega-mesothermic elements (Subtropical trees)
	<i>Cathaya</i>
	Mesothermic elements (Warm-temperate trees)
	<i>Pinus</i>
	Meso-microthermic elements (Mid-altitude trees)
	Microthermic elements (High-altitude trees)
	Non-significant elements
	Cupressaceae
	Mediterranean xerophytes
	Herbs
	Steppe elements

Moreover, they are also convenient for comparison with oxygen isotope curves in order to contribute to reconstruction of paleoclimate evolution. The groups used in the synthetic diagrams are from left to right:

- Megathermic (tropical) elements: *Avicennia alba*, a mangrove tree; Euphorbiaceae, Rubiaceae, Rutaceae, Arecaceae, etc.;
- Mega-mesothermic (subtropical) elements: mainly Taxodiaceae (including *Taxodium* type and *Glyptostrobus*), *Engelhardia*, Sapotaceae, *Microtropis fallax*, *Distylium*;
- *Cathaya*, a conifer living today at mid-altitude in subtropical China;

- Mesothermic (warm-temperate) elements: deciduous *Quercus*, *Carya*, *Pterocarya*, *Carpinus orientalis*, *Juglans*, *Juglans* cf. *cathayensis*, *Celtis*, *Zelkova*, *Ulmus*, *Tilia*, *Acer*, *Liquidambar* cf. *orientalis*, *Alnus*, *Salix*, *Populus*, *Fraxinus*, *Buxus sempervirens* type, *Betula*, *Fagus*, *Hedera*, *Lonicera*, *Ilex*, *Tilia*, etc.;
- *Pinus*;
- Meso-microthermic (mid-altitude) elements: *Cedrus* and *Tsuga*;
- Microthermic (high-altitude) trees: *Abies* and *Picea*;
- Non-significant elements: some cosmopolitan or widely distributed elements such as Rosaceae and Ranunculaceae;
- Cupressaceae;
- Mediterranean xerophytes: *Quercus ilex* type, *Olea*, *Phillyrea*, *Ligustrum*, etc.;
- Herbs: Poaceae, Amaranthaceae-Chenopodiaceae, Asteraceae Asteroideae, Asteraceae Cichorioideae, *Geranium*, *Convolvulus*, *Erodium*, Lamiaceae, *Plantago*, *Euphorbia*, Brassicaceae, Apiaceae, *Rumex*, *Polygonum*, Cyperaceae, Campanulaceae, Ericaceae, Solanaceae, etc.; some halophytes such as Caryophyllaceae, Plumbaginaceae are included within the herbs; some herbs contain water plants such as; *Potamogeton*, *Sparganium* and Typhaeae,
- Steppe elements: *Artemisia*, *Ephedra* and *Hippophae rhamnoides*.

PLATE 1

- 1, *Abies* (Ptolemais Base);
- 2-4, *Acer* (Ptolemais Base);
- 5-7, *Galium* (Ptolemais Base);
- 7-11, *Cistus* (Ptolemais Base);
- 12-14, *Fagus* (Ptolemais Base);
- 15-16, Lamiaceae (Ptolemais Base);
- 17-19, *Myrica* (Ptolemais Base);
- 20, *Typha* (Ptolemais Base);
- 21, Rosaceae (Ptolemais Base);
- 22, *Zelkova* (Ptolemais Base);
- 23, *Alnus* (Ptolemais Notio);
- 24, Apiaceae (Ptolemais Notio);
- 25, Asteraceae Asteroideae (Ptolemais Notio);
- 26, *Carya* (Ptolemais Notio);
- 27, Caryophyllaceae (Ptolemais Notio);
- 28, *Engelhardia* (Enez);
- 29, deciduous *Quercus* (Ptolemais Base);

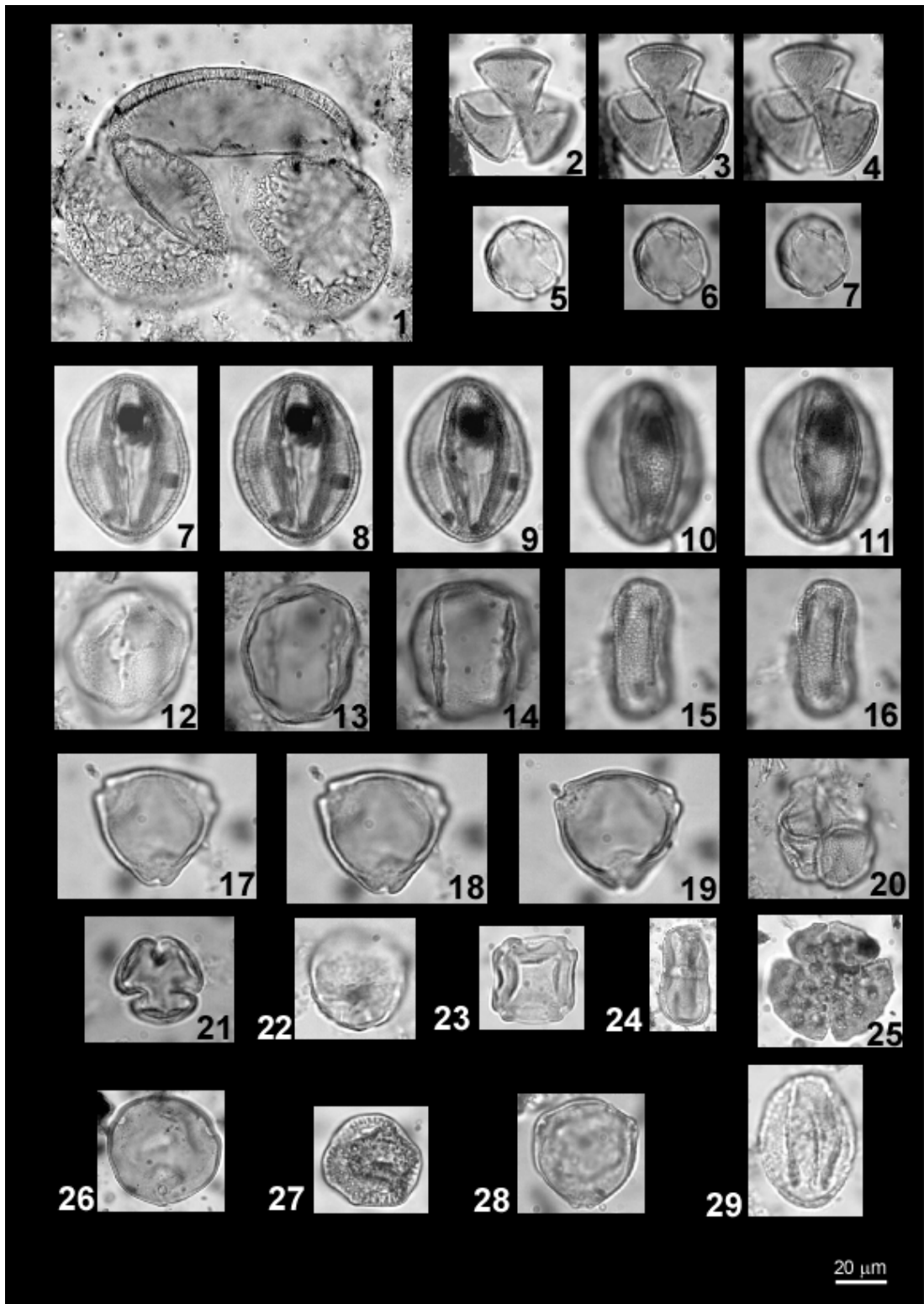


Figure 3.1 : Some pollen photos from the studied regions.

PLATE 2

- 30**, *Cedrus* (Ptolemais Notio);
- 31**, *Tsuga* (Ptolemais Notio);
- 32**, *Lonicera* (Ptolemais Notio);
- 33**, *Avicennia alba* (DSDP Site 380);
- 34**, *Polygonum* (Ptolemais Notio);
- 35**, *Tilia* (Ptolemais Notio);
- 36**, *Pterocarya* (Ptolemais Base);
- 37**, *Carpinus orientalis* (Enez);
- 38**, Amaranthaceae-Chenopodiaceae (Enez);
- 39**, Taxodiaceae: probably *Glyptostrobus* (DSDP Site 380);
- 40**, *Sparganium* (Enez);
- 41**, *Artemisia* (DSDP Site 380);
- 42**, *Corylus* (Trilophos);
- 43**, Poaceae (DSDP Site 380);
- 44**, Asteraceae Cichorioideae (Ptolemais Notio).

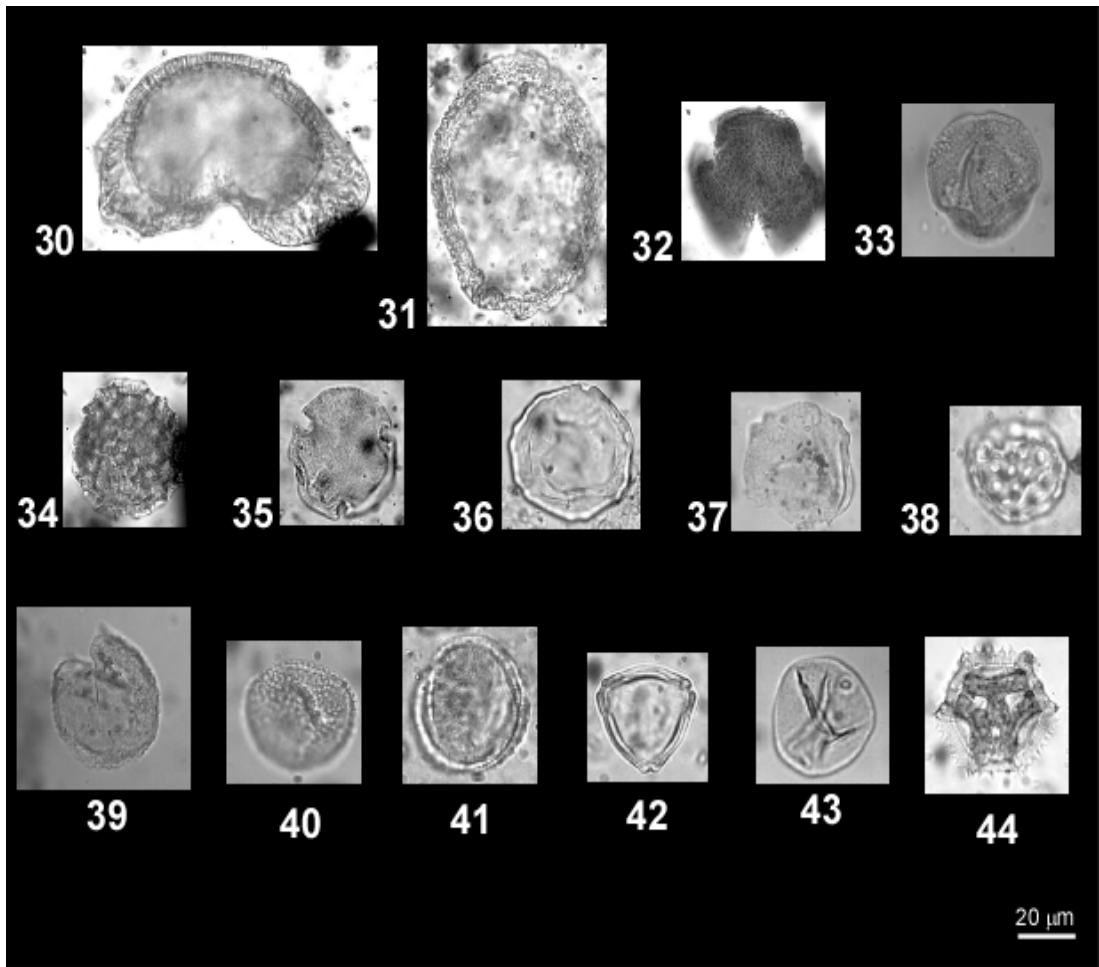


Figure 3.2 : Continued.

4. CHRONOLOGY OF THE STUDIED SECTIONS

A total of 10 sections and 436 samples have been studied for pollen analysis (in Table 1). The chronology of studied sections are mainly supported by calcareous nanoplankton data and other biostratigraphic data (Table 4.1). The chronostratigraphy of the studied locations are given in Figure 4.1. In the DSDP Black Sea core, firstly, seventeen samples were selected corresponding to warm phases in the pollen diagram for nanofossils. These depths are 219, 223.02, 326.14, 334.50, 368.43, 461.53, 471.50, 476.46, 504.35, 509.35, 518, 548.50, 586.49, 682.95, 708.20, 748.45, and 840.07 mbsf. The eight of the seventeen samples yielded nanofossils. The corresponding depths are 219, 223.02, 326.14, 368.43, 476.46, 504.35, 748.45, and 840.07 mbsf. These chronological limitations are assigned in the sediments using ages of the lowest occurrence (LO), highest occurrence (HO), lower consistent occurrence (LCO) and highest consistent occurrence (HCO) of the species as determined by Raffi *et al.* (2006):

- at 840.07 m depth, *Triquetrorhabdulus rugosus* and *Ceratolithus acutus* are observed. The age is between 5.345 Ma (*C. acutus* LO) and 5.279 Ma (*T. rugosus* HO) (early Zanclean);
- at 748.45 m depth, *Reticulofenestra pseudoumbilicus* displays an age older than 3.839-3.79 Ma (*R. pseudoumbilicus* HO) (late Zanclean);
- at 476.46 m and 504.35 m depth, *Discoaster brouweri* displays an age older than 2.06 – 1.926 Ma (*D. brouweri* HO) (late Gelasian);,
- at 368.43 m depth, medium-sized *Gephyrocapsa* shows an age younger than 1.73 – 1.67 Ma (medium-sized *Gephyrocapsa* spp. LO) (Calabrian),
- at 326.14 m depth, *Helicosphaera sellii* exhibits an age older than 1.34-1.256 Ma (*H. sellii* HO) (Calabrian).
- at depths 223.02 and 219 m, the presence of *Reticulofenestra asanoi* displays that these samples are between 1.136 Ma (*R. asanoi* LCO) and 0.901 Ma (*R. asanoi* HCO) (Calabrian).

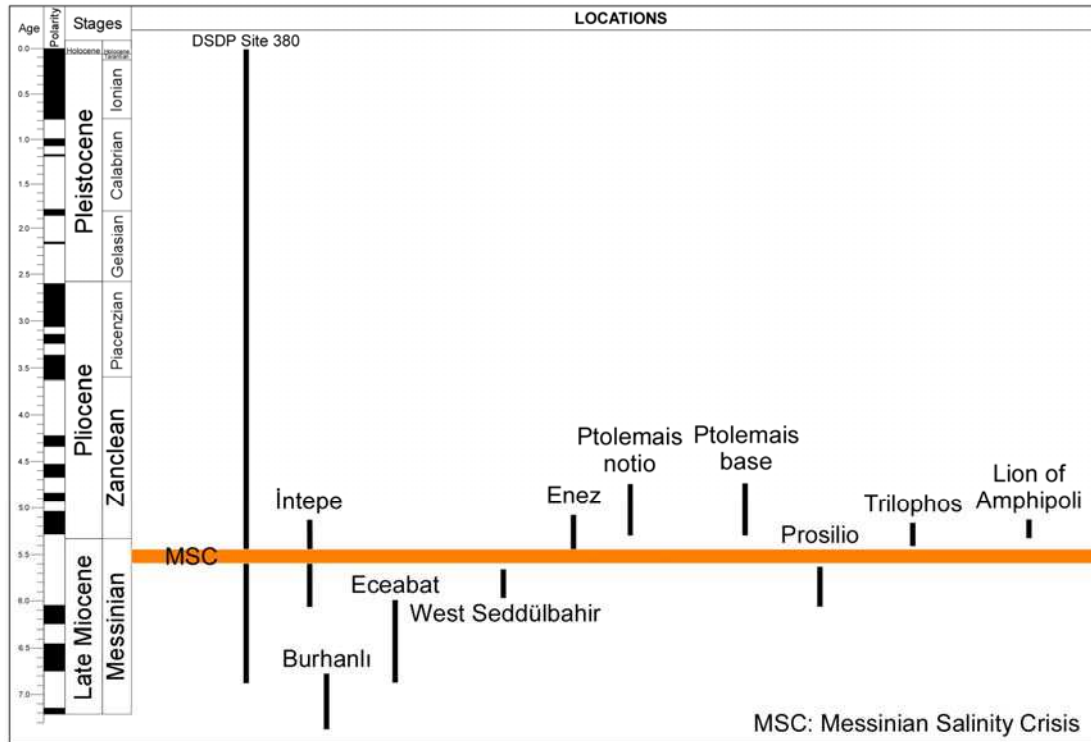


Figure 4.1 : The chronostratigraphic position of the studied sections from the Late Miocene to the Early Pleistocene.

Samples from the studied sections in the Gulf of Saros (Enez) and Dardanelles regions (İntepe, west Seddülbahir, Burhanlı, Eceabat) were analysed for nannoplankton. The Enez section contain poor to moderate nannoflora in 7 samples. They indicate the co-occurrence of *Triquetrorhabdulus rugosus* and *Ceratolithus acutus*. They represents NN12b nannofossil subzone indicating the extreme end of Messinian (after the MSC) to earliest Zanclean (Melinte *et al.*, 2009). The studied sections in the Dardanelles are correspond with the Messinian erosional surface (Melinte *et al.*, 2009).

The nannoflora content of Eceabat indicates poor to moderate preservation and few reworked specimens. They contain *Amaurolithus primus*, *Reticulofenestra pseudoumbilicus*, *R. Rotaria* (samples 1, 2, 4, 5), *Nicklithus amplificus* (samples 1 and 3) and *Triquetrorhabdulus rugosus*. This nannoflora indicates NN11c nannofossil subzone. It belongs to an early Messinian age (Melinte *et al.*, 2009). The nannofloral community of west Seddülbahir includes *Triquetrorhabdulus rugosus*, *Reticulofenestra pseudoumbilicus*, *Ceratolithus acutus*.

Table 4.1: Age control of the study areas.

Study Location	Country	Age determination	Age	Pollen Analysis
DSDP Site 380	Turkey, near the Bosphorus	Melinte, M. C. (personal information)	Pliocene-Lower Pleistocene	S. Boroi, D. Biltekin, S.-M. Popescu
İntepe	Turkey	Melinte et al., 2009	Early-Late Messinian-Early Pliocene	J.-P. Suc, D. Biltekin
Eceabat	Turkey	Melinte et al., 2009	Early Messinian	D. Biltekin
Burhanlı	Turkey	Melinte et al., 2009	Latest Tortonian-Early Messinian	D. Biltekin
West Seddülbahir	Turkey	Melinte et al., 2009	Latest Messinian-Earliest Zanclean	J.-P. Suc
Enez	Turkey	Melinte et al., 2009	Messinian (after MSC)-Earliest Zanclean	D. Biltekin
Ptolemais Notio and Ptolemais Base	Macedonia	van Vugt et al., 1998, Steenbrink et al., 1999	Early Pliocene	D. Biltekin
Prosilio	Greece	Steenbrink et al., 2000,2006	Late Miocene	D. Biltekin
Lion of Amphipoli	Greece	Melinte, M. C. (personal information)	Early Zanclean	J.-P. Suc
Trilophos	Greece	Melinte, M. C. (personal information)	Latest Messinian-Earliest Zanclean	D. Biltekin

The age of this section is from NN12a to NN12b subzones, from the latest Messinian to the earliest Zanclean (Melinte *et al.*, 2009). In the Burhanlı section, nannoflora community; *Reticulofenestra pseudoumbilicus*, *Reticulofenestra rotaria*, *Triquetrorhabdulus rugosus* and *Nicklithus amplificus* were recorded in the samples. According to this nannoflora assemblages, age of section is the latest Tortonian to early Messinian (upper part : NN11b subzone; lower part: NN 11c subzone). In the İntepe section (samples from 18 to 24), the nannofossil content of sediments are *Amaurolithus primus*, *Reticulofenestra rotaria* (samples 14-18), *Nicklithus amplificus* (samples 1-7), *Triquetrorhabdulus rugosus* (samples 1-31) and *Ceratolithus acutus* corresponding to NN11c and maybe NN12a subzone.

The age of samples from Western Macedonia and Northern Greece (Ptolemais Notio and Base, Prosilio, Trilophos and Lion of Amphipoli) were also determined. The age of the Ptolemais Formation is based on paleontological data (small mammals) and magneto- and cyclostratigraphy and $^{40}\text{Ar}/^{39}\text{Ar}$ dating, according to which it is the Early Pliocene (MN 14 and 15) (van de Weerd, 1979; van Vugt *et al.*, 1998; Steenbrink *et al.*, 1999). In Trilophos and Lion of Amphipoli, datation is based on nannofossils. According to this, Lion of Amphipoli is in the Early Zanclean age (Melinte, M.C., personal correspondence). The nannoflora of Trilophos was analysed in five samples.

Only two samples (samples 4 and 5) have nannoplankton content. The nannoplankton assemblages in Trilophos contain *Triquetrorhabdulus rugosus*, *Reticulofenestra pseudoumbilicus*, *Ceratolithus acutus*, which belongs to NN12 a, b subzones (the latest Messinian to the earliest Zanclean) (Melinte, M.C., personal correspondence). The indirect age determination for Prosilio section is based on correlation of thick green clay bed with abundant fish teeth and vertebrate.

This bed has been found in the 5 km easterly Lava quarry dated as 6.57 Ma years (Steenbrink *et al.*, 2000). The correlation of polarity sequence in Prosilio section (Late Miocene) with geomagnetic polarity time scale gives the lower normal polarity; subchron C3An.2n, middle normal interval with C3An.1n and the upper interval with Thvera (Steenbrink *et al.*, 2006).

5. RESULTS

5.1 DSDP Site 380

The Black Sea borehole was taken from near the Bosphorus on the basin apron in a water depth of 2107 meters (southwestern Black Sea). The length of the core is 1073.5 meters (42°05.94'N and 29°36.82'E). In this thesis, 319.03 to 702.4 mbsf interval was studied which correspond to Units (Unit 2 and Unit 4(4a) in Figure 5.1.

5.1.1 Lithology

The sedimentary sequence of the core is divided into five main units and 13 subunits (Fig. 5.1) (Ross, 1978). These units and subunits are described below:

UNIT 1 (0-332.5 m)

In this unit includes mainly terrigenous sediments. The sediments are silty clay, sandy silts, and rare sands as thin laminae. The silts, sands and muds comprise feldspars, quartz, clay minerals, detrital carbonates, pyrite, organic matter, heavy minerals and diatoms. The clay minerals consist mainly of illite and smectite, with smaller amounts of kaolinite and chlorite. In addition, detrital carbonates exist in a small amounts. Unit 1 contains sediments which were deposited during the marine incursions and the intervening lacustrine periods. This unit is subdivided into five subunits, the first two of which were not recovered by the DSDP coring:

Subunit 1a:

This subunit is generally represented by a 30 cm-thick laminated in Black Sea cores. In general, this subsunit is a typical sediment of the present Black Seadeposited in the last 3000 a. It consists of nannofossil (coccolithophore) ooze (Ross and Degens, 1974).

Subunit 1b (0-2 m):

The Subunit 1b is a dark gray sapropel and rich in organic matter and diatoms. Its age spans from 8 ka to 3 ka.

Subunit 1c (2-42 m):

The subunit 1c includes muds and sandy silts. This subunit is the one of the sandy intervals at this hole. Silty sands compose of micas, detrital carbonates, quartz, feldspars, heavy minerals, clays, opaque minerals and shell components. The terrigenous sediments are micaceous.

These sediments were deposited under lacustrine, fresh to brackish water environment. This is supported by the presence of fresh-water diatoms, such as; *Stephanodiscus* and *Melosira*.

Subunit 1d (45-76 m):

This subunit constitutes chiefly diatomaceous muds. During the deposition of this unit, marine influence was dominant. Diatoms are generally marine. However, The scarcity of foraminifers and nannofossil communities show that the environment was not under fully marine conditions. The presence of *Gephyrocapsa sp.* indicates that salinity of Black Sea was more than 18‰ (Percival, 1978 and Bukry, 1973). This subunit is the first brackish-marine sequence below the Holocene (Marine Isotope Stage 5e).

Subunit 1e (76-142.5 m):

This subunit includes terrigenous sediments. The silts and muds consist of quartz, feldspars, clay minerals and detrital carbonates. The one interval contains diatoms of some brackish-water species.

Subunit 1f (142.4-171 m):

The sediments of this subunits are greenish gray to dark greenish gray. The Diatoms are abundant. Thin sandy silts layers are common. They are in terms of quartz and feldspar. The content of diatom species indicate brackish-marine condition.

Subunit 1g (171-266 m):

Subunit 1g chiefly contains muds. The thin silt and clay intervals are common. One interval is diatomaceous with fresh-water species. The lithology of this subunit is alike subunits 1c and 1e.

Subunit 1h (266-332.5 m):

This subunit includes muds and turbidite intervals. It includes two diatom-rich levels, containing fresh-water species in 294.5-304 m. This subunit also contains *Ammonia beccarii*, that is abundant at the bottommost part of this subunit. Thus, this indicates that this subunit were deposited in a brackish-marine environment.

UNIT 2 (332.5-446.5 m)

The Unit 2 is represented by several interbedded of carbonate-rich layers. The upper part of the unit includes aragonitic sediments. The bottom part of the unit contains the lowest occurrence of siderite-rich sediments. Siderite-rich marls are observed in thin layers or laminae. In addition, calcareous oozes are present in calcite.

The other sediment is aragonite. Also the carbonates, sapropelic and diatomaceous muds, laminated and varve-like clays and sandy silts are observed. The dominant lithology of this unit usually is mud. It consists of quartz, feldspars, clay minerals and a little amount of detrital carbonates.

The color varies from greenish gray to olive gray or to dark greenish gray. The darker sediments are rich in terms of pyrite. However, the olive/light olive gray sediments include diatoms and carbonates. The chemical sediments contain aragonite, siderite and calcite. Siderite mostly is in marls. The siderite-rich layers are light olive gray in color and from a few to numerous centimeters thickness.

Calcite-rich marls and oozes or seekride are also represented in the core. The upper section of this unit was deposited under marine-brackish conditions. The presence of the *Braarudosphaera* flora indicates that Black Sea was effected by strong marine influence, the salinity may have reached 22‰ (Percival, 1978 and Bukry, 1973). The oldest sediments of this unit may have been formed in a fresh or brackish lake.

UNIT 3 (446.5-644.5 m)

This unit is featured by the existence of seekreide. The dominant content of this unit are muds, marls and seekreide. The upper section of the unit still includes siderite. The bottom part of this unit is placed just above the diatomaceous ooze. Also this unit consists of an ostracode fauna such as; *Candona-Loxoconcha* assemblages that show the deposition in fresh-water lakes (Benson, 1978 and Olteanu, 1978).

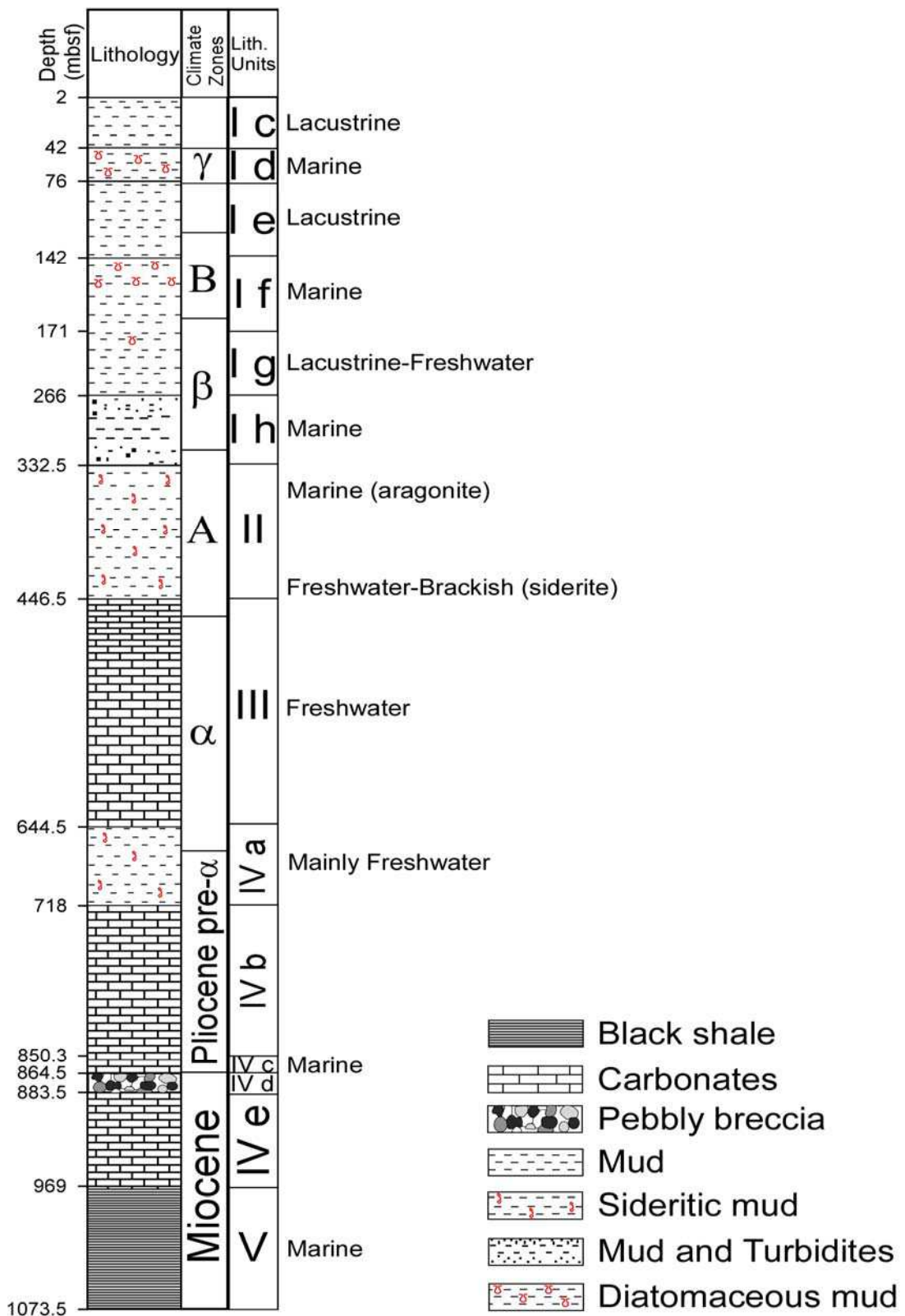


Figure 5.1 : Lithology of DSDP 380 Site Black Sea core (Ross, 1978). Climate zones in the diagram: γ (Glacial), B (Interglacial), β (Glacial), A (Interglacial), α (Glacial). Studied intervals cover 319.03 to 702.4.

UNIT 4 (644.6-969 m)

This unit contains the various sediment types including also chemical sediments. The upper part of the unit includes siderite layer in 664.6 meters. The bottom of the unit is transitional to an underlying black shale. In this unit, diatoms and carbonate-rich sediments are also present. Besides, it is noteworthy to mark the presence of pebbly mudstones and breccias. This unit is divided into five subunits:

Subunit 4a (644.6-718 m):

This subunit is represented by the existence of several manganosiderite intercalations in diatomaceous clay. In the upper and the bottom levels are characterized by the siderite layers. The main lithology of this subunit are mud, diatomaceous clay and the terrigenous sediments. In the upper section, clays are usually structureless. However, at the lower part, they have some distinct laminations. The structureless clay levels contain chiefly clay minerals and numerous amounts of diatoms.

The main clay mineral is smectite with illite, and a small amount of kaolinite and chlorite. The laminated layers contain diatom-rich and clay-rich lamina. At the same time, siderite is common in this subunit. The siderite-rich sediments are pale olive color, thin layers or as nodules. The diatom content of the subunit suggests that depositional environment was possibly from fresh to brackish (Schrader, 1978). Besides, dinoflagellates are present abundantly. These suggest the marine flux period.

Subunit 4b (718-850.3 m):

This subunit constitute seekreide. Diatomaceous clays and marls are also presented. The upper boundary this subunit is represented by the base of the siderite. The main sediments in this subunit are clays, calcite (chemical) and diatoms. The seekreide varves contain calcite-rich light greenish gray and clay-rich dark greenish gray lamina. The diatomite varves comprise light olive green calcite-bearing diatomaceous marl and darker olive green diatomaceous clay. At the base, dinoflagellates and acritarchs are common. The toward to upper part, they are presented as a less amount.

Subunit 4c (850.3-864.5 m):

This subunit is defined by the existence of aragonite and magnesian calcite. The main lithology of the subunit is diatomaceous shales in olive-black color. The sediments in this subunit were formed under brackish-marine condition.

The abundance of *Braarudosphaera* flora shows that the salinity may have reached 22‰ (Percival, 1978 and Bukry, 1973). The existence of *Bolivina* indicates stenohaline conditions (Gheorghian, 1978). Dinoflagellates and acritarchs are common that indicate marine influence.

Subunit 4d (864.5-883.5 m):

The subunit is characterized by pebbly mudstones, stromatolitic dolomites and conglomerates. The dolomite was deposited such in an intertidal to supratidal environment (Stoffers, 1978). The sea level in the Black Sea was possibly very shallow. This is also supported by shallow habitat diatoms (Schrader, 1978). The major lithology is conglomerate, slump breccia or pebbly mudstone.

Subunit 4e (838.5-969 m):

This subunit contains dolomite which is in the form of laminated seekreide and marls. The upper part of this subunit is above the base of the pebbly mudstone. The main lithology is calcareous mud or marl. It has dark greenish color. Interbedded in the marl sequence are calcitic, aragonitic and dolomitic sediments. These chemical sediments form in three distinct sediments content: laminated marl, carbonate varves and dolomite.

UNIT 5 (969-1073.5 m)

This unit is characterized by the presence of black shales with zeolitic sandstones and dolomite. The black shales are in greenish black and fissile. They contain clays, organic matter, quartz, feldspars and pyrite. The content of small benthic foraminifers in the sequence indicate that the black shales were deposited in a brackish-marine environment.

5.1.2 High-resolution pollen record of DSDP 380

In DSDP Site 380 Black Sea hole, studied interval is from 319,03 m to 702,40 m below sea floor (mbsf) corresponding to the Early Pliocene-Early Pleistocene. High-resolution pollen analysis of the core provides significant data for paleovegetation and paleoclimate during the Early Pliocene to Early Pleistocene (from Zanclean to Gelasian). The vegetation is characterized by different plants groups. Most of them are inherited from the Miocene. Along the study intervals, the flora is dominated by mostly two vegetation types (Fig. 5.3). They are thermophilous plants and herbs characterizing steppe. Thermophilous vegetation is characterized by megathermic (tropical), mega-mesothermic (subtropical) and mesothermic (warm-temperate) elements.

Megathermic elements are Euphorbiaceae, Rubiaceae, Arecaceae, Rutaceae and *Avicennia alba*. However, they are in small amount in the studied intervals. Mega-mesothermic elements are characterized by Taxodiaceae (chiefly *Glyptostrobus*), *Taxodium* type, *Engelhardia*, *Platycarya* and Sapotaceae. Among them, particularly Taxodiaceae swamp forests show high abundances. Percentage of Taxodiaceae reaches up around 80% (Figs. 5.2-5.3). Mesothermic elements contain deciduous *Quercus*, *Betula*, *Corylus*, *Juglans*, *Pterocarya*, *Buxus sempervirens*, *Liquidambar orientalis*, *Nyssa*, *Acer*, *Castanea*, etc.

These evergreen and deciduous mixed forest include a riparian vegetation composed of *Salix*, *Alnus*, *Carpinus orientalis*, *Zelkova*, *Carya*, *Ulmus*, etc. The mesothermic plants are presented frequently along studied intervals. *Quercus* reaches up 10% in some levels and *Zelkova* reaches up 11%. Herbs are involved by mainly Amaranthaceae-Chenopodiaceae, Poaceae, Asteraceae Astroideae, Asteraceae Cichorioideae, Brassicaceae, Caryophyllaceae, Lamiaceae, *Rumex*, Apiaceae, *Centaurea*, etc. At the same time, herbs include some fresh-water plants such as; *Sparganium*, *Potamogeton*, *Typha*, *Myriophyllum*. Among herbs, Amaranthaceae-Chenopodiaceae has higher amount. Its percentage approaches 88%. Steppe elements comprise mainly *Artemisia*, *Ephedra* and *Hippophae rhamnoides*. *Artemisia* is represented abundantly with a percentage of around 84% (Figs. 5.2-5.3). The rest of steppe elements (*Ephedra* and *Hippophae rhamnoides*) do not vary significantly.

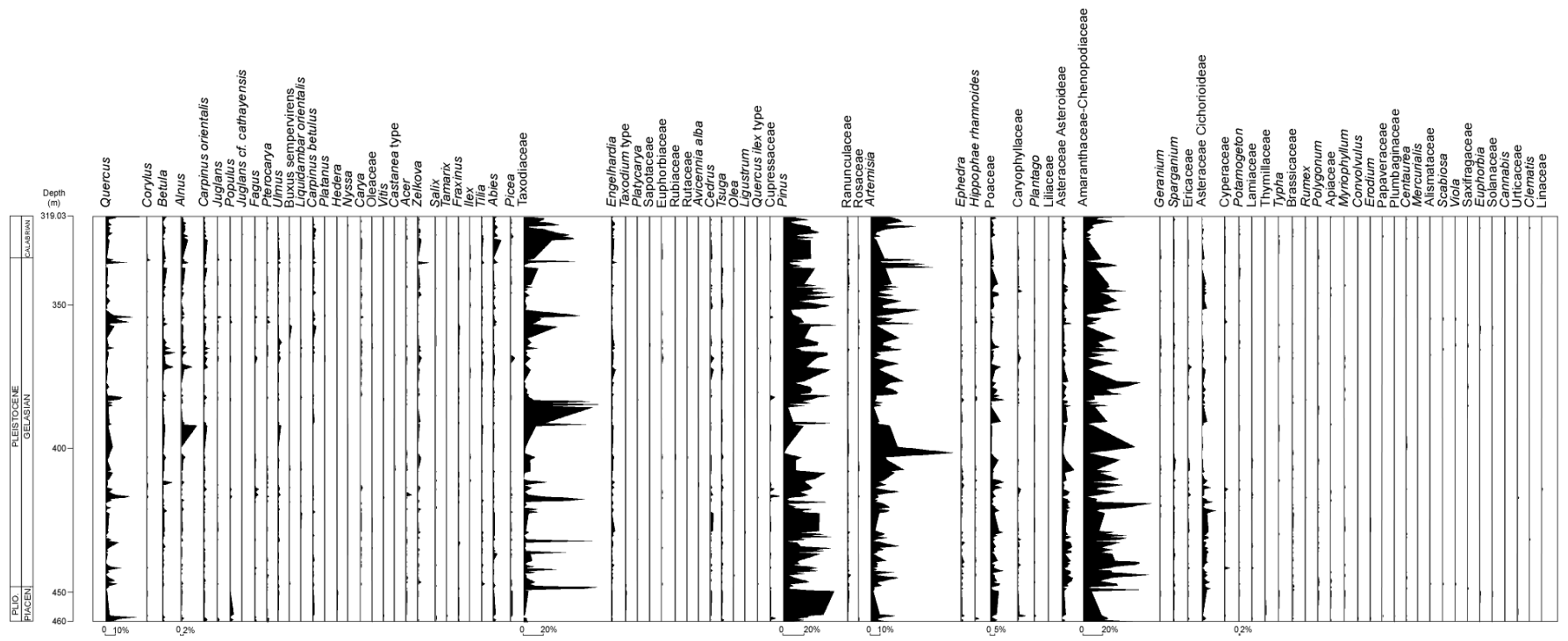


Figure 5.2 : Detailed pollen diagram of DSDP Site 380 between 319.03-460 m.

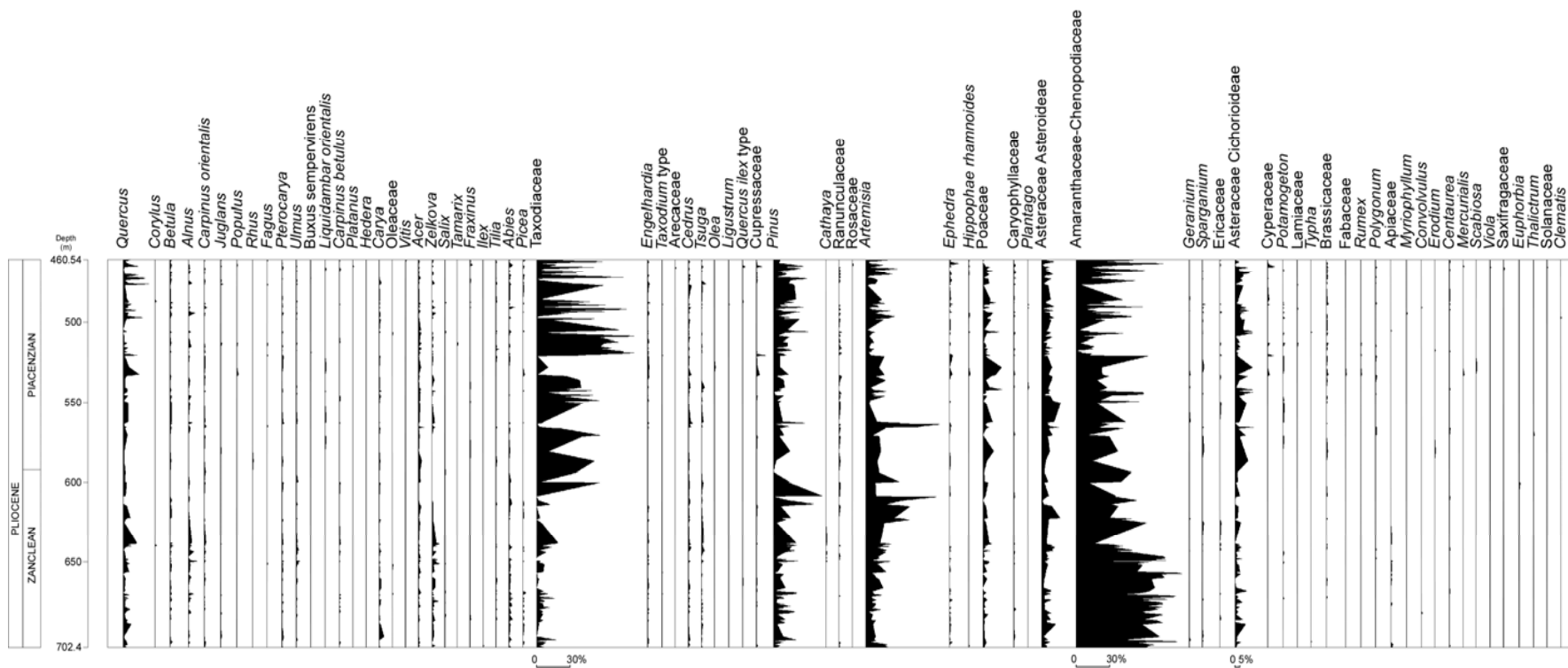


Figure 5.3 : Detailed pollen diagram of DSDP Site 380 between 460.54-702.4 m.

In addition, altitudinal coniferous trees such as; microthermic elements (*Abies* and *Picea*) and meso-microthermic elements (*Cedrus* and *Tsuga*) appear in a small number. Also, *Cathaya* has a less amount. *Cathaya* is a gymnosperm, living today in the subtropical mid-altitude forest of southern China.

Pollen groups in the synthetic pollen diagram are: 1; Megathermic elements (*Avicennia alba*, Rutaceae, Arecaceae, Rubiaceae), 2; Mega-mesothermic elements (Taxodiaceae, *Engelhardia*, *Taxodium* type, *Platycarya*, Sapotaceae), 3; *Cathaya*, 4; Mesothermic elements (deciduous *Quercus*, *Betula*, *Alnus*, *Carya*, *Pterocarya*, *Zelkova*, *Ulmus*, *Fagus*, etc.), 5; *Pinus*, 6; Meso-microthermic elements (*Cedrus* and *Tsuga*), 7; Microthermic elements (*Abies* and *Picea*), 8; Cupressaceae, 9; Herbs (Amaranthaceae-Chenopodiaceae, Poaceae, Asteraceae Astroideae, Asteraceae Cichorioideae, Brassicaceae, Caryophyllaceae, Lamiaceae, *Rumex*, Apiaceae, *Polygonum*, etc., 10; Steppe elements (*Artemisia*, *Ephedra* and *Hippophae rhamnoides*).

Mediterranean xerophytes and non-significant elements have small amounts. Therefore, they were excluded from the synthetic pollen diagram. *Pinus* is represented abundantly. Its percentage gets at 53%. The pollen record of the core enables the identification of the different vegetation stages with subdivisions. Additionally, these stages are correlated with oxygen isotope curve (with MIS). The stages are described below (Popescu *et al.*, 2010):

Pollen zone 2 (624-702,40 meters): This zone is divided into three subzones (2a, 2b, 2c) (Fig. 5.4). These pollen subzones are defined by Zagwijn, 1960; Zagwijn and Suc, 1984. Pollen zone 2 is characterized by the abundance of herbs (mainly Amaranthaceae-Chenopodiaceae). This show that drier climate conditions existed during this time. On the contrary, thermophilous trees are not very much. Nevertheless, *Artemisia* steppes also have a decrease in this zone. At the top of zone 2, *Artemisia* displays an increase.

Pollen zone 3 (603-624 meters): In this zone, herbs are abundant with *Artemisia*, reaching up 59%. On the other hand, thermophilous plants have a small amounts. This time intervals corresponds the earliest glacials in the Northern Hemisphere. This zone matches Marine Isotope Stages (MIS 104-96).

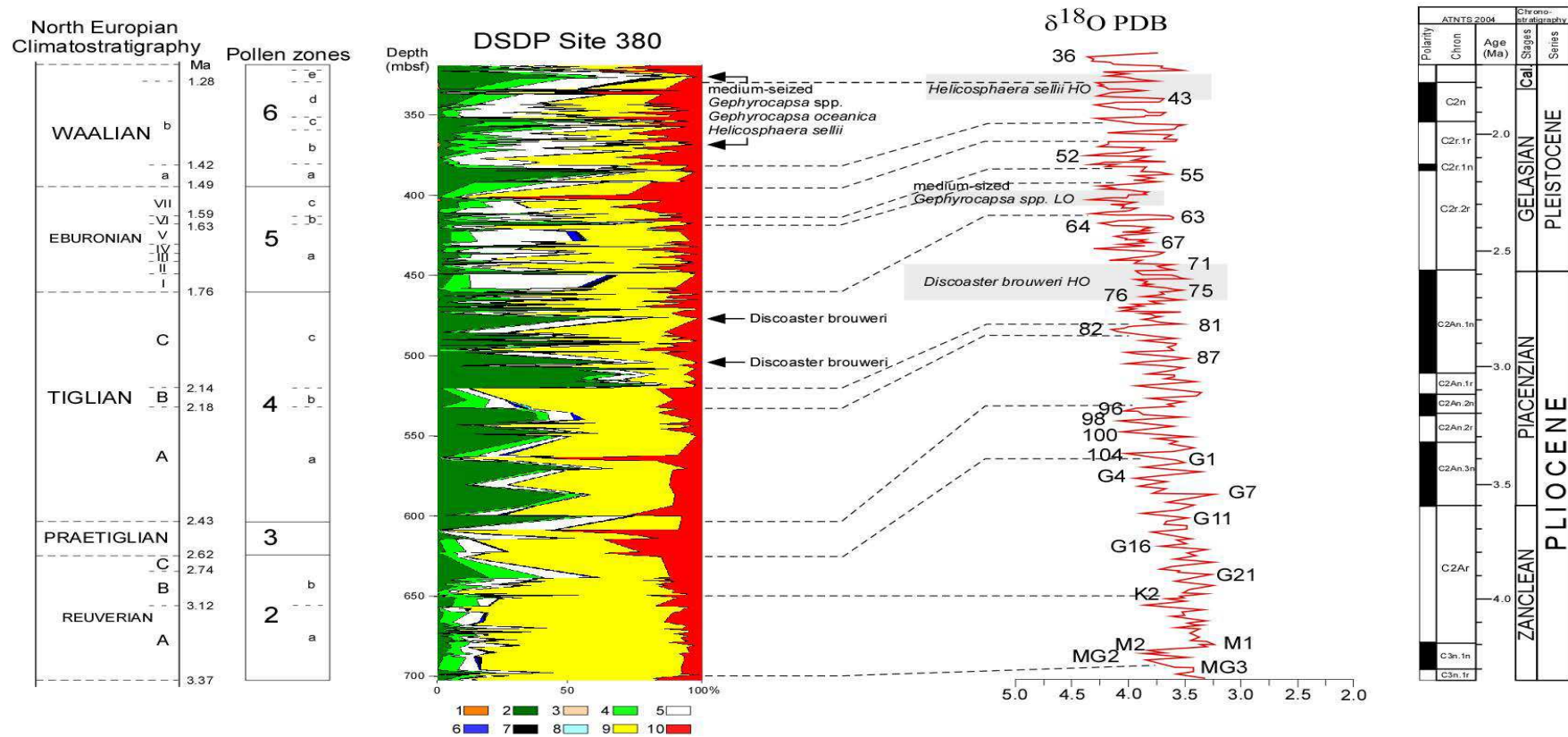


Figure 5.4 : The synthetic pollen diagram of DSDP Site 380 obtained in this study. Pollen groups in the diagram: 1; Megathermic elements, 2; Mega-mesothermic elements, 3; *Cathaya*, 4; Mesothermic elements, 5; *Pinus*, 6; Meso-microthermic elements, 7; Microthermic elements, 8; Cupressaceae, 9; Herbs, 10; Steppe elements (see for explanation in the next page). The synthetic pollen diagram with oxygen isotope curve showing Marine Isotope Stages (Shackleton *et al.*, 1990, 1995), pollen zones, NW European climatostratigraphy (Zagwijn, 1960, 1998) and nannofossil biohorizons (Raffi *et al.*, 2006). Chronostratigraphy, Lourens *et al.* (2004).

Pollen zone 4 (603-461 meters): Pollen zone 4 is divided into three subzones. These are 4a, 4b and 4c. This zone is dominated by chiefly thermophilous forests. Among them, subtropical trees are particularly abundant (probably mainly *Glyptostrobus*). Thermophilous trees are quickly replaced by herbs. In this zone, herb elements are represented abundantly. *Artemisia* is not abundant. Its percentage is around 11% in average. Climate fluctuations shows warmer-moister phases opposed to cooler-drier ones, probably corresponding to glacial-interglacial cycles. This zone corresponds the Tiglian warm period (Zagwijn, 1960; 1963; Zagwijn and Suc, 1984).

Pollen zone 5 (395-461 meters): In this zone, herbs are prominent (mostly Amaranthaceae-Chenopodiaceae). With herbs, *Artemisia* shows higher frequency. Subtropical trees do not change very much. Besides, mesothermic elements have an increase. This zone corresponds to the Eburonian stage (MIS 62-50) (Zagwijn, 1975).

Pollen zone 6 (319,030-392,010 meters): In this zone, Herbs are abundant with *Artemisia* steppes. Nevertheless, mega-mesothermic elements and mesothermic elements are prominent. This zone corresponds Waalian phase. The subdivisions are 6a and 6b in the study intervals.

The other important result is *Avicennia alba* (Mangrove) and some tropical Euphorbiaceae plants. *Avicennia* was observed between 781.63 meters and 1018.85 m in the lower part of the section (Popescu, 2006). In this study, it was observed at 412.53 m. On the other hand, *Avicennia* disappeared from North Mediterranean 14 Ma ago (Serravalian) and from North Africa at 5.3 Ma (Chikhi, 1992; Bachiri Taoufiq *et al.*, 2001).

According to these results, thermophilous plants persisted up till the Early Pleistocene in the region more recently than in the other regions of Mediterranean. Thermophilous plants were well recorded during the Pliocene time and the Pleistocene (Fig. 5.5). Relict plants such as *Carya*, *Carpinus orientalis*, *Pterocarya*, *Liquidambar orientalis*, *Zelkova* are still living in the Anatolia. This situation can be explained by the Asian monsoon climate effect.

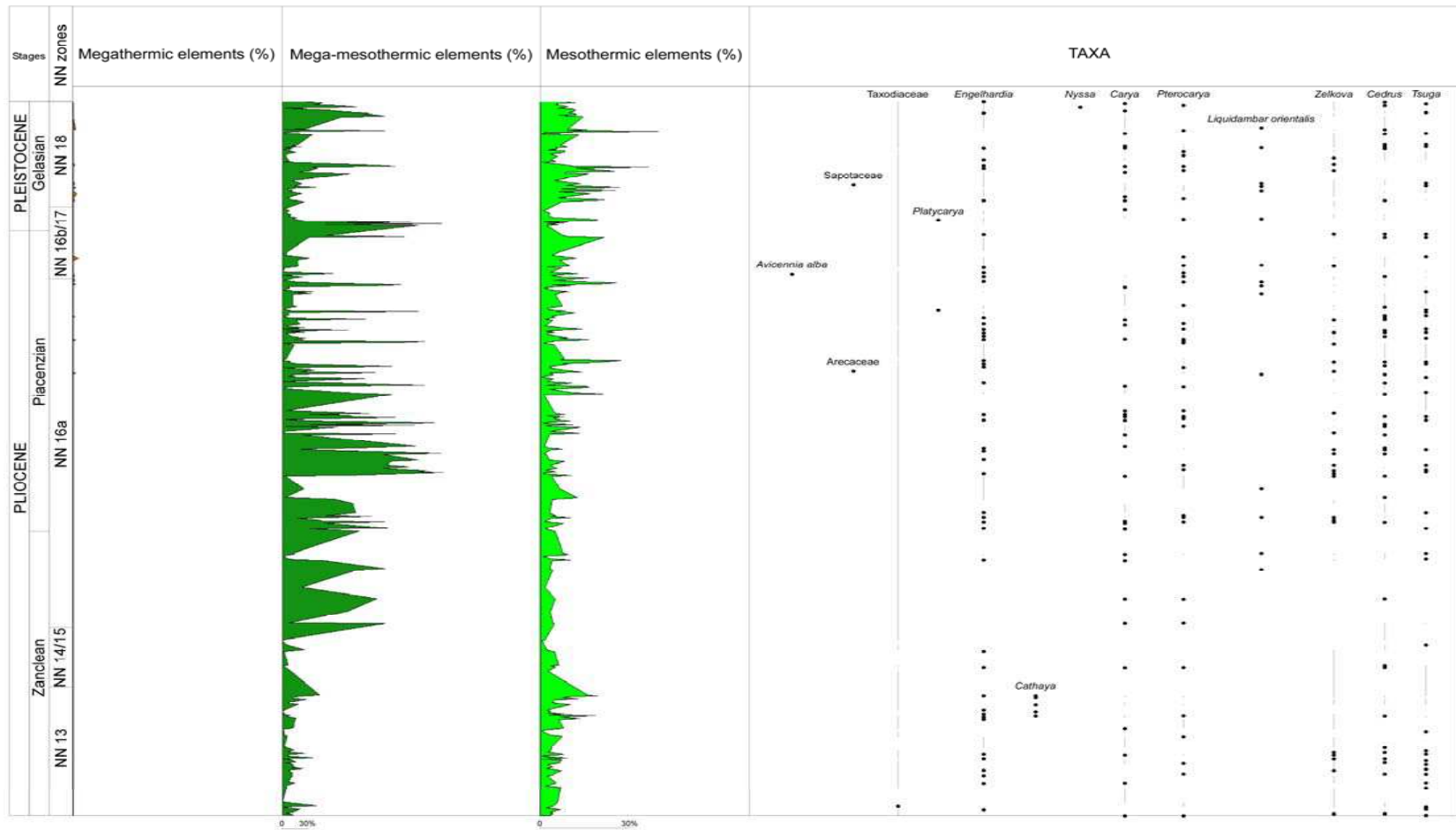


Figure 5.5 : The distribution of thermophilous trees during the Pliocene-Pleistocene in the DSDP Site 380.

5.2 Gulf of Saros

5.2.1 Enez

Enez is located in the eastern shoreline of the Enez lagoon (40°46'24" N, 26°04' E) near the border of Turkey with Greece. The study area includes the Pliocene and the Late Quaternary deltaic deposits of Meriç River overlying the Kirazlı Formation (Çağatay *et al.*, 1998, 2006). The seven samples of eight brownish clay sediments (thickness ~8 m) from the Pliocene bottomset deposits in the Enez section are rich in pollen grains. The flora are characterized by the herbaceous vegetation and warm-temperate trees in all the samples (mesothermic elements) (Fig. 5.6). Herbs reach up more than 75% in the lowest part of the section. Inside this group; Poaceae, Amaranthaceae-Chenopodiaceae, Asteraceae Asteroideae, Asteraceae Cichorioideae are abundant in the samples. The other herbs elements are: Caryophyllaceae, Plumbaginaceae, Solanaceae, *Scabiosa*, Papavaraceae, *Centaurea*, etc. Herbs elements also contain some water plants such as; *Potamogeton* and *Sparganium*.

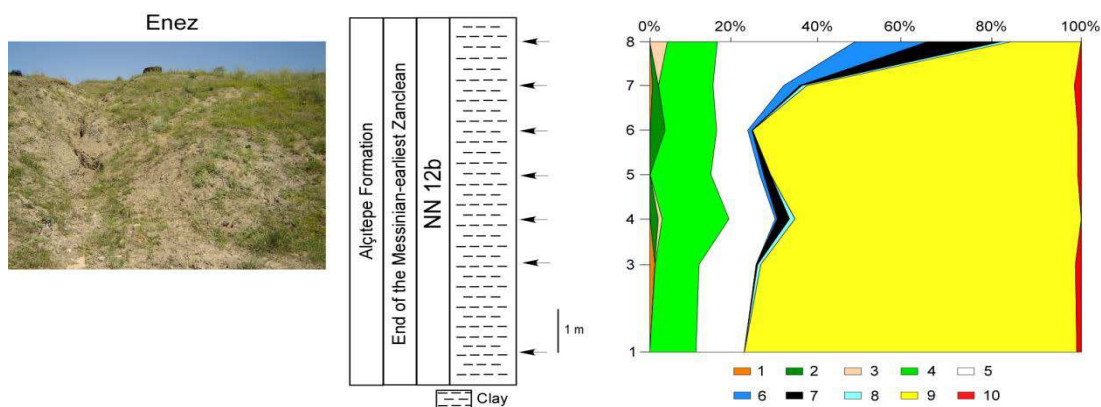


Figure 5.6 : The synthetic pollen diagram of Enez section. Note that only the samples with statistically significant pollen (minimum 150) numbers were analysed. The numbers in the diagram show the pollen groups: 1; megathermic elements (*Arecaceae*, *Sapotaceae*), 2; mega-mesothermic elements (*Taxodiaceae*, *Engelhardia*, *Ginkgo*, *Loropetalum* and *Distylium*), 3; *Cathaya*, 4; mesothermic elements (*Quercus*, *Carya*, *Pterocarya*, *Zelkova*, *Carpinus orientalis*, *Alnus*, *Ulmus*, *Corylus*, etc.), 5; *Pinus*, 6; meso-microthermic elements (*Cedrus*, *Tsuga*), 7; microthermic elements (*Abies*, *Picea*), 8; Cupressaceae, 9; herbs (*Asteraceae Asteroideae*, *Asteraceae Cichorioideae*, *Poaceae*, *Amaranthaceae-Chenopodiaceae*, *Brassicaceae*, *Plumbaginaceae*, etc.) and include some water plants (*Sparganium*, *Potamogeton*), 10; steppe elements (*Artemisia*).

Mesothermic elements (warm-temperate trees) are characterized by the abundance of deciduous *Quercus* (reaches up 8%). The other mesothermic elements in the samples are presented by *Alnus*, *Carya*, *Pterocarya*, *Liquidambar orientalis*, *Corylus*, *Zelkova*, *Ulmus*, *Carpinus orientalis*, *Juglans*, *Buxus sempervirens*, etc. In addition, altitudinal trees (mainly *Tsuga* and *Abies*, *Cedrus*, *Picea*) are also presented frequently in the samples.

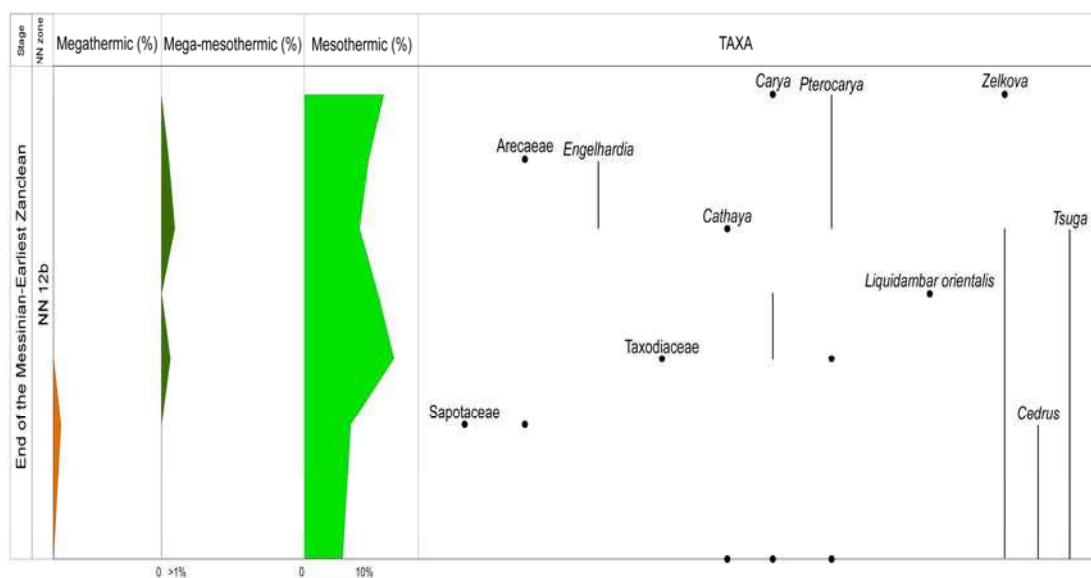


Figure 5.7 : The distribution of thermophilous trees in Enez section during the end of the Messinian (after MSC)-the earliest Zanclean.

Megathermic trees are rare in the sediments. Mega-mesothermic elements are not abundant in the samples. They are frequent in samples 4 and 6. Among them; *Taxodiaceae*, *Engelhardia*, *Ginkgo*, *Loropetalum* and *Distylium* were recorded. *Ginkgo* (gymnosperm) was observed rarely in sample 7. This plant disappeared from Europe 1.7-2.7 Ma ago. They are living in subtropical China today (Gong *et al.*, 2008). *Cathaya* is recorded frequently in samples 1 and 6.

Pinus is also abundant in the samples and its abundance increases towards the top of the section. *Cupressaceae* is frequent in samples 1, 3 and 6. The augmentation in herbs groups in the lower part of the Enez section indicates more open and drier conditions. Thermophilous plants dominated during the end of the Messinian and the earliest Zanclean in Enez section (Fig. 5.7). All taxas in the samples are shown in the detailed pollen diagram (Fig. 5.8).

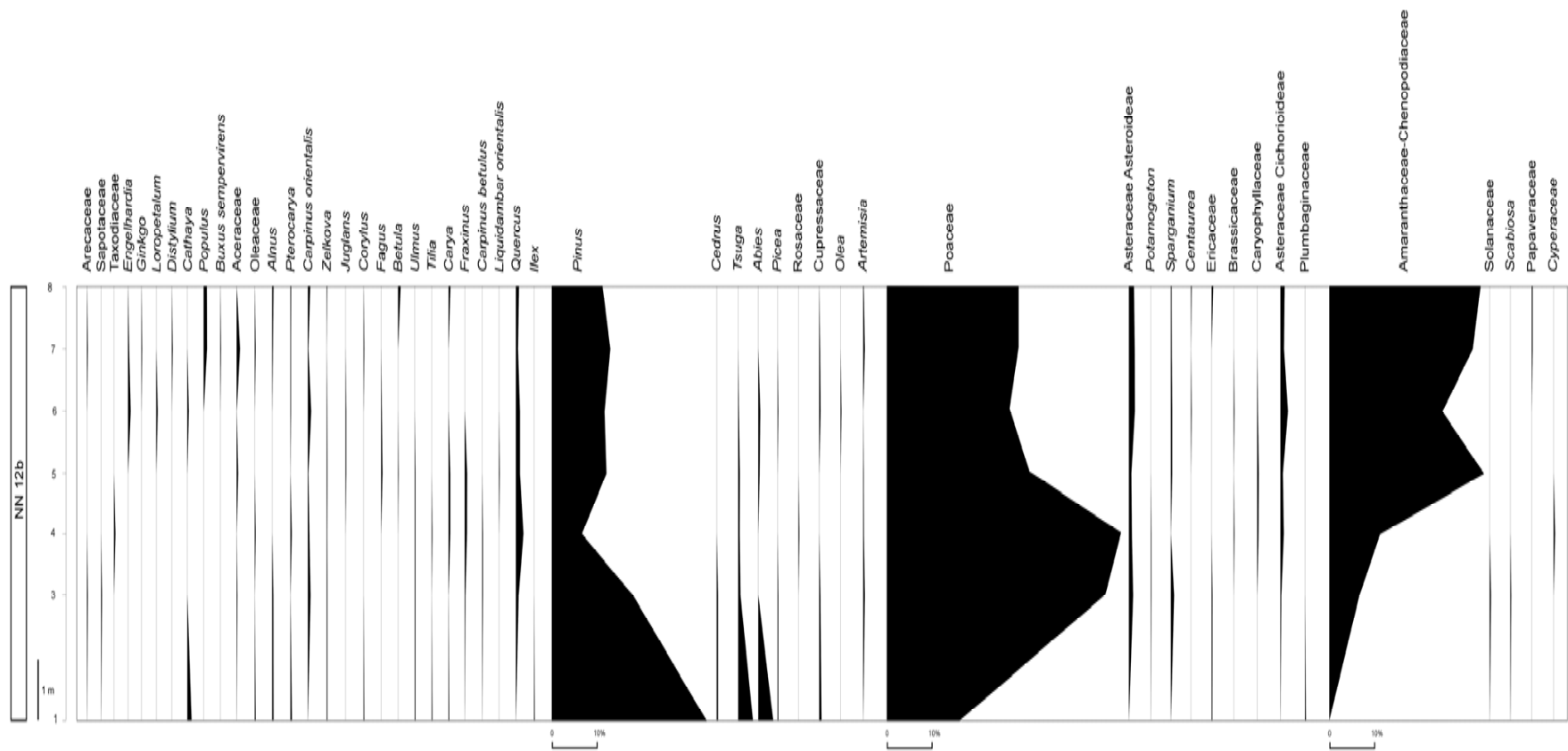


Figure 5.8 : The detailed pollen diagram of Enez section.

5.3 Dardanelles Strait

5.3.1 İntepe

İntepe is located in the south of Dardanelles Strait (40°1'27" N, 26°20'33" E, Fig. 1.2). İntepe section possesses approximately 77 m thickness (Gillet *et al.*, 1978; Sakınç and Yaltırak, 2005). The 36 m of İntepe section was studied in this study. Studied section includes clays, sands, calcareous sandstones and thin limestones (Fig. 5.9). Upper part of İntepe section comprises yellowish sands and pebbly sandstones. *Maetra* shells abundant in the section. In addition, *Melanopsis* shells are observed. Middle part of the section contains a 5 cm thick lignite which correspond to the unconformity related to the MSC (Gillet *et al.*, 1978). The unconformity is overlain by a 2 cm thick sand and *Maetra*. The sediments were dated by nannofossil. The nannofossil content of sediments are *Amaurolithus primus*, *Reticulofenestra rotaria* (samples 14-18), *Nicklithus amplificus* (samples 1-7), *Triquetrorhabdulus rugosus* (samples 1-31), *Ceratolithus acutus* (Melinte *et al.*, 2009). According to nannoflora, the samples (between 18 and 24) belong to NN11c and probably NN12a subzone (Melinte *et al.*, 2009). Among the samples, only 8 samples are rich in terms of pollen grains. Pollen analysis of İntepe section shows that changes in vegetation before and after the Messinian Salinity Crisis (MSC). While the vegetation is characterised by herbs and arboreal trees (chiefly warm-temperate trees) before the MSC, besides herbs and arboreal trees, subtropical elements, mid- and high altitude trees, *Pinus* and *Cathaya* also display an increase after the MSC. Herbs are dominated by Poaceae, Asteraceae Asteroideae, Asteraceae Cichorioideae, and Amaranthaceae-Chenopodiaceae. Among them, Poaceae reaches up 20% and Amaranthaceae-Chenopodiaceae reaches up 10% (Fig. 5.10). Arboreal vegetation is dominated by warm-temperate trees such as; *Quercus*, *Zelkova*, *Carpinus orientalis*, *Carya*, *Pterocarya*, *Acer*, *Ulmus*, *Juglans*, etc. Nevertheless, subtropical elements (Taxodiaceae, *Engelhardia*) have low amount before the MSC. After the MSC, increase in the mega-mesothermic trees, *Pinus* and altitudinal trees such as *Cedrus*, *Abies* and *Picea* may demonstrate more distal location with respect to the paleoshoreline. On the other hand, some aquatic plants (*Sparganium*, *Potamogeton*, *Typha*, *Myriophyllum* and Alismataceae) are well represented after the MSC.

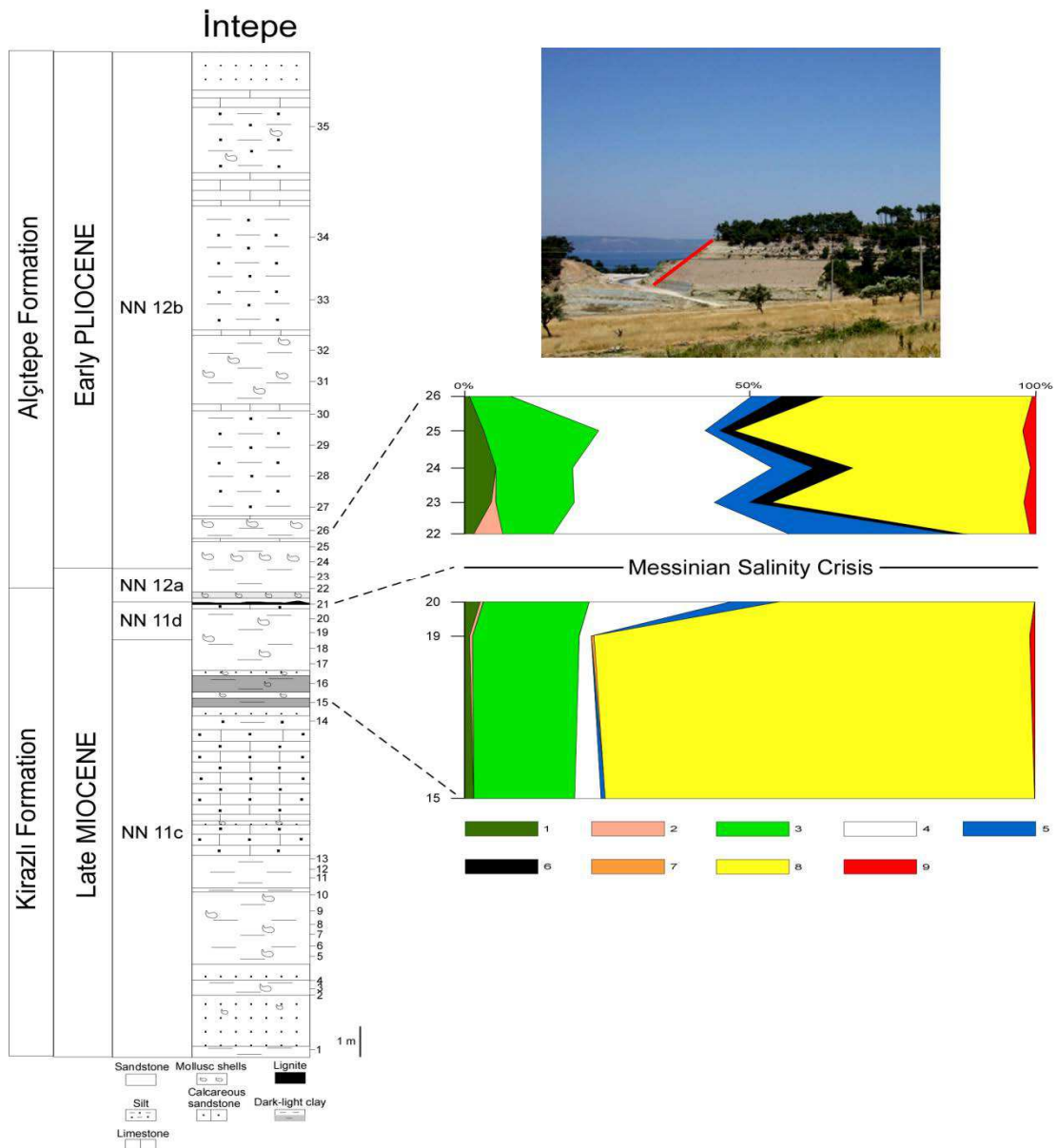


Figure 5.9 : The synthetic pollen diagram of İntepe section with a lithological log. Note that only the samples with statistically significant pollen (minimum 150) numbers were analysed. The numbers in the diagram show the pollen groups: 1; mega-mesothermic elements (*Taxodiaceae*, *Engelhardia*), 2; *Cathaya*, 3; mesothermic elements (*Quercus*, *Carya*, *Pterocarya*, *Zelkova*, *Carpinus orientalis*, *Alnus*, etc.), 4; *Pinus*, 5; meso-microthermic elements (*Cedrus*), 6; microthermic elements (*Abies* and *Picea*), 7; mediterranean xerophytes 8; herbs (Asteraceae Asteroideae, Asteraceae Cichorioideae, Poaceae, Amaranthaceae-Chenopodiaceae, Apiaceae, etc.), and include some fresh water plants (*Sparganium*, *Potamogeton*, *Typha*, etc), 9; steppe elements (*Artemisia*, *Ephedra*).

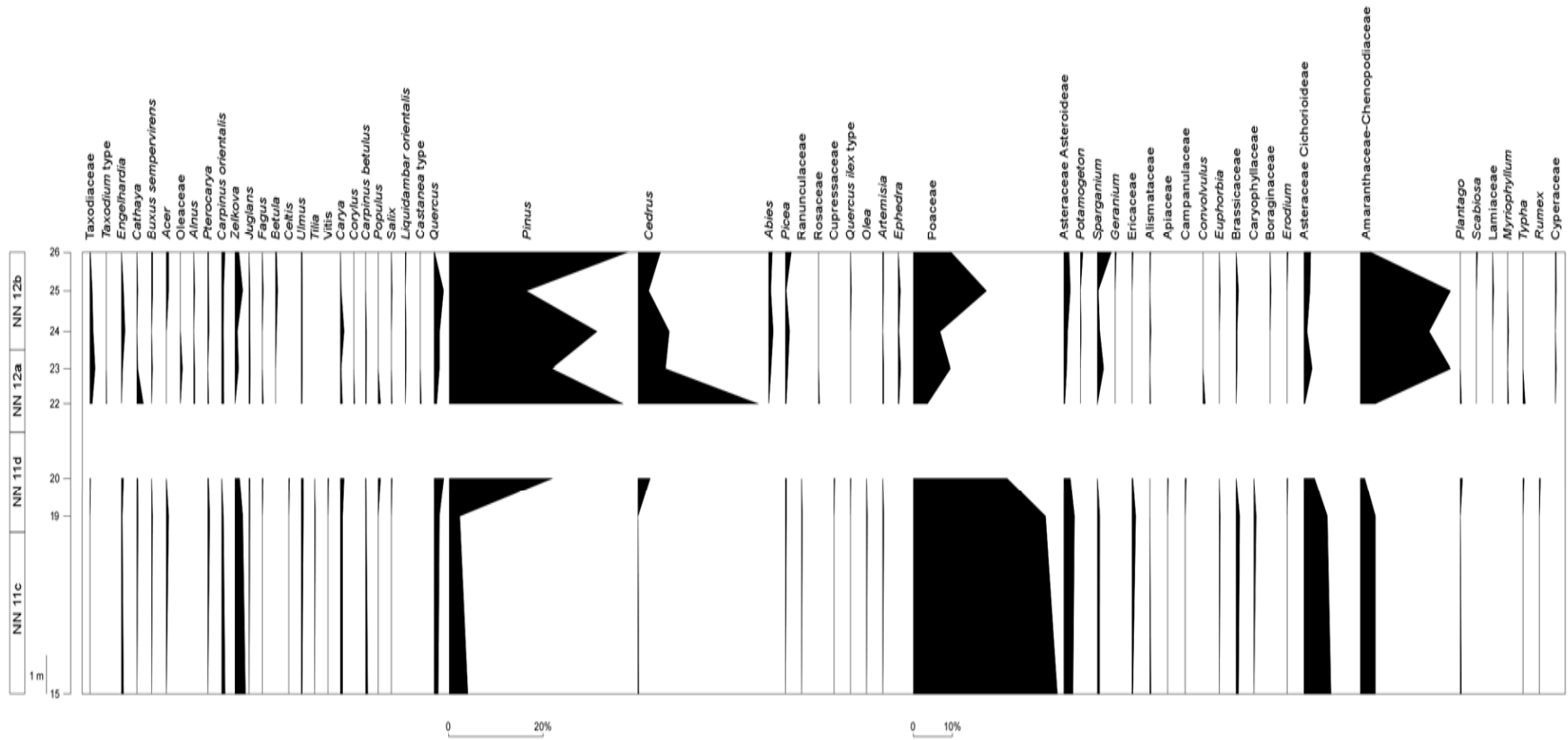


Figure 5.10 : The detailed pollen diagram of Intepe section.

Hence, presence of Amaranthaceae-Chenopodiaceae and aquatic plants demonstrate nearby coastal environments in the region after the MSC (Fig. 5.9). The increasing of altitudinal trees (mainly *Cedrus*, *Abies* and *Picea*) could indicate uplift of the area during the Late Messinian (Melinte *et al.*, 2009). Calculation of mean annual temperature from paleoclimatic transfer function based on pollen assemblages (Fauquette *et al.*, 1998a, 1999) in order to estimate minimum palaeoaltitude of the nearby massif. The result indicate that in the İntepe samples (from 22 to 26), mean annual temperature is 16.5°C (range: 15-18.5°C). Thermophilous plants are well observed before and after the MSC (Fig. 5.11).

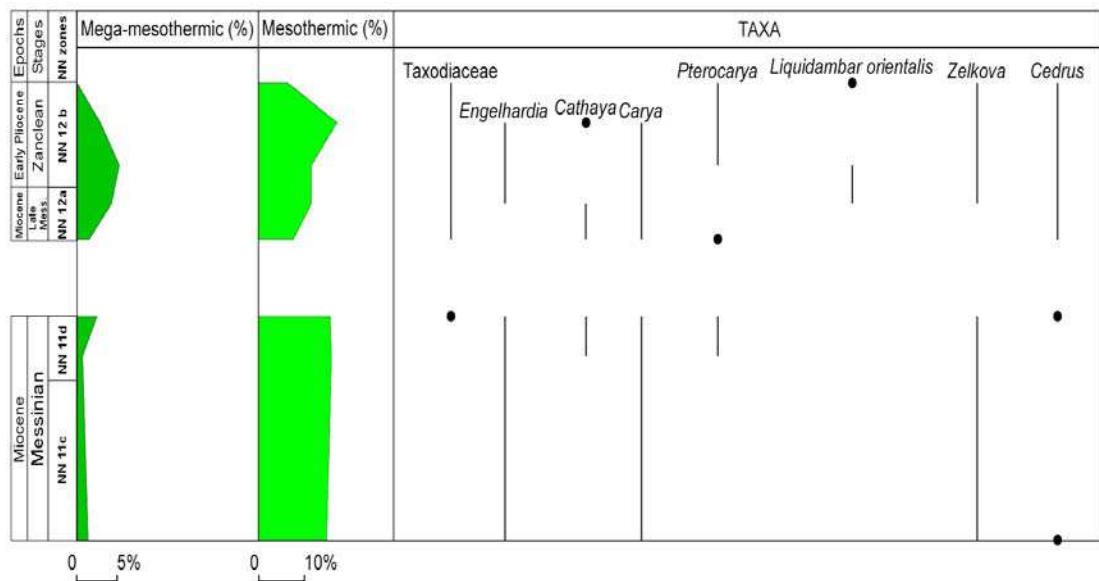


Figure 5.11 : The distribution of thermophilous plants in İntepe section before and after the Messinian Salinity Crisis (MSC).

Moreover, dinoflagellate cyst flora of İntepe section was analysed for reconstruction of coastal marine environment. They contain 12 taxa. *Pediastrum* (fresh water algae) and *Botryococcus* can be added to dinoflagellate cyst. They indicate a fresh water input. Dinoflagellate community include oceanic species, neritic species : *Spiniferites mirabilis*, *Spiniferites membranaceus* and marine autotrophic cosmopolitan species: *Lingulodinium machaerophorum*, *Operculodinium centrocarpum* sensu Wall and Dale, *Spiniferites bentorii*, *Spiniferites bentorii* subsp. *truncates*, *Spiniferites hyperacanthus*, *Spiniferites ramosus*, *Spiniferites bulloideus*, *Spiniferites* spp (Melinte *et al.*, 2009). Besides, dinoflagellate assemblages contain Paratethyan brackish species such as; *Galeacysta etrusca* and *Impagidinium globosum*.

Samples from 15 to 19, marine euryhaline species dominated at that time (*Operculodinium centrocarpum*, *Lingulodinium machaerophorum*, *Spiniferites bulloideus*, *Spiniferites ramosus*, *Spiniferites bentorii*, *Spiniferites bentorii* subsp. *truncates*, *Spiniferites hyperacanthus*). The relative abundance of *Spiniferites* spp. reaches up above 50%.

The presence of this species indicates marine conditions. Sample 15 contains only Paratethyan brackish species. In samples from 20 to 23, *Pediastrum* indicates an increase. This suggests that fresh-brackish water conditions dominated during that time with less than 4.6 ‰ salinity, sometimes with the marine interrupting conditions. Samples 24 and 26 indicate an increase of salinity once again (Melinte *et al.*, 2009).

5.3.2 West of Seddülbahir

West of Seddülbahir (40°02'38" N, 26°10'55" E, Fig.1.2), the studied section consists of ~30 m thick clays with carbonate, coquina and sandstone intercalations. They are rich in molluscs. The nannofloral community of west Seddülbahir includes *Triquetrorhabdulus rugosus*, *Reticulofenestra pseudoumbilicus*, *Ceratolithus acutus*. This section belongs to NN12a and NN12b subzones, corresponding to the Latest Messinian to the Earliest Zanclean (Melinte *et al.*, 2009). Only sample 5 and 3 are rich in pollen grains. The flora of west of Seddülbahir are characterized by herbs, mesothermic elements, meso-microthermic elements and *Cathaya* (Fig. 5.12). Non-boreal flora includes herbs with smaller amount of steppe elements (only *Ephedra*).

Herbs are Amaranthaceae-Chenopodiaceae, Poaceae, Asteraceae Asteroideae, Asteraceae Cichorioideae, Apiaceae, Caryophyllaceae, Ericaceae, *Rumex*, Saxifragaceae, etc., and include some fresh water plant such as *Typha*. Mid-altitudinal trees (mainly *Cedrus* and *Tsuga*) are abundant in the region after the MSC. This suggests that some uplift events occurred in the region after the Messinian Salinity Crisis. *Pinus* conifer pollen is also abundant during that time. They are overspread due to its prolific character. Nevertheless, *Cathaya* is abundant with subtropical plants (Taxodiaceae, *Distylium*, *Microtropis fallax* and *Engelhardia*) in the west of Seddülbahir.

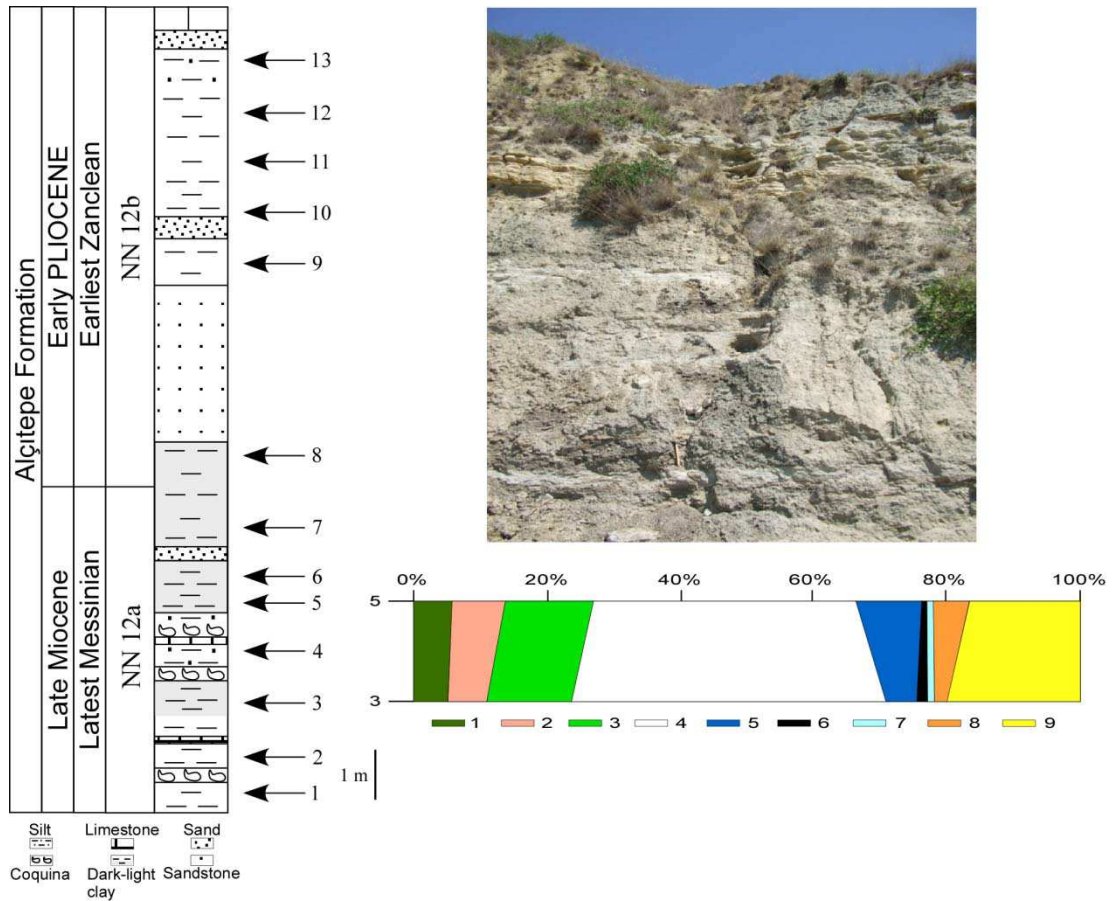


Figure 5.12 : The synthetic pollen diagram of west of Seddülbahir section with a lithological log. Note that only the samples with statistically significant pollen (minimum 150) numbers were analysed. The numbers in the diagram show the pollen groups: 1; mega-mesothermic elements (*Taxodiaceae*, *Distylium*, *Microtropis fallax* and *Engelhardia*), 2; *Cathaya*, 3; mesothermic elements (*Quercus*, *Carya*, *Pterocarya*, *Zelkova*, *Carpinus orientalis*, *Alnus*, etc.), 4; *Pinus*, 5; meso-microthermic elements (*Cedrus* and *Tsuga*), 6; microthermic elements (*Abies* and *Picea*), 7; Cupressaceae, 8; mediterranean xerophytes 9; herbs (Asteraceae Asteroideae, Asteraceae Cichorioideae, Poaceae, Amaranthaceae-Chenopodiaceae, Apiaceae, etc.), and include some fresh water plant (*Typha*).

Among mesothermic elements, *Quercus*, *Carpinus orientalis*, *Pterocarya*, *Juglans*, *Betula*, *Zelkova*, *Carpinus betulus*, *Ulmus*, *Buxus sempervirens*, etc. were recorded. High altitudinal trees *Abies* and *Picea* were observed rarely. Mediterranean xerophytes such as *Quercus ilex* type, *Ligustrum*, *Olea* and *Phillyrea* are presented frequently. Cupressaceae does not vary significantly, but it is presented frequently. All pollen taxa in the west of Seddülbahir are shown in the detailed pollen diagram (Fig. 5.13).

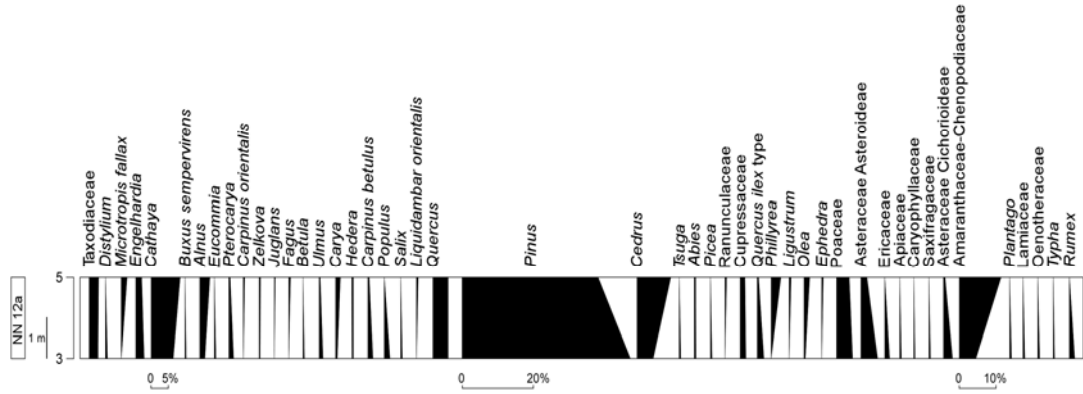


Figure 5.13 : The detailed pollen diagram of west of Seddülbahir.

5.3.3 Eceabat

At Eceabat (40°11'30" N, 26°21'18" E, Fig.1.2), four samples are the whitish clayey base (20 m thick) belonging to Kirazlı Formation and one sample (10 m higher) is a clayey intercalation with calcareous tabular deposits belonging to Alçitepe Formation (Sakinç *et al.*, 1999). Eceabat nannoflora exhibits poor to moderate preservation and few reworked specimens. They include *Amaurolithus primus*, *Reticulofenestra pseudoumbilicus*, *R. Rotaria* (samples 1, 2, 4, 5), *Nicklithus amplificus* (samples 1 and 3) and *Triquetrorhabdulus rugosus*. These nannoflora belong to the NN11c nannofossil subzone, corresponding to an Early Messinian age (Melinte *et al.*, 2009). Five samples were analysed palynologically. However, only one sample (sample 2) was rich in pollen grains (Fig. 5.14).

Pollen flora in Eceabat is characterized by mainly herbs elements. In this group, they are dominated by mainly Amaranthaceae-Chenopodiaceae, Asteraceae Asteroideae, Asteraceae Cichorioideae, Poaceae, etc. with fresh water plant *Sparganium*. Steppe elements are represented by *Artemisia* and *Ephedra*. Subtropical trees are indicated by Taxodiaceae and *Engelhardia*. Taxodiaceae is presented frequently. *Engelhardia* has less amount. Among mesothermic elements (warm-temperate trees) *Quercus*, *Carya*, *Zelkova*, *Alnus*, *Hedera*, *Salix* are observed. Mid-altitudinal tree *Tsuga* is rare as well as Mediterranean xerophytes and Cupressaceae in the sample 2. *Pinus* is also presented abundantly.

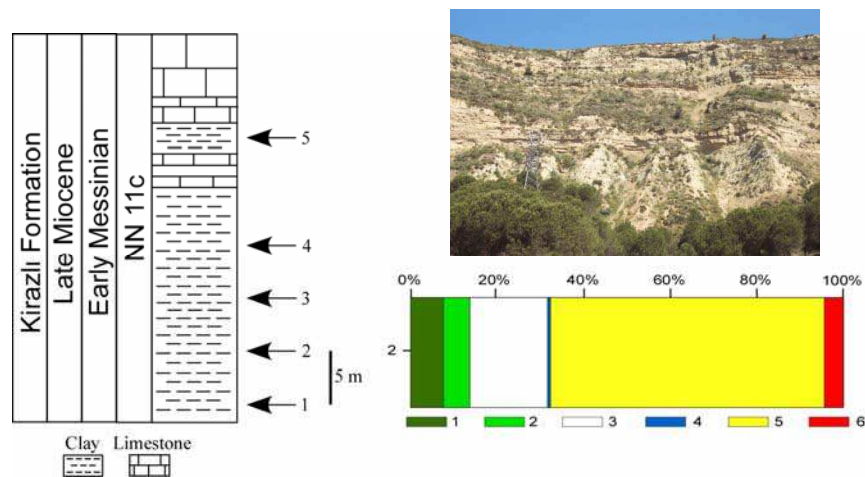


Figure 5.14 : The synthetic pollen diagram of Eceabat section with a lithological log. Note that only the samples with statistically significant pollen (minimum 150) numbers were analysed. The numbers in the diagram show the pollen groups: 1; mega-mesothermic elements (*Taxodiaceae* and *Engelhardia*), 2; mesothermic elements (*Quercus*, *Carya*, *Zelkova*, *Alnus*, etc.), 3; *Pinus*, 4; meso-microthermic elements (*Tsuga*), 5; herbs (*Asteraceae* *Asteroideae*, *Asteraceae* *Cichorioideae*, *Poaceae*, *Amaranthaceae*-*Chenopodiaceae* etc., and include fresh water plant *Sparganium*.

5.3.4 Burhanlı

Burhanlı is located in the Gelibolu Peninsula (40°18'17" N, 26°33'08" E, Fig.1.2). The nannoflora community, *Reticulofenestra pseudoumbilicus*, *Reticulofenestra rotaria*, *Triquetrorhabdulus rugosus* and *Nicklithus amplificus*, were found in the samples. According to this nannoflora assemblages, age of the samples ranges from the Latest Tortonian to the Early Messinian (upper part : NN11b subzone; lower part: NN 11c subzone). Six clay samples with alternating sands belonging to Kirazlı Formation were analysed palynologically. However, only one sample (sample 3) has an enough pollen grains. The vegetation is dominated by herbs (Fig. 5.15). They are recorded by chiefly *Asteraceae* *Cichorioideae*, *Asteraceae* *Asteroideae*, *Amaranthaceae*-*Chenopodiaceae*, *Poaceae*, etc. with fresh water plant *Potamogeton*. Warm-temperate trees (*Carpinus orientalis*, *Zelkova*, *Liquidambar orientalis*, *Carpinus betulus*, *Ulmus* and *Carya* are represented frequently. In addition, subtropical trees (*Taxodiaceae* and *Engelhardia*) and mid-altitudinal trees (*Cedrus*) are observed frequently in the sample 3. *Pinus* is abundantly recorded. The percentage of *Pinus* reaches up 30%. Steppe elements (*Artemisia* and *Hippophae rhamnoides*) are also represented frequently. High altitudinal trees (*Picea*) and *Rosaceae* (non-significant elements) are rare in sample 3.

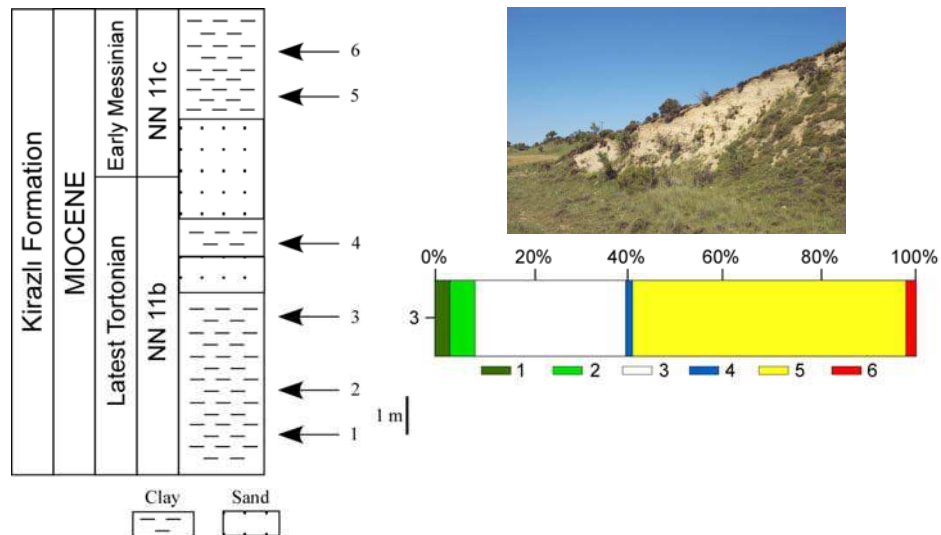


Figure 5.15 : The synthetic pollen diagram of Burhanlı section with a lithological log. Note that only the samples with statistically significant pollen (minimum 150) numbers were analysed. The numbers in the diagram show the pollen groups: 1; mega-mesothermic elements (*Taxodiaceae* and *Engelhardia*), 2; mesothermic elements (*Carya*, *Zelkova*, *Carpinus orientalis*, *Liquidambar orientalis*, etc.), 3; *Pinus*, 4; meso-microthermic elements (*Cedrus*), 5; herbs (*Asteraceae* Asteroideae, *Asteraceae* Cichorioideae, *Poaceae*, *Amaranthaceae-Chenopodiaceae* etc., and include fresh water plant *Potamogeton*, 6; steppe elements (*Artemisia* and *Hippophae rhamnoides*).

5.4 Western Macedonia

5.4.1 Ptolemais notio

The sediments of Ptolemais Notio region cover the Early Pliocene age. The vegetation in the region is characterized by the herbs and mesothermic elements (Fig. 5.16). Herbs are dominated chiefly by *Poaceae*, *Asteraceae* Asteroideae, *Asteraceae* Chichorioideae, *Amaranthaceae-Chenopodiaceae* and *Sparganium*. The mesothermic elements are characterized by the abundances of *Alnus*, more than 10% (Fig. 5.17). The other evergreen-deciduous mixed forest, such as deciduous *Quercus*, *Betula*, *Carpinus orientalis*, *Zelkova*, *Tilia*, etc., are present in the detailed pollen diagram (Fig. 5.17). The deciduous *Quercus* is present in abundance with percentage of deciduous *Quercus* reaching up to 10% in the samples. Megathermic trees such as *Taxodiaceae* and *Engelhardia* are commonly presented frequently. *Poaceae* is more than 20%, and the other herbs such as, *Asteraceae* Asteroideae, *Asteraceae* Cichorioideae have been observed abundantly. Mid-altitude and high altitude trees (such as; *Cedrus*, *Tsuga*, *Abies* and *Picea*) are present commonly.

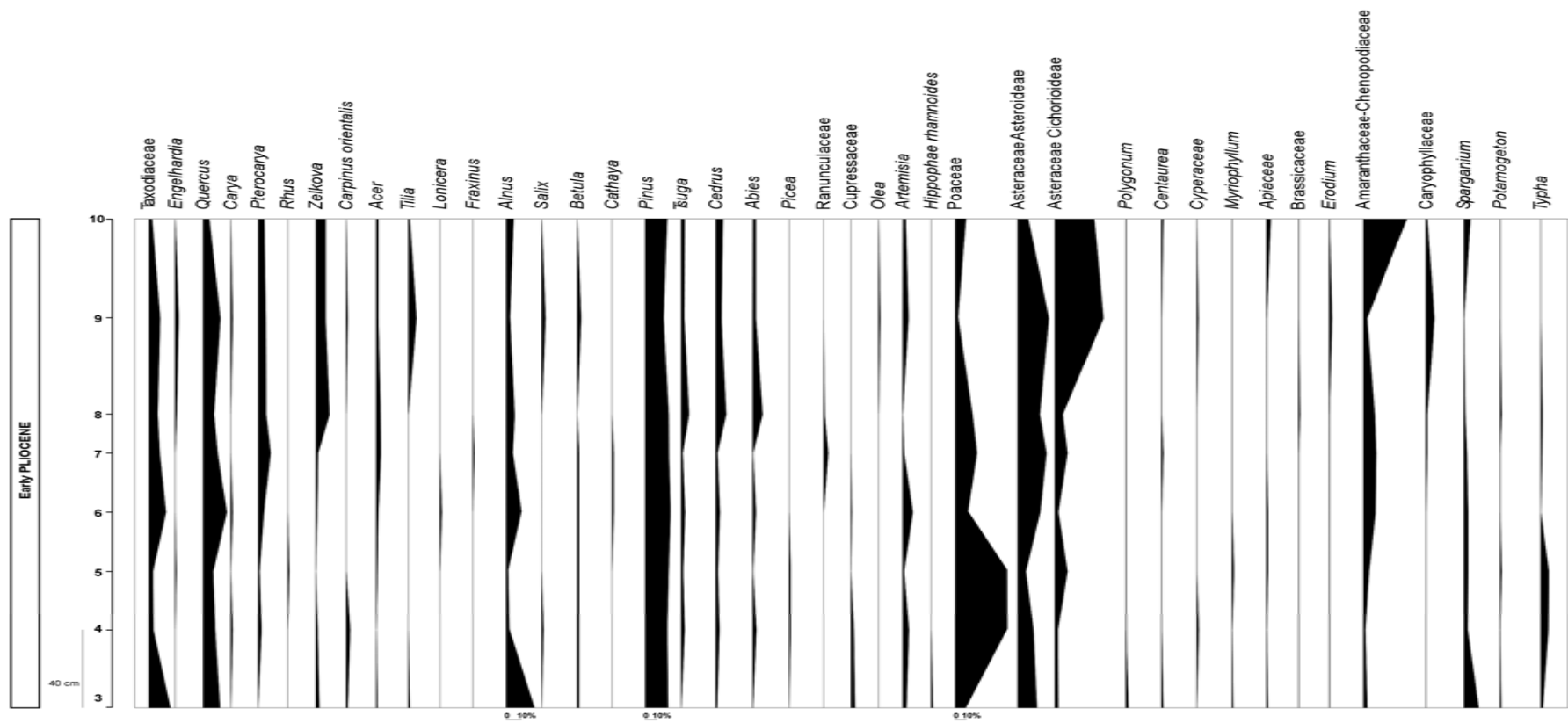


Figure 5.17 : Detailed pollen diagram of Ptolemais Notio.

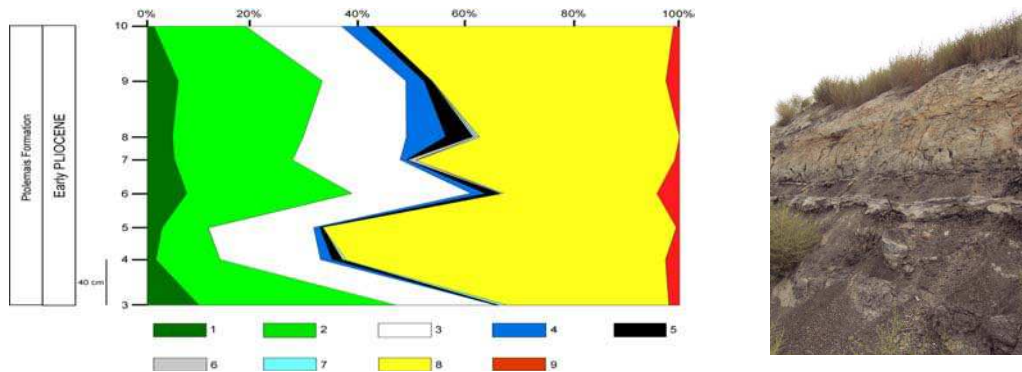


Figure 5.16 : The synthetic pollen diagram of Ptolemais Notio. Note that only the samples with statistically significant pollen (minimum 150) numbers were analysed. The numbers in the diagram show the pollen groups: 1; mega-mesothermic elements (*Taxodiaceae*, *Engelhardia*), 2; mesothermic elements (*Quercus*, *Carya*, *Pterocarya*, *Zelkova*, *Carpinus orientalis*, *Fraxinus*, *Alnus*, etc.), 3; *Pinus*, 4; meso-microthermic elements (*Cedrus* and *Tsuga*), 5; microthermic elements (*Abies* and *Picea*), 6; non-significant (*Ranunculaceae*), 7; Cupressaceae, 8; herbs (*Asteraceae* Asteroideae, *Asteraceae* Cichorioideae, *Poaceae*, *Amaranthaceae* *Chenopodiaceae*, *Apiaceae*, *Polygonum*, etc. and include some water plants (*Sparganium*, *Potamogeton*, *Typha*), 9; steppe elements (*Artemisia*, *Hippophae rhamnoides*).

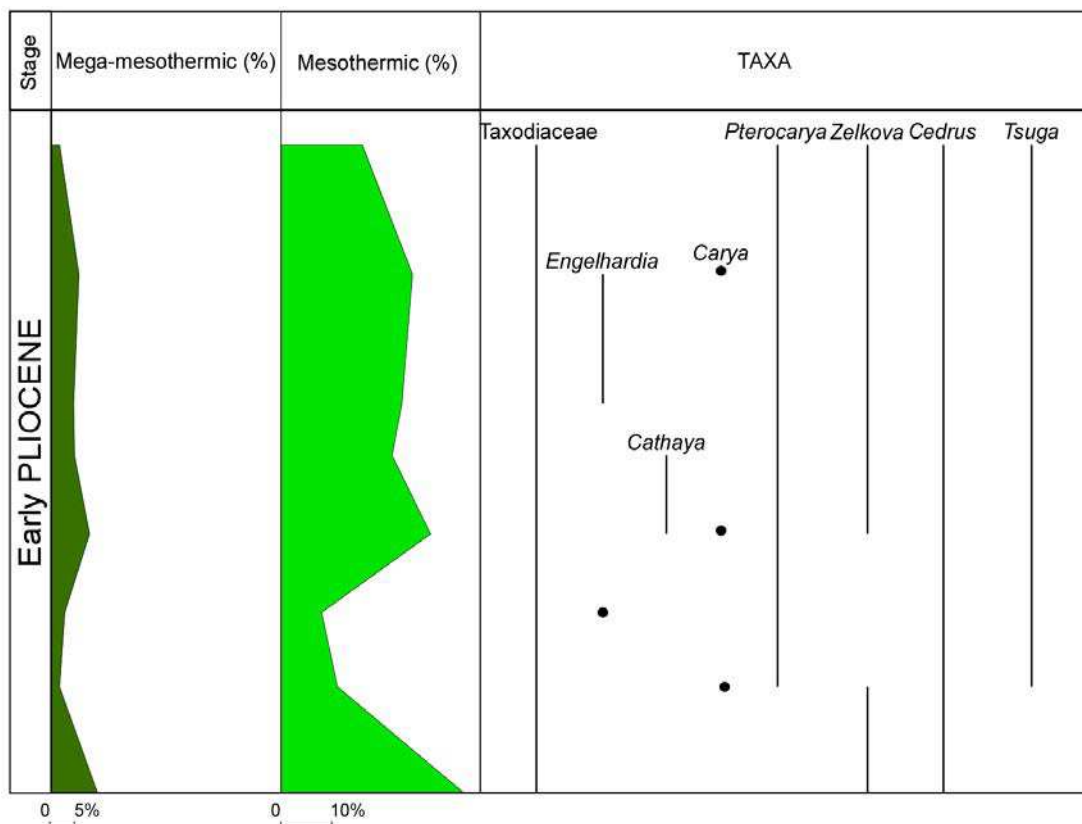


Figure 5.18 : The distribution of thermophilous plants during the Early Pliocene in Ptolemais Notio.

Nevertheless, *Cathaya* do not vary significantly during this time. Besides, *Pinus* is abundant and reaches up 20%. Cupressaceae and non-significant elements (Ranunculaceae) are not much abundant. Mediterranean xerophytes are very scarce in the samples. Because of this, it is not included in the synthetic pollen diagram. Steppe elements are common and represented in the synthetic pollen diagram. *Artemisia* is frequent. However, *Hippophae rhamnoides* is rare in the samples. Thermophilous plants were well recorded in the Ptolemais Notio section. The distribution of them during the Early Pliocene are shown in Figure 5.18.

5.4.2 Ptolemais base

The vegetation of Ptolemais Base region is characterized by mainly warm-temperate trees, herbs and steppes (Fig. 5.19). The evergreen-deciduous mixed forest includes deciduous *Quercus*, *Alnus*, *Betula*, *Carpinus orientalis*, *Zelkova*, *Liquidambar*, Oleaceae, *Fagus* etc. Some of them, especially, deciduous *Quercus* has high abundance during this time. Percentage of deciduous *Quercus* reaches up 36% in the samples. Also, *Fagus* is commonly present with its percentage reaching up to 6%.

Herbs also became more abundant with steppes (mainly *Artemisia* and *Ephedra*). *Poaceae* is abundant with an average of 17%, and Amaranthaceae-Chenopodiaceae has been observed frequently. Mega-mesothermic (Taxodiaceae and *Engelhardia*) elements are not abundant. Mid-altitude and high altitude trees (i.e., *Cedrus*, *Tsuga*, *Abies* and *Picea*) are also frequently present. The average percentages of *Cedrus* and *Abies* reach up 4% and 3% respectively.

Cathaya and Cupressaceae do not vary significantly during this time. Ranunculaceae and Rosaceae (non-significant elements) are frequent. Mediterranean xerophytes (*Olea* and *Quercus ilex* type) are present in small amounts in the samples. Thermophilous trees were observed in the samples during the Early Pliocene in Ptolemais Base. They are exhibited in Figure 5.20. The high abundance of mesothermic plants and herbs with steppes may be due to warm-temperate climate conditions in the region. *Pinus*, a conifer tree, is very abundant, probably due to the capacity of its saccate pollen for long distance transport (Heusser 1988; Suc and Drivaliari, 1991; Cambon *et al.*, 1997; Beaudouin, 2003). Moreover, all taxa with relatively high percentages are represented in the detailed pollen diagram (Fig. 5.21).



Figure 5.19 : The synthetic pollen diagram of Ptolemais Base. The numbers in the diagram show the pollen groups: 1; mega-mesothermic elements (*Taxodiaceae*, *Engelhardia*), 2; mesothermic elements (*Quercus*, *Carya*, *Pterocarya*, *Zelkova*, *Carpinus orientalis*, *Liquidambar*, *Fraxinus*, *Alnus*, etc.), 3; *Pinus*, 4; meso-microthermic elements (*Cedrus* and *Tsuga*), 5; microthermic elements (*Abies* and *Picea*), 6; non-significant (*Ranunculaceae* and *Rosaceae*), 7; mediterranean xerophytes (*Olea*, *Quercus ilex* type), 8; herbs (*Asteraceae* Asteroideae, *Asteraceae* Cichorioideae, *Poaceae*, *Amaranthaceae*-*Chenopodiaceae*, *Cistus*, etc. and include some water plants (*Sparganium*, *Potamogeton*, *Typha*), 9; steppe elements (*Artemisia*, *Ephedra*).

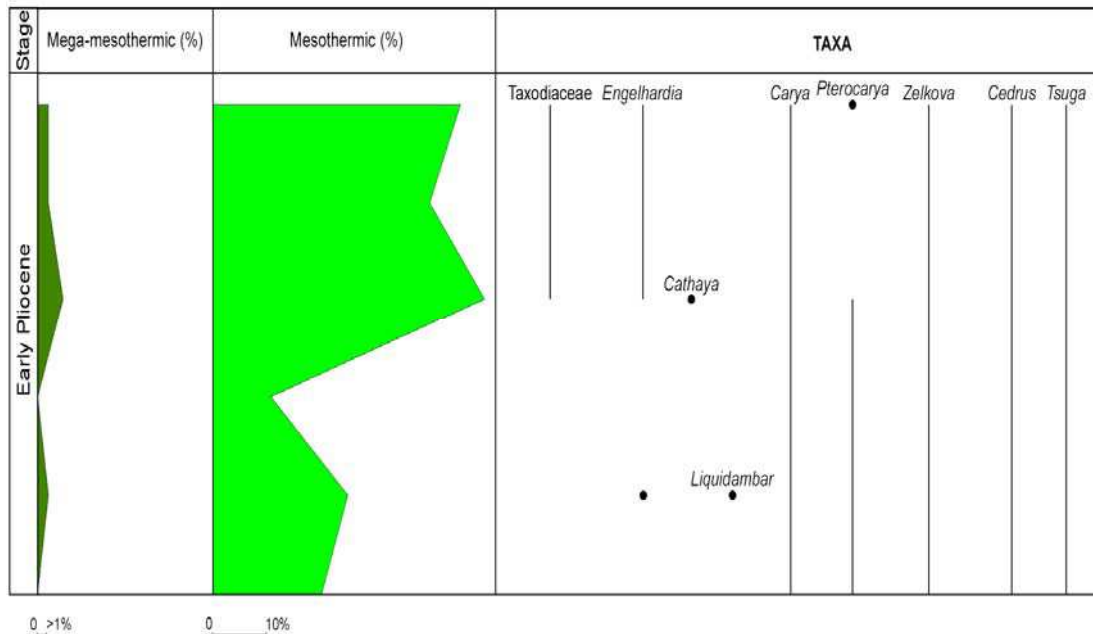


Figure 5.20 : The distribution of thermophilous trees during the Early Pliocene in Ptolemais Base section.

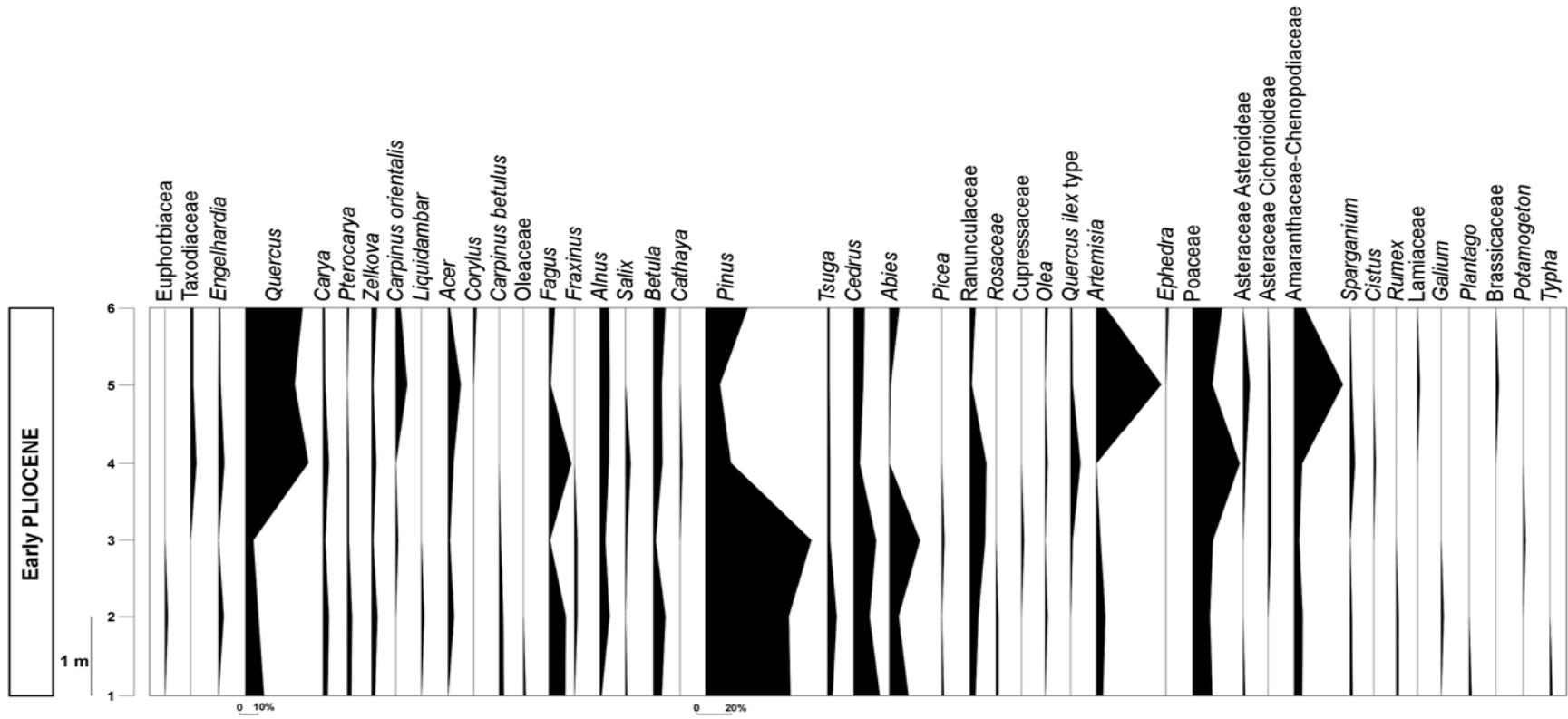


Figure 5.21 : Detailed pollen diagram of Ptolemais Base.

5.5 Northern Greece

5.5.1 Trilophos

Trilophos is located (40°45'90" N, 22°98'57" E, Fig.1.2) The section belongs to NN12 biozone corresponding to the Latest Messinian-Earliest Zanclean. The vegetation is represented by the abundance of warm-temperate trees, herbs and altitudinal elements (Fig. 5.22). The evergreen-deciduous mixed forest, such as deciduous *Quercus*, *Alnus*, *Betula*, *Carpinus orientalis*, *Zelkova*, etc., are presented in the detailed pollen diagram (Fig. 5.23). Especially, *Alnus* and deciduous *Quercus* have shown high abundance during this time. Percentage of deciduous *Quercus* reaches up to 7%. The amount of *Alnus* is 10% percent. Herbs also are represented highly. *Poaceae* has an average abundance of approximately 10%. Other herbs, Amaranthaceae-Chenopodiaceae and Asteraceae Cichorioideae have been observed frequently. Mid-altitude and high altitude trees (such as, *Cedrus*, *Tsuga*, *Abies*) also show abundance. *Tsuga* is abundant and *Abies* is 6%. Nevertheless, *Cedrus* is present commonly. Subtropical trees (Taxodiaceae and *Engelhardia*) have less amount in the samples.

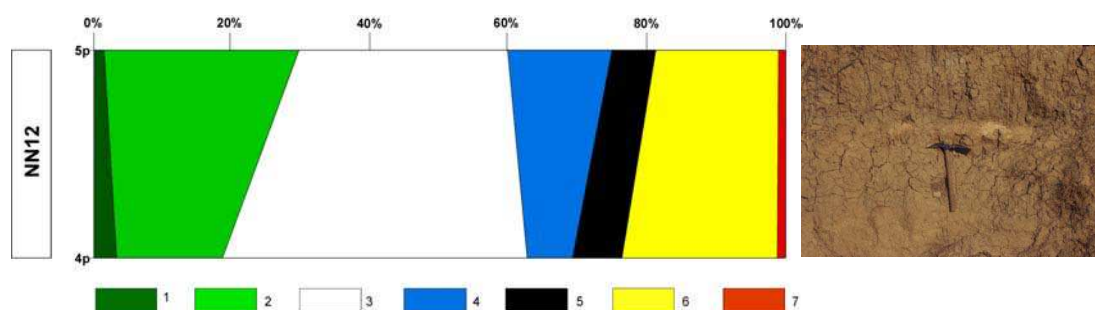


Figure 5.22 : The synthetic pollen diagram of Trilophos. Note that only the two samples of five with statistically significant pollen (minimum 150) numbers were analysed. The numbers in the diagram show the pollen groups: 1; mega-mesothermic elements (*Taxodiaceae*, *Engelhardia*), 2; mesothermic elements (*Quercus*, *Carya*, *Pterocarya*, *Zelkova*, *Carpinus orientalis*, *Betula*, *Alnus*, etc.), 3; *Pinus*, 4; meso-microthermic elements (*Cedrus* and *Tsuga*), 5; microthermic elements (*Abies*), 6; herbs (Asteraceae Asteroideae, Asteraceae Cichorioideae, *Poaceae*, Amaranthaceae-Chenopodiaceae, *Geranium*, etc. and include some water plants (*Sparganium*, *Potamogeton*, *Typha*), 7; steppe element (*Artemisia*).

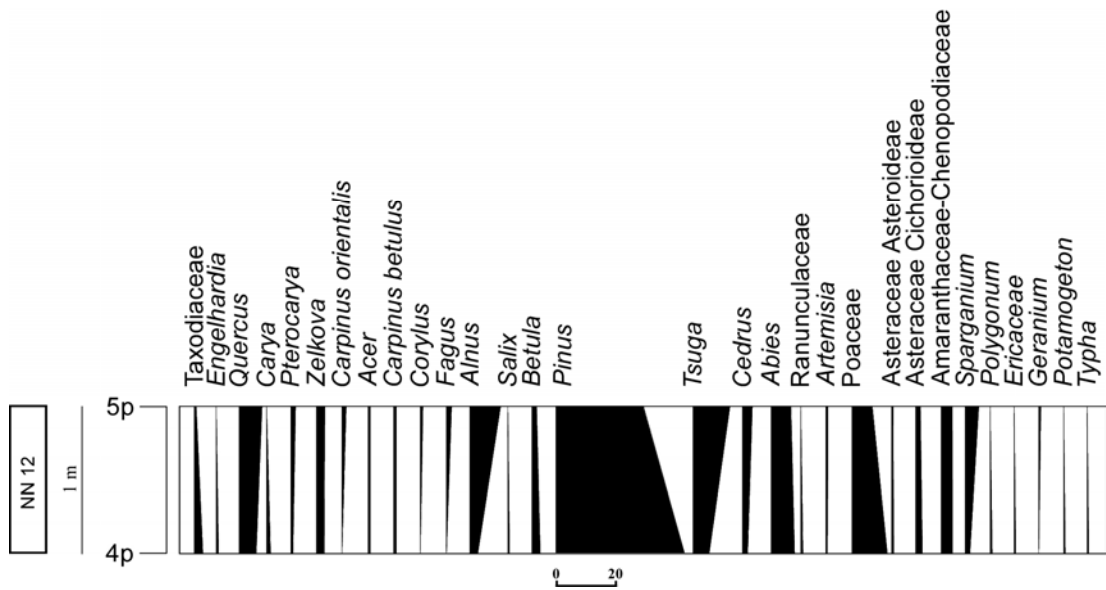


Figure 5.23 : Detailed pollen diagram of Trilophos.

Pinus also is abundant during this time. All taxa with percentages are represented in the detailed pollen diagram (Fig. 5.23).

5.5.2 Prosilio

The Prosilio section is located in 10 km SW of Servia. The vegetation in Prosilio section is characterized by the altitudinal trees (mid- and high altitude trees) and Cupressaceae (Fig. 5.24). The altitudinal trees are dominated by *Tsuga*, *Abies* and *Picea*. The percentage of *Tsuga* reaches up to 39%. *Abies* is about 17% and *Picea* is about 6%. *Cathaya* is abundant in sample 3. Herbs are presented frequently in the samples. They are Asteraceae Asteroideae, Asteraceae Cichorioideae, Poaceae, Amaranthaceae-Chenopodiaceae and fresh water plant *Sparganium*. Steppe elements (*Artemisia* and *Hippophae rhamnoides*) are the same as herbs.

They reach up to 5% in sample 2. Mesothermic trees (*Quercus*, *Ulmus* and *Alnus*) have low abundance in the samples. All taxa in the samples are shown in the detailed pollen diagram (Fig. 5.25). *Pinus* is also abundant with about 20% on average. In addition, Prosilio sediments contain *Botryococcus* colonies. *Botryococcus* is a green algae, generally live in freshwater (swamps, ponds, and lakes) (Gray, 1960; Tappan, 1980, Guy-Ohlson, 1992). Some forms of them also tolerates brackish environments (Wake and Hillen, 1980; DeDecker, 1988).

Botryococcus is commonly accepted that fossil colonies of *Botryococcus* indicate freshwater input and depositional settings affected by freshwater (Batten and Grenfell, 1996). The abundance of *Botryococcus* show lake-level fluctuations during that time in Prosilio. Besides, Cupressaceae is very abundant in sample 2. The percentage of Cupressaceae reaches up to 61% in sample 2. Distribution of Cupressaceae shows changes from warm-humid conditions to dry and warm to cold climatic conditions.

Using their morphology, it is difficult to determine them. If Cupressaceae profile is parallel to Taxodiaceae profile, which is thought to be a subtropical tree *Chamaecyparis* (Popescu, 2001). However, Cupressaceae profile in Figure 5.24 is fit with high altitudinal conifer trees (*Abies* and *Picea*). Therefore, the high presence of Cupressaceae may indicate an existing dry and cold climatic conditions corresponding to a decrease in temperature. Moreover, the mid- and high altitudinal trees could indicate some uplift of the surrounding area.

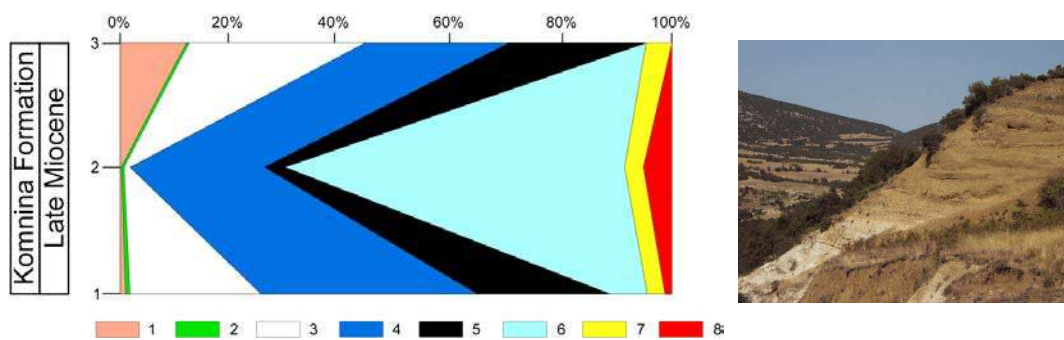


Figure 5.24 : The synthetic pollen diagram of Prosilio. Note that only the three samples of six with statistically significant pollen (minimum 150) numbers were analysed. The numbers in the diagram show the pollen groups: 1; *Cathaya*, 2; mesothermic elements (*Quercus*, *Alnus* and *Ulmus*), 3; *Pinus*, 4; meso-microthermic elements (mainly *Tsuga*), 5; microthermic elements (*Abies* and *Picea*), 6; Cupressaceae, 7; herbs (Asteraceae Asteroideae, Asteraceae Cichorioideae, Poaceae, Amaranthaceae-Chenopodiaceae and include water plant *Sparganium*, 8; steppe element (*Artemisia* and *Hippophae rhamnoides*).

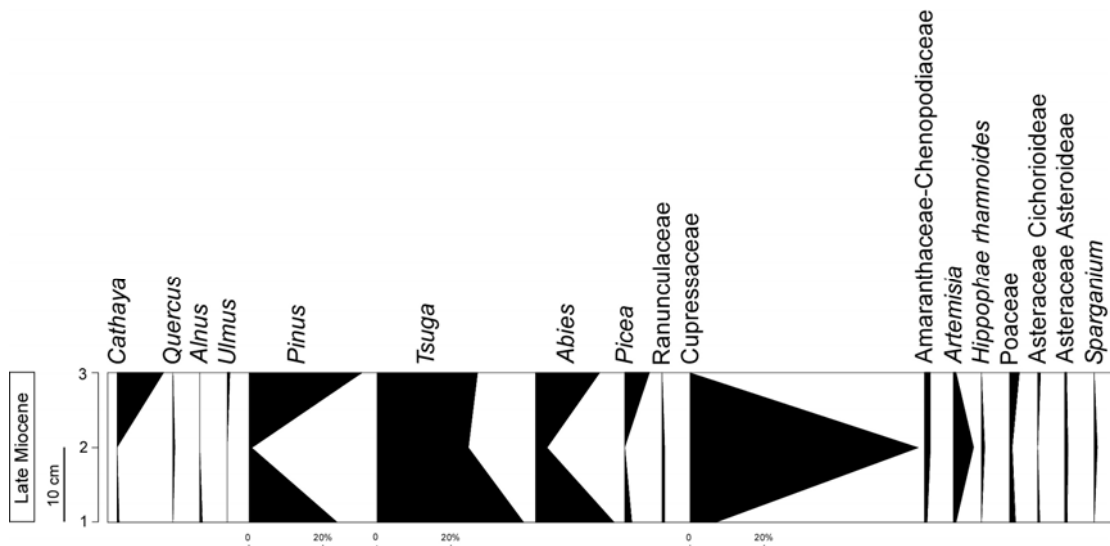


Figure 5.25 : The detailed pollen diagram of Prosilio.

5.5.3 Lion of Amphipoli

The Lion of Amphipoli section represents the Early Zanclean. During this time vegetation is characterized by mega-mesothermic, mesothermic, mid- and high altitude trees, herbs and *Cathaya* (Fig. 5.26). Mega-mesothermic trees, belonging to these plant assemblages, such as Taxodiaceae, *Engelhardia* and *Taxodium* type are observed.

Taxodiaceae has a frequency, its percentage reaches up to 3%. *Engelhardia* and *Taxodium* type are rare. The deciduous forest are represented by deciduous *Quercus*, *Populus*, *Buxus sempervirens*, *Carya*, *Zelkova*, *Ulmus*, *Pterocarya*, *Juglans*, *Fagus*, *Betula*, *Acer* and *Tilia*. Among this plant associations, deciduous *Quercus* is abundant with 7%. The mid-altitude trees such as, *Cedrus* are less abundant (4%). High altitude trees such as *Abies* and *Picea* are also observed. *Abies* is rare. However, *Picea* is frequent as well as *Cedrus* (4.7%).

Cathaya does not change significantly (1.6%). The group of the herbs (mainly Poaceae, Amaranthaceae-Chenopodiaceae, Asteraceae Asteroideae, Brassicaceae, *Potamogeton*, Cyperaceae, *Plantago*, Caryophyllaceae, and Asteraceae Cichorioideae) are abundant, the percentage of herbs reaches up 10%. In addition, it should be mentioned that conifer pollen, mainly *Pinus* and indeterminate Pinaceae are particularly abundant. This is due to the resistance of saccate pollen to long distance transportation.

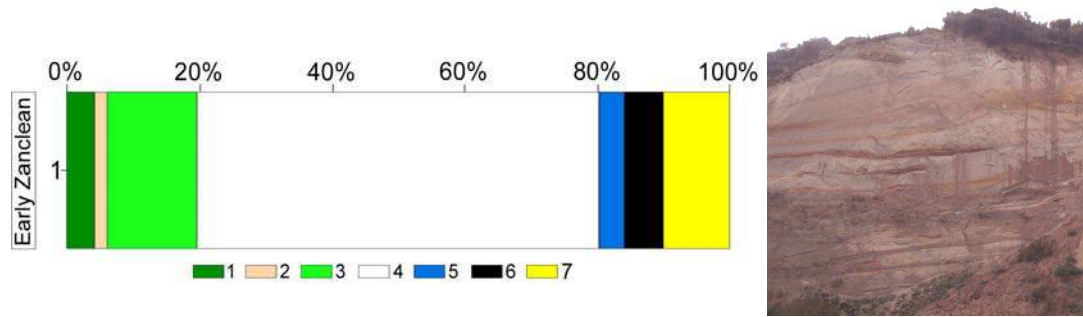


Figure 5.26 : The synthetic pollen diagram of Lion of Amphipoli. Note that only the samples with statistically significant pollen (minimum 150) numbers were analysed. The numbers in the diagram show the pollen groups: 1; mega-mesothermic elements (*Taxodiaceae*, *Engelhardia*, *Taxodium* type), 2; *Cathaya*, 3; mesothermic elements (*Quercus*, *Carya*, *Pterocarya*, *Zelkova*, *Ulmus*, etc.), 4; *Pinus*, 5; meso-microthermic elements (*Cedrus*), 6; microthermic elements (*Abies* and *Picea*), 7; herbs (*Asteraceae* *Asteroideae*, *Asteraceae* *Cichorioideae*, *Poaceae*, *Amaranthaceae*-*Chenopodiaceae*, etc. and include water plant *Potamogeton*).

6. DISCUSSION

6.1 Flora and Floristic Refuges

A total of 11 sections and 436 samples have been studied for pollen analysis in this study. Totally 107 different taxa were identified. The list of identified taxa are indicated in Table 3.2. Flora of the study areas is diversified in terms of thermophilous elements which are characterized by a peculiar story; they are arranged according to the Nix's (1982) classification:

- (1) megathermic elements (tropical): *Avicennia alba*, Euphorbiaceae, Rubiaceae and Rutaceae;
- (2) mega-mesothermic elements (subtropical): Taxodiaceae including *Taxodium*-type, *Engelhardia*, *Platycarya*, Sapotaceae, *Distylium*, *Microtropis fallax*, *Ginkgo*, *Loropetalum*, Arecaceae and *Cathaya*;
- (3) mesothermic elements (warm-temperate): *Carpinus orientalis*, *Juglans*, *Juglans* cf. *cathayensis*, *Carya*, *Pterocarya*, *Liquidambar orientalis*, *Platanus*, *Nyssa*, *Ulmus*, *Zelkova*, *Celtis* and *Eucommia*;
- (4) meso-microthermic elements (cool-temperate): *Cedrus* and *Tsuga*.
- (5) Microthermic elements (boreal): *Abies* and *Picea*.

During the Late Miocene (early-late Messinian) and Earliest Zanclean, floras are generally characterized by mesothermic trees such as *Quercus*, *Alnus*, *Carya*, *Buxus sempervirens*, *Ulmus*, *Juglans*, *Betula*, *Carpinus orientalis*, *Celtis*, *Carpinus betulus*, *Eucommia*, *Pterocarya*, *Liquidambar orientalis* etc. in the North Aegean and Northern Greece [i.e. İntepe, West Seddülbahir, Enez, Eceabat, Burhanlı (the latest Tortonian - early Messinian) and Prosilio]. Subtropical trees are Taxodiaceae (including *Taxodium* type), *Engelhardia*, *Ginkgo*, *Loropetalum*, *Distylium* and *Microtropis fallax*, Arecaceae and Sapotaceae. They are common during this time-interval in the North Aegean. Subtropical elements are not abundant in İntepe, West Seddülbahir, Enez, Eceabat, and Burhanlı.

Among subtropical trees, *Ginkgo* is only observed in the Enez section. Today, *Ginkgo biloba* is the only species of Ginkgoaceae; it is living in China (Gong, 2008). The earlier record of Ginkgoaceae in Anatolia was found in Seyitömer Basin during the Early-Middle Miocene (Yavuz Işık, 2007). In addition, macrofossil (leaf) of Ginkgoaceae was found at the Early-Late Pliocene boundary in western Hungary (Hably and Kvaček, 1998). Among the herbs, Poaceae, Amaranthaceae-Chenopodiaceae are common. *Pinus* is overrepresented in most of the samples.

Meso-microthermic and microthermic trees (*Cedrus* and *Tsuga*, *Abies* and *Picea*) are recorded in the study areas. *Tsuga* pollen is abundant at Enez and Prosilio. *Cedrus* is abundant at İntepe (after the MSC) and West Seddülbahir. *Cathaya* is observed at İntepe, West Seddülbahir, Enez and Prosilio.

Subtropical elements are frequent in DSDP Site 380 and mainly represented by Taxodiaceae (including *Taxodium*- and *Sequoia*-types, *Sciadopitys*), *Engelhardia*, *Myrica*, Sapotaceae, *Microtropis fallax*, *Distylium* cf. *sinensis*, Araliaceae, *Nyssa*, etc. during the Late Miocene (Popescu, 2006). Tropical trees are few and they are represented by *Amanoa*, *Fothergilla*, *Exbucklandia*, *Avicennia*, Euphorbiaceae, Sapindaceae, Loranthaceae and Acanthaceae in the lower part of the 380 pollen record (Popescu, 2006).

Pollen records from the other time-spans of the Miocene have also shown the existence of thermophilous trees in Anatolia. The pollen results from Ermenek (central Taurus, Turkey) pointed out thermophilous plants during the Aquitanian: Euphorbiaceae, Rubiaceae, Sapotaceae, Taxodiaceae, *Engelhardia*, *Liquidambar orientalis*, *Carya*, *Ulmus*, *Pterocarya*, *Zelkova*, *Carpinus betulus*, Anacardiaceae, *Carpinus orientalis*, *Juglans*, *Platanus*, *Rhus*, etc. (Biltekin, unpublished). During that time, especially *Cedrus* is very abundant within sediments from the region. Today, *Cedrus libani* is mostly found in the Taurus (Turkey), but also in Syria and Lebanon (Hajar *et al.*, 2010).

Cedar belt is located between 1200 and 1400 meters in Eastern Mediterranean (rainfall: 1000-2000 mm/year) (Quézel, 1998). For this region, *Cedrus libani* might be an endemic species in the Taurus. In future studies, after detailed morphological analysis, it could be correlated with *Cedrus* of Ermenek. In addition, *Cedrus* is still existed as relict in Morocco, Algeria, Cyprus and Lebanon (Quézel, 1998; Quézel and Médail, 2003). *Cathaya* is also found in the region during the early Miocene.

Pollen results of Seyitömer Basin (Kütahya, Western Anatolia) have shown that flora was rich in terms of thermophilous plants (Taxodiaceae, *Engelhardia*, *Carya*, *Zelkova*, *Liquidambar*, *Cedrus*, etc. during the Early-Middle Miocene (Yavuz Işık, 2007). During the same time-interval, Taxodiaceae, *Engelhardia*, Hamamelidaceae, *Nyssa*, *Myrica*, Sapotaceae, Araliaceae, *Carpinus orientalis*, *Liquidambar*, *Parrotia persica*, *Ulmus*, *Carya*, *Zelkova*, *Pterocarya*, *Juglans*, *Cedrus* are presented in the central Turkey (Pelitçik Basin) (Yavuz Işık, 2009). During the Burdigalian, Euphorbiaceae, Taxodiaceae, Cyrillaceae-Clethraceae, Sapotaceae, Hamamelidaceae, *Engelhardia*, *Pterocarya*, *Carya*, *Juglans*, *Celtis*, *Ulmus*, *Zelkova*, *Carpinus*, *Liquidambar*, Araliaceae, *Cathaya*, *Cedrus* existed in the Güvem Basin (NW Central Anatolia) (Yavuz Işık, 2008).

In Çatakbağyaka (west-south Turkey), thermophilous trees such as Euphorbiaceae, *Mussaenda*-type, Rubiaceae, *Alchornea*, Passifloraceae, Taxodiaceae, Arecaceae, *Myrica*, Sapotaceae, *Distylium*, Hamamelidaceae, *Engelhardia*, Celastraceae, *Carya*, *Juglans*, *Pterocarya*, *Liquidambar*, *Parrotia persica*, Anacardiaceae, *Eucommia*, *Zelkova*, *Carpinus*, *Carpinus orientalis*, *Celtis*, *Cathaya* and *Cedrus* were found during the Langhian (~14.8-15.0 Ma) (Jiménez-Moreno, 2005).

Pollen records are also available from the nearby areas and other areas of the Mediterranean region for the Miocene. Thermophilous trees such as Sapotaceae, Araliaceae, Theaceae, *Reevesia*, *Pandanus*, Schizaeaceae, Gleicheniaceae, Taxodiaceae, *Engelhardia*, *Alangium*, *Symplocos*, *Itea*, *Chloranthus*, *Myrica*, *Liquidambar*, *Celtis*, *Nyssa*, *Planera*, *Zelkova*, *Ulmus*, *Platanus*, *Carpinus*, *Juglans*, *Carya*, *Pterocarya*, *Tsuga*, etc. lived in NW Bulgaria during the Badenian (Middle Miocene) (Ivanov, 2002). In the west Bulgaria (Beli Breg Coal), subtropical plants are in low quantity (*Engelhardia*, *Platycarya*, *Symplocos*, Sapotaceae and Arecaceae). Mid-high altitude trees (*Tsuga*, *Cedrus* and *Cathaya*) are also important in the pollen flora. *Carya*, *Pterocarya*, *Ulmus*, *Zelkova*, *Eucommia*, *Juglans* are common during the Late Miocene (Ivanov, 2007).

During the Late Tortonian-Messinian, thermophilous elements are Mimosaceae, Euphorbiaceae, Rubiaceae, Taxodiaceae (*Sequoia* type in Samos, *Taxodium* type in the Pikermi area), *Engelhardia*, Sapotaceae, Arecaceae, *Symplocos*, *Nyssa*, *Myrica*, *Carya*, *Juglans* are recorded in the southern-central and northern Greece (Ioakim, 2005).

The main difference with these regions is the high abundance of Taxodiaceae in the Late Miocene localities in this study. Other differences are abundance of *Tsuga* (in Enez and Prosilio) and *Cedrus* (at İntepe after the MSC). In addition, Cupressaceae (Juniper family) are more abundant (reaching up to 61%) at Prosilio during this time. Cupressaceae contain species living in a warm-humid conditions and some others in dry-cold conditions (Suc and Popescu, 2005; Popescu, 2006).

It is difficult to assess a finer identification than the family level because of the very poor variability of morphological characters of Cupressaceae. In this situations, their interpretation is made according to their behavior in the pollen records. Here, Cupressaceae show a parallel curve to those of mid- and high-altitude elements, steppes (*Artemisia* and *Hippophae rhamnoides*) and herbs. This could indicate lowering in temperature. Indeed, studies on modern and fossil species of Cupressaceae (*Thuja*) show that this taxon can survive under the cold to freezing conditions (LePage, 2003).

There are studies on macroflora data in Turkey for the Miocene and Pliocene (Kasaplıgil, 1977; Sakıncı, 2007) and neighbouring areas (Kovar-Eder, 2006; Kovar-Eder, 2008; Velitzelos, 1990). Sakıncı (2007) examined silicated trees in Thrace from Late Miocene-Pliocene age. Within silicated tree assemblages, Podocarpaceae, Anacardiaceae, Fagaceae, Juglandaceae, *Engelhardia*, Lauraceae, Fabaceae Caesalpinoideae, Fabaceae Mimosoideae, Rosaceae Prunoideae (*Prunus*), Asteraceae have been observed. These silicated tree assemblages are comparable and convenient with pollen results from this study. *Engelhardia*, *Fagus*, *Juglans*, Asteraceae are also recorded in Enez and DSDP Site 380.

Kovar-Eder *et al.* (2006) reconstructed and mapped the vegetation using macroplant data from southern Europe (Greece and adjacent areas, Italy, southern France and Spain) from the Late Miocene to Early Pliocene. The results show that sclerophyllous oaks developed during the Late Miocene and humid subtropical conditions dominated in Italy during the Early Pliocene. Southern France and Spain recorded a decrease in thermophilous plants during that time-interval. Pollen flora for the Pliocene is dominated by swampy component (with mainly *Glyptostrobus*), and an evergreen-deciduous mixed assemblage.

Within them, Taxodiaceae (*Glyptostrobus*) is very abundant and. *Glyptostrobus* is almost observed in the most of samples of DSDP core between 702.4 and 319.03 m depth with changing quantity. A detailed scanning electronic microscope analysis of pollen grains indicates that Taxodiaceae pollen grains have the same morphology with *Glyptostrobus pensilis* (i.e. *Glyptostrobus lineatus*). The last occurrence of *Glyptostrobus* in the Black Sea region was expected during the Late Pliocene to Early Pleistocene. On contrary, analyses of DSDP Site 380 document its persistence up to Recent. *Glyptostrobus* was occupying the deltaic coastal areas. Taxodiaceae disappeared earlier from the northern Mediterranean region (3.6 Ma), later from the southern Mediterranean (2.6 Ma), from Italy and Crete (1.3 Ma) and disappeared from Black Sea and Lake Baikal very recently (Suc *et al.*, 2004; Popescu *et al.*, 2010) (Fig. 6.1).

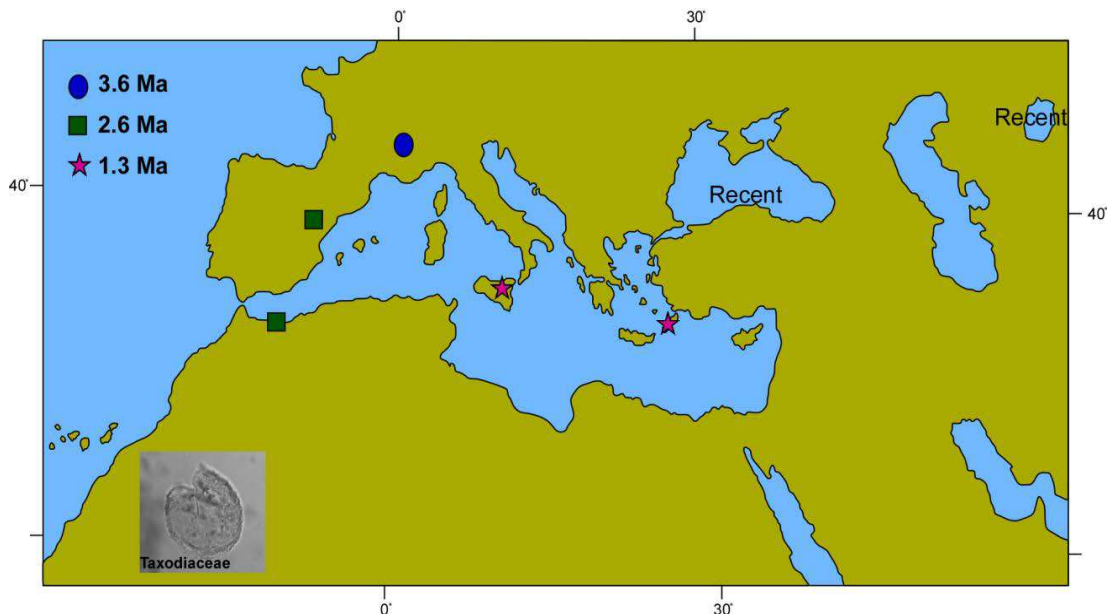


Figure 6.1 : Latest records of Taxodiaceae swamps in the Mediterranean region.

Quercus is also abundant in the pollen flora. *Alnus* is generally seen in most of the sediments as well as *Carpinus orientalis*, *Zelkova*, *Abies*. *Cathaya* is not very frequent and *Cedrus* and *Tsuga* are not abundant but they are usually recorded. Microthermic trees such as *Abies* and *Picea* are not frequent. Other thermophilous trees are Euphorbiaceae, Rubiaceae, Arecaceae, Rutaceae, *Avicennia alba*, *Engelhardia*, *Platycarya*, Sapotaceae, *Juglans*, *Juglans cf. cathayensis*, *Pterocarya*, *Ulmus*, *Liquidambar orientalis*, *Carpinus betulus*, *Platanus*, *Nyssa*, *Carya*, and *Zelkova*.

Avicennia is a mangrove element, it was scarcely recorded in the previous work of DSDP Site 380 (at 1018.85 and 781.63 m depth; Popescu, 2006). In the pollen records of this study, *Avicennia alba* is very rare and has been only observed at 412.53 m depth. *Avicennia* disappeared from the northern Mediterranean at 14 Ma (Serravalian), from southern Mediterranean and Sicily at ca. 5.3 Ma (Bessedik, 1985; Suc and Bessais, 1990), and at ca. 1.6 Ma from the southern Black Sea (Popescu *et al.*, 2010) (Fig. 6.2). This suggests that tropical trees persisted in Anatolia longer than in the other regions areas of the Mediterranean region. Among the other flora components, herbs are dominated by Poaceae, Amaranthaceae-Chenopodiaceae, Asteraceae Asteroideae, Asteraceae Cichorioideae. Steppe assemblages include *Artemisia*, *Hippophae rhamnoides* and *Ephedra*. Within them, *Artemisia* is very abundant.

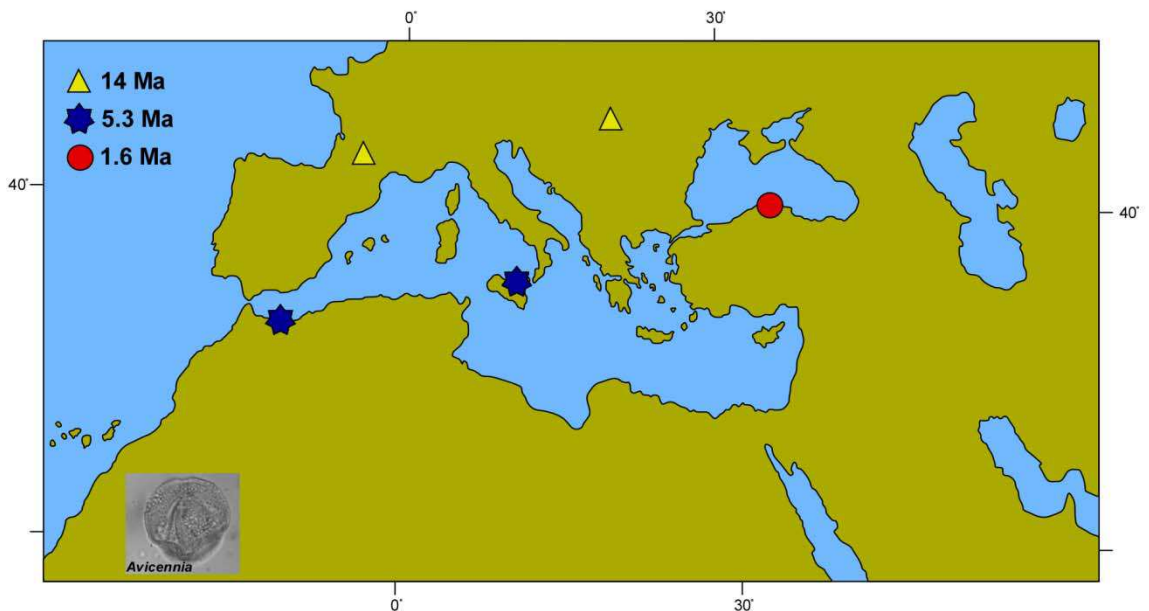


Figure 6.2 : Latest records of *Avicennia* mangrove in the Mediterranean region.

Pinus and Mediterranean xerophytes (*Quercus ilex* type, *Olea*, *Ligustrum*) are not frequent. Pollen records have similar floristic patterns to the Early Pliocene recorded at Garraf1 (NW Mediterranean), Susteren 752.72 (Netherlands), Rio Maior F16 (Portugal), Wolka Ligezawska (Poland) (Suc, 1984; Zagwijn, 1960; Diniz, 1984; Popescu *et al.*, 2010). Kasapligil (1977) recorded plant macrofossils (cones, fruits, seeds, leaves and branches) in Güvem Basin which is located at 125 km from the Black Sea coastline (NW Central Anatolia). In the Pliocene Güvem macroflora, *Glyptostrobus europoeus* is abundant.

This situation agrees with the pollen results of DSDP Site 380. Other common species is *Sequoia langsdorfii*. Among other species, there are *Carpinus miocenica*, *Magnolia sprengeri*, *Menispermum*, *Myrica banksiaefolia*, *Persea indica fossilis*, *Platanus*, *Platycarya miocenica*, *Pterocarya pterocarpa fossilis*, *Zelkova ungeri*, *Liquidambar europaeum*, *Acer angustilobum*, several species of *Quercus*, *Castanopsis*, *Ulmus*, *Alnus*, *Betula aff. Luminifera*, *Populus tremula fossilis*, *Fagus*, *Castanea*, *Castanopsis*, *Tsuga*, *Salvinia*, *Potamogeton*, *Typha*, *Pinus*, *Picea*, etc. Kasaplıgil (1977) also examined pollen grains. Pollen grains include *Alnus*, *Betula*, *Menispermum*, *Pterocarya*, *Nyssa*, *Ulmus*, *Zelkova*, *Quercus*, *Salix*, *Cedrus*, *Picea*, etc.

In NW Macedonia and Western Greece (Ptolemais Notio, Ptolemais Base, Trilophos and Lion of Amphipoli), flora is depicted by mesothermic trees (*Quercus*, *Carya*, *Pterocarya*, *Zelkova*, *Ulmus*, *Liquidambar*, *Carpinus orientalis*, *Juglans*, etc.). Among them, *Quercus*, *Pterocarya*, *Zelkova*, *Alnus*, *Betula* are abundant. Tropical trees are scarcely found. Subtropical plants (i.e. Taxodiaceae, *Engelhardia* and *Taxodium* type) are presented in small amounts. *Cathaya* is not very important in the regions except at Lion of Amphipoli.

Cedrus and *Tsuga* are frequent. Among herbs, Poaceae, Amaranthaceae-Chenopodiaceae, Asteraceae Asteroideae, Asteraceae Cichorioideae are recorded. Within them, Poaceae is very abundant in Ptolemais Notio section. Mid- and high-altitude conifers are represented by *Cedrus*, *Tsuga*, *Abies* and *Picea*. The previous palynological studies from the Ptolemais Basin show that the flora is dominated by Taxodiaceae, Cyperaceae, deciduous *Quercus* and Poaceae (Kloosterboer-van Hoeve *et al.*, 2001, 2006). In this study, more taxa have been identified when comparing with the previous microfloristic studies in the Ptolemais Basin. In addition, Cyperaceae are not abundant in the samples.

Other differences from previous studies are the abundance of mid- and high-altitude conifers (*Cedrus*, *Tsuga*, *Abies* and *Picea*) during the Early Pliocene. This could display the presence of elevated nearby reliefs. Macroflora (leaves, fruits, seeds) from the Ptolemais area evidences mixed-mesophytic forest assemblages during the Pliocene (Velitzelos, 1990). This macrofloristic results are comparable with pollen data from Ptolemais Notio and Ptolemais Base.

Pollen records of the studied areas indicate that prominent changes occurred in the flora. Results show how Anatolia recorded the floral extinctions. The Neogene successive coolings began at 14 Ma and resulted in the vanishing of thermophilous plants in the Northern Hemisphere mid-latitudes. As a consequence, two residual refuge areas developed in the Mediterranean region. One of them locates in the Northeastern Mediterranean region as documented by the persisting taxa *Zelkova*, *Pterocarya*, *Liquidambar* and *Cedrus*. The other refuge area is in the Southwestern Mediterranean region. *Laurus*, *Argania* (Sapotaceae) and *Cedrus* are relict plants in this area (Quézel and Médail, 2003). On the Anatolia coastlines, *Pterocarya fraxinifolia* and *Liquidambar orientalis* are the only thermophilous elements to persist near slopes of coastal ranges (Fig. 6.3).

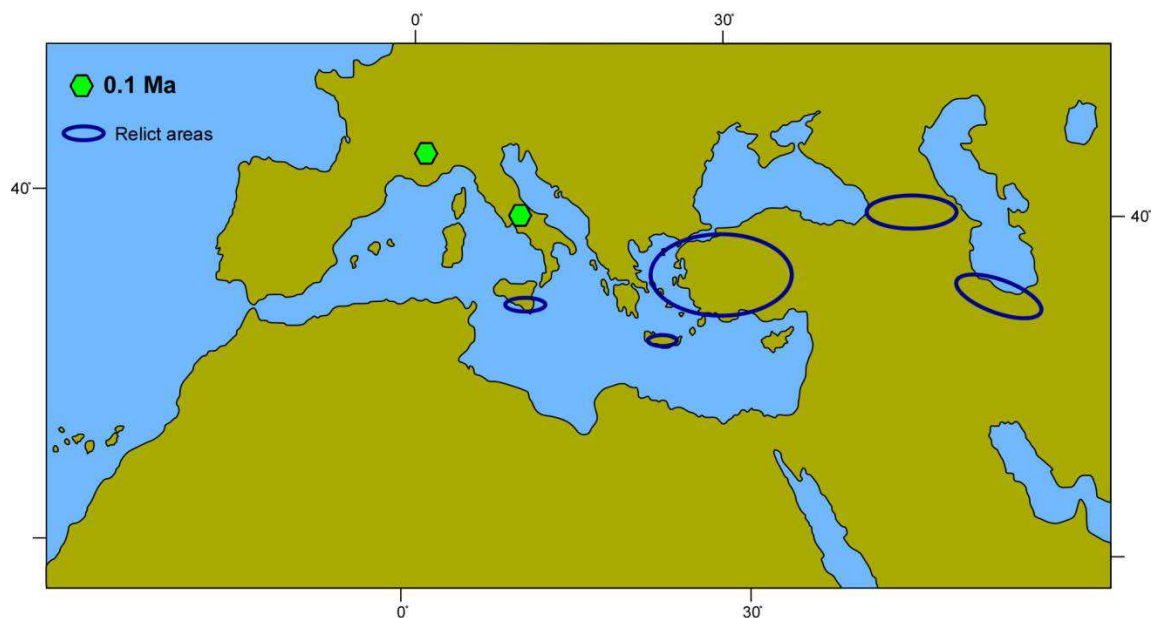


Figure 6.3 : Latest records of some thermophilous warm-temperate trees in the Mediterranean region. Dark blue circles indicate refuge areas.

In the pollen records of this study, they have been observed since the Late Miocene. This makes the study area the most important refuge domain in the region (Zohary, 1973; Quézel and Médail, 2003). Relict plants were well-defined in the pollen records. They were living in Anatolia during the Pliocene-Pleistocene, during the Early Pliocene and Latest Miocene. Most of them, such as *Carya*, *Parrotia persica*, *Cathaya*, *Cedrus* and *Tsuga* persisted in the region up today. Their disappearance seems to have happened during the Middle Pleistocene. Taxodiaceae were still living on the Rhodes Island 500 kyrs ago (Suc and Popescu, 2005).

However, Taxodiaceae disappeared from the Euxinian-Hyrcanian region sub-recently (Fig. 6.1). The persistence of relict plants in Anatolia could be explained by the effective influence of the Asiatic monsoon which almost continuously provided water masses along a longitudinal gradient allowing the maintain of plants requiring warm and humid climatic conditions despite the successive Quaternary glaciations.

6.2 Vegetation

Observed changes in vegetation according to this study will be described since the Late Miocene and discussed in this section. Abundance and diversity of identified pollen grains enable a reliable comparison with the present-day plant ecosystems. The most crucial parameters controlling the vegetation organization in altitude are both temperature and precipitation. Therefore, vegetation reconstructed from this study must be compared with the organization in altitudinal belts of present-day forest in southeastern China (Wang, 1961) (Fig. 6.4), as it is the closest living example for the Miocene European flora (Suc, 1984; Axelrod *et al.*, 1996; Jiménez-Moreno, 2005; Jiménez-Moreno *et al.*, 2005; Jiménez-Moreno, 2006; Jiménez-Moreno *et al.*, 2007a,b; 2008a,b; Jiménez-Moreno *et al.*, 2010). Thus, the North-Aegean Late Neogene vegetation could be split into ecologically different environments:

- (1) open lowlands were characterized by open vegetation with steppe elements such as Poaceae, Amaranthaceae-Chenopodiaceae, *Convolvulus* and *Ephedra*, *Artemisia*, etc., and both some halophytes such as Caryophyllaceae, Plumbaginaceae and in some places an aquatic ecosystem constituted by *Potamogeton*, *Sparganium*, *Typha*, *Thalictrum*, Liliaceae, etc.; and the Mediterranean xerophytes such as *Quercus ilex* type, *Olea*, *Ligustrum*, etc.;
- (2) a broad-leaved evergreen forest, from sea level to around 700 m altitude composed by *Glyptostrobus*, *Rhus*, Euphorbiaceae, Rutaceae, *Engelhardia*, Sapotaceae, *Distylium*, *Ilex*, etc.;
- (3) an evergreen and deciduous mixed forest, above 700 m in altitude characterized by deciduous *Quercus*, *Engelhardia*, *Taxodium* type, *Platycarya*, *Carya*, *Pterocarya*, *Carpinus orientalis*, *Celtis*, *Fagus*, *Acer*, *Hedera*, *Liquidambar* cf. *orientalis*, etc.

Within this vegetation belt, riparian vegetation is identified, composed of *Alnus*, *Salix*, *Carya*, *Carpinus*, *Zelkova*, *Ulmus*, *Liquidambar*, etc. The shrub level is dominated by *Ilex*, Caprifoliaceae, Ericaceae, etc.;

- (4) a mid-altitude deciduous and coniferous mixed forest, above 1000 m with *Betula*, *Fagus*, *Cathaya*, *Pinus*, *Cedrus* and *Tsuga*;
- (5) a high-altitude coniferous forest, above 1800 m in altitude with *Abies* and *Picea*;
- (6) herbaceous meadows in high altitude, above 2800 m, develop in more humid areas.

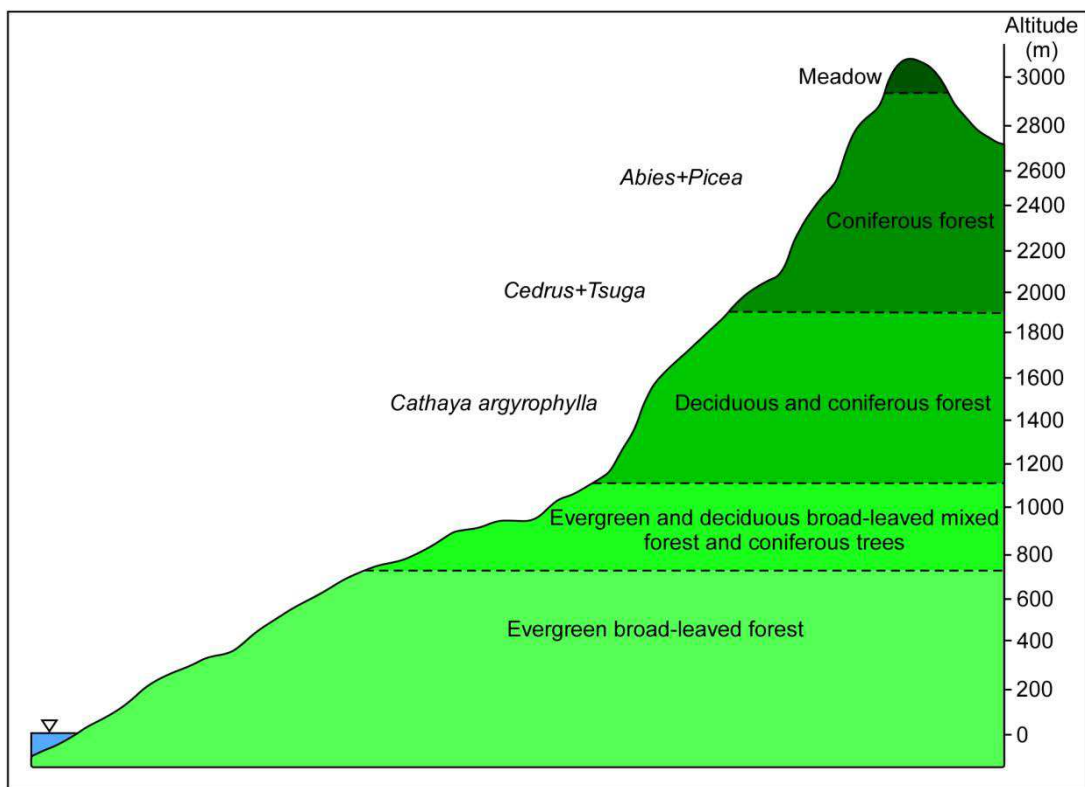


Figure 6.4 : The vegetation organization in altitude in the southeast China (ca. 25-30° of latitude) (from Wang, 1961).

The vegetation is mainly characterized by herbs in İntepe, Burhanlı and Eceabat areas (Fig. 6.5). Among them Poaceae, Asteraceae Asteroideae, Asteraceae Cichorioideae, and Amaranthaceae-Chenopodiaceae are dominated in the regions during the Early Messinian. Arboreal elements are not abundant and constituted of warm-temperate trees such as deciduous *Quercus*, *Zelkova*, *Carpinus orientalis*, *Carya*, *Pterocarya*, etc. *Pinus* was abundant in the Eceabat and Burhanlı areas.

The other elements are subtropical trees, mid- and high-altitude trees, mediterranean xerophytes, steppe elements, non-significant trees and Cupressaceae. They are not prevalent in the pollen floras from that time. During the Late Miocene, the vegetation was mainly dominated by altitudinal coniferous trees (mid- and high-altitude elements) such as chiefly *Tsuga*, *Abies* and *Picea* and Cupressaceae in Prosilio (northern Greece).

Herbs (Asteraceae Asteroideae, Asteraceae Cichorioideae, Poaceae, Amaranthaceae-Chenopodiaceae) and steppe elements (*Artemisia* and *Hippophae rhamnoides*) are in small amounts. Also mesothermic trees (*Quercus*, *Ulmus* and *Alnus*) display low abundance in the pollen floras. *Pinus* is also abundant. In addition, sediments include *Botryococcus* colonies. The presence and abundance of *Botryococcus* indicate freshwater input and lake-level fluctuations during that time. Besides, Cupressaceae is very common in the area. The vegetation is depicted by generally warm-temperate elements and herbs during the Late Miocene (latest Messinian)-Early Pliocene (earliest Zanclean) in the region (Enez, İntepe, West Seddülbahir, Ptolemais Notio, Ptolemais Base, Lion of Amphipoli and Trilophos).

In open vegetation, mainly Poaceae, Asteraceae Asteroideae, Asteraceae Cichorioideae, and Amaranthaceae-Chenopodiaceae, etc. (with water plants: *Sparganium*, *Typha*, *Potamogeton*) are found. This agrees with outcomes of the CARAIB vegetation model (Favre, 2007). Potential vegetation maps constructed from interpolation of pollen data obtained for most of them before this study confirm that herbs and mesothermic plants were largely developed in the region during the Zanclean (Figs. 6.6 and 6.7). An evergreen and deciduous mixed forest was composed of mesothermic elements such as deciduous *Quercus*, *Carya*, *Pterocarya*, *Fagus*, *Acer*, *Carpinus orientalis*, *Liquidambar orientalis*, *Ilex*, also *Engelhardia*, etc. Within this vegetation belt, a riparian vegetation is identified with *Salix*, *Alnus*, *Carya*, *Carpinus orientalis*, *Zelkova*, *Ulmus*, *Liquidambar*, etc.

In addition, mid- and high-altitude trees (*Cedrus*, *Tsuga*, *Abies* and *Picea*) increased in the region during the Late Miocene-Early Pliocene. This could be caused by some uplift of the surrounding massifs. *Cathaya*, a mid-altitude conifer, does not vary significantly in the region during that time. Mediterranean xerophytes, Cupressaceae and steppe (*Artemisia*) elements are in small amounts. Nevertheless, *Pinus* seems to be over-represented.

During the Late Miocene-Early Pliocene, vegetation on the Southwest Black Sea shorelines (as illustrated by the DSDP Site 380 pollen content) is characterized by thermophilous plants and herbs with steppe assemblages. Among thermophilous trees, subtropical (Taxodiaceae including *Taxodium* type, *Sequoia* type, *Sciadopitys*, *Engelhardia*, *Myrica*, etc.) and warm-temperate trees (i.e., deciduous *Quercus*, *Carya*, *Pterocarya*, *Juglans*, *Zelkova*, *Ulmus*, etc.) are recorded (Popescu, 2006).

Within herb and steppe elements, Poaceae, Amaranthaceae-Chenopodiaceae and *Artemisia* are abundant during that time. The similar vegetation trends were observed in southwestern Romania during the Early Pliocene where developed swampy forests competing with herbaceous vegetation (Popescu, 2006). The significant changes occurred in the vegetation during the Late Pliocene (early Piacenzian)-Early Pleistocene (Gelasian). The most of the plants were inherited from the Miocene. Most of the thermophilous plants disappeared from the region in contrast to a continuous increase in mesothermic trees.

In DSDP Site 380, it is seen that the competition between two vegetation types prevailed during the studied time-interval, opposing forest assemblages and herbs with *Artemisia* steppes. At the end of the Zanclean, herbaceous environments (with mainly Amaranthaceae-Chenopodiaceae, Poaceae, Asteraceae Asteroideae, Asteraceae Cichorioideae) dominated in the region with *Artemisia* steppes. The percentage of Amaranthaceae-Chenopodiaceae reaches up around 88%. During this time, subtropical trees were not abundant with mesothermic plants. At the early Piacenzian, corresponding to Pollen zone 4 (603-460.540 m) (see for detail Popescu *et al.*, 2010), swamp forests were well developed in contrast to herb landscapes with steppe elements.

Within swamp forests, Taxodiaceae (mainly probably *Glyptostrobus*) prevailed with *Engelhardia*, Sapotaceae, *Nyssa*, etc. Deciduous mixed forests mainly composed of mesothermic elements such as deciduous *Quercus*, *Betula*, *Alnus*, *Liquidambar*, *Fagus*, *Carpinus orientalis*, *Carpinus betulus*, *Tilia*, *Acer*, *Ulmus*, *Zelkova*, *Carya*, *Pterocarya*, etc. were largely developed during this time, but situated at higher altitude. Within this vegetation belt, riparian forest also developed with *Salix*, *Alnus*, *Carya*, *Carpinus orientalis*, *Zelkova*, *Ulmus*, *Liquidambar*, etc.

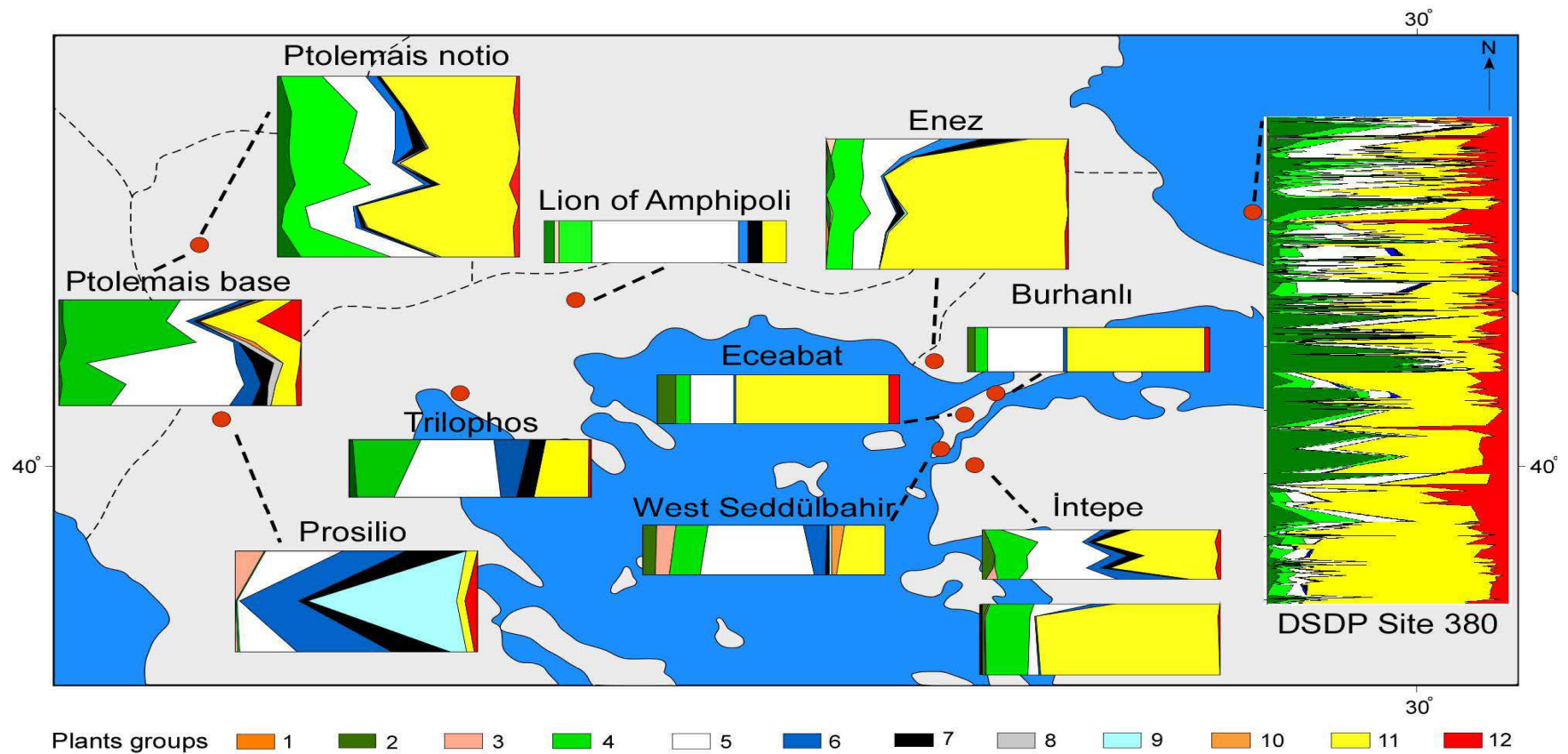


Figure 6.5 : Late Neogene synthetic pollen diagrams in the study region. Numbers show the plants groups in synthetic pollen diagrams: 1, Megathermic elements; 2, Mega-mesothermic elements; 3, *Cathaya*; 4, Mesothermic elements; 5, *Pinus*; 6, Meso-microthermic elements; 7, Microthermic elements; 8, Non-significant elements; 9, Cupressaceae; 10, Mediterranean xerophytes; 11, Herbs; 12, Steppe elements.

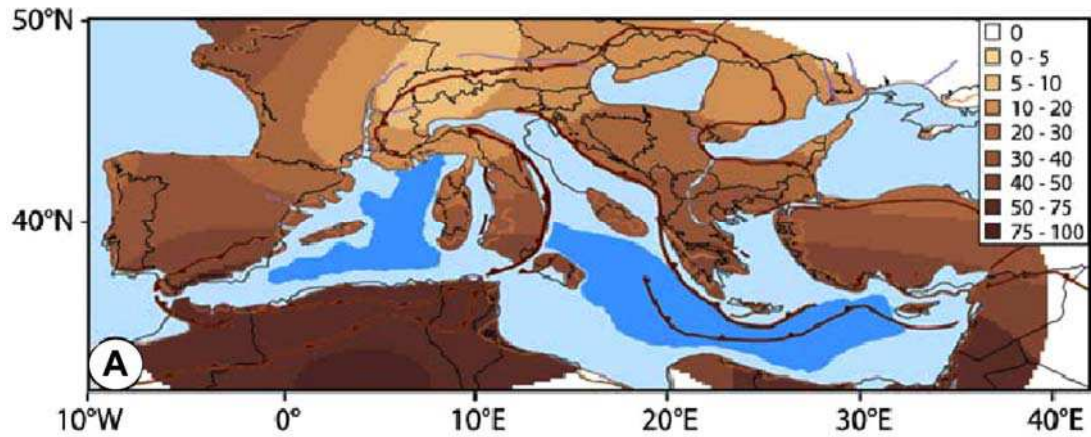


Figure 6.6 : Interpolated vegetation map for herbs during the Zanclean (Favre, 2007).

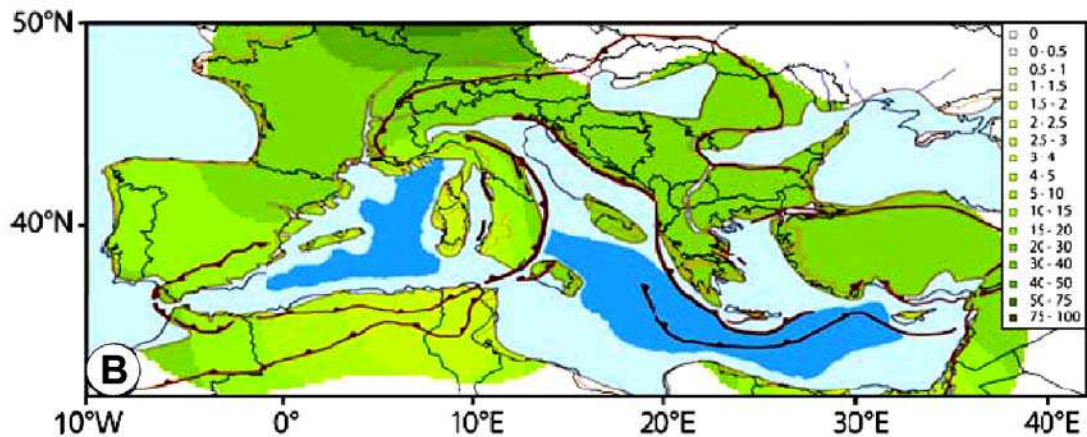


Figure 6.7 : Interpolated vegetation map for mesothermic trees during the Zanclean (Favre, 2007).

The BIOME4 and paleodata reconstructions indicate that temperate forest dominated in northeastern Europe during the Middle Pliocene (Salzmann *et al.*, 2008). Herb assemblages were mainly composed of Amaranthaceae-Chenopodiaceae, Poaceae, Asteraceae Asteroideae, Asteraceae Cichorioideae, Caryophyllaceae, Brassicaceae, *Polygonum*, *Rumex*, etc.

Steppe elements (i.e., *Artemisia*, *Ephedra*, *Hippophae rhamnoides*) were frequent during that time. At the beginning of the Pleistocene, glacial-interglacial cycles occurred with a major decrease in temperature. This caused strong alternations in vegetation. Glacial-interglacial changes in vegetation are marked by alternations of *Artemisia* steppes with herbs and forest assemblages (composed of mesothermic trees). This situation is well observed in the studied interval of DSDP Site 380.

At the Early-Middle Pleistocene (early-middle Gelasian-early Calabrian), herbs are common with steppes (*Artemisia*, *Ephedra* and *Hippophae rhamnoides*), including mostly Amaranthaceae-Chenopodiaceae, Poaceae, Asteraceae Asteroideae, Asteraceae Cichorioideae, Brassicaceae, etc. Mega-mesothermic trees are not abundant, but mesothermic plants (i.e., mainly deciduous *Quercus*, *Alnus*, *Betula*, *Carpinus orientalis*, etc.) show somewhat increasing trends.

Nevertheless, the same vegetation trend is observed in the southern Apennines (Italy). Here the vegetation is characterized by the competition between steppe taxa and forest assemblages during the Lower-Middle Pleistocene (Sabato *et al.*, 2005). The other observed vegetation types through study intervals are altitudinal forests made of microthermic and meso-microthermic trees, mediterranean xerophytes, non-significant elements and Cupressaceae.

Microthermic (*Abies* and *Picea*) and meso-microthermic (*Cedrus* and *Tsuga*) conifers are not frequent as well as *Pinus*, mediterranean xerophytes (*Olea*, *Quercus ilex* type, *Ligustrum*), non-significant elements (Rosaceae and Ranunculaceae) and Cupressaceae.

6.2.1 The development of *Artemisia* steppes

Artemisia is the well-known cosmopolitan wind-pollinated sagebrush. Past evidences of *Artemisia* steppes have probably existed since the Middle Tertiary from arid or subarid areas of temperate Asia (Wang *et al.*, 2003; Yunfa *et al.*, 2010). Development of *Artemisia* in mid-altitudes of central Asia was strongly encouraged by uplift of the Tibetan Plateau during the Miocene and the *Artemisia* development and expansion is drawn versus the global cooling curve and Tibetan uplift history (in Fig. 6.8). The Moreover, the other effects on diversification and distribution of *Artemisia* are global cooling and Asian monsoon in that area.

The presence of open vegetation without a significant development of *Artemisia* steppes in other regions of Mediterranean (i.e., in the southern Mediterranean) is established since the Earliest Miocene (Suc *et al.*, 1995a, b; Bachiri Taoufiq *et al.*, 2001; Jiménez-Moreno and Suc, 2007). Pollen results from the studied area enable information on the earliest development of *Artemisia* steppes in Anatolia in time and space.

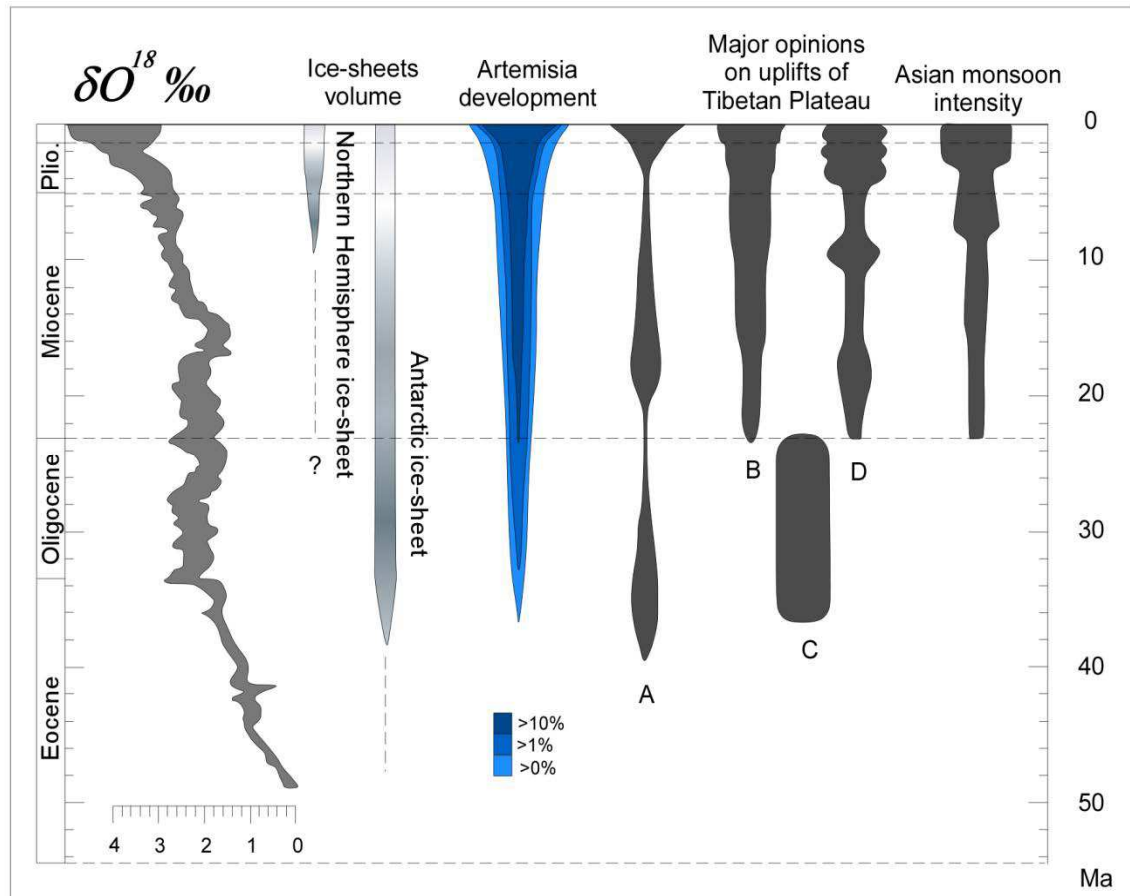


Figure 6.8 : Diagram indicating the origin and development of *Artemisia* (from Yunfa *et al.*, 2010), with global climate (Zachos *et al.*, 2008), capital letters in the diagram: A, B, C, D are adapted from Li, 1991; Li and Fang, 1999; An *et al.*, 2006; Rowley and Currie, 2006; d. Wan *et al.*, 2007) and the Asian monsoon intensity (Wan *et al.*, 2007).

The occurrence of *Artemisia* in Anatolia could be divided into three parts as the Miocene, Pliocene and Pleistocene. The earliest records of *Artemisia* steppes in Anatolia concern the Early Miocene (Aquitanian~23.0-20.4 Ma) from the central Taurus, more precisely the Ermenek region (Biltekin, unpublished). In this area, *Artemisia* is observed in almost all the samples and reaches up to around 10%.

In addition, *Artemisia* steppes were found in Çatakbağyaka (southwestern Aegean region) during the Middle Miocene (Langhian) (Jiménez-Moreno, 2005). Also *Artemisia* was found in western Anatolia (Seyitömer Basin, Kütahya) at the Late Early-Middle Miocene (Yavuz Işık, 2007).

In other parts of the world, it was common in the western part of the Tibetan Plateau during the Miocene (Yunfa *et al.*, 2010) and in the Snake River Plain (America) during the Miocene (~12 Ma) (Davis and Ellis, 2010), in the western north America at the Early Miocene, in the Northeastern America at the Middle Miocene and in the central Europe during the Late Oligocene (Graham, 1996).

The main development of the *Artemisia* steppes with open herbaceous vegetation in Anatolia began during the Late Miocene-Early Pliocene (Zanclean) and in the Ponto-Euxinian region during the earliest glacial phases. In the other studied regions i.e., Eceabat, Burhanlı, İntepe, *Artemisia* is present but in very small amounts.

The marked changes occurred between the Miocene and the Pliocene. Because of this, high resolution pollen records of the Black Sea DSDP Site 380 are very informative about the development of *Artemisia* steppes in Anatolia (Fig. 6.9). In the studied intervals, the increase of *Artemisia* continued through the Pliocene.

It reached up to approximately 62% during the Pliocene. When the glacial-interglacial cycles began at the beginning of the Pleistocene, *Artemisia* was very abundant. The abundance of *Artemisia* steppes have continued along the whole Pleistocene until present. Maximum abundance of *Artemisia* occurred at 401.44 m in DSDP Site 380. In this depth, *Artemisia* reaches up about 85%.

According to the pollen results, the earliest settlement of sagebrush (*Artemisia*) steppes seems to be extended to the Early Miocene (Aquitainian) in the central Taurus (Biltekin, unpublished). Overall the development of *Artemisia* in Anatolia could result from the combined effects of uplift of the Tibetan Plateau, onset of global cooling and reinforcement of the Asian monsoon (Zhisheng *et al.*, 2001, Yunfa *et al.*, 2010).

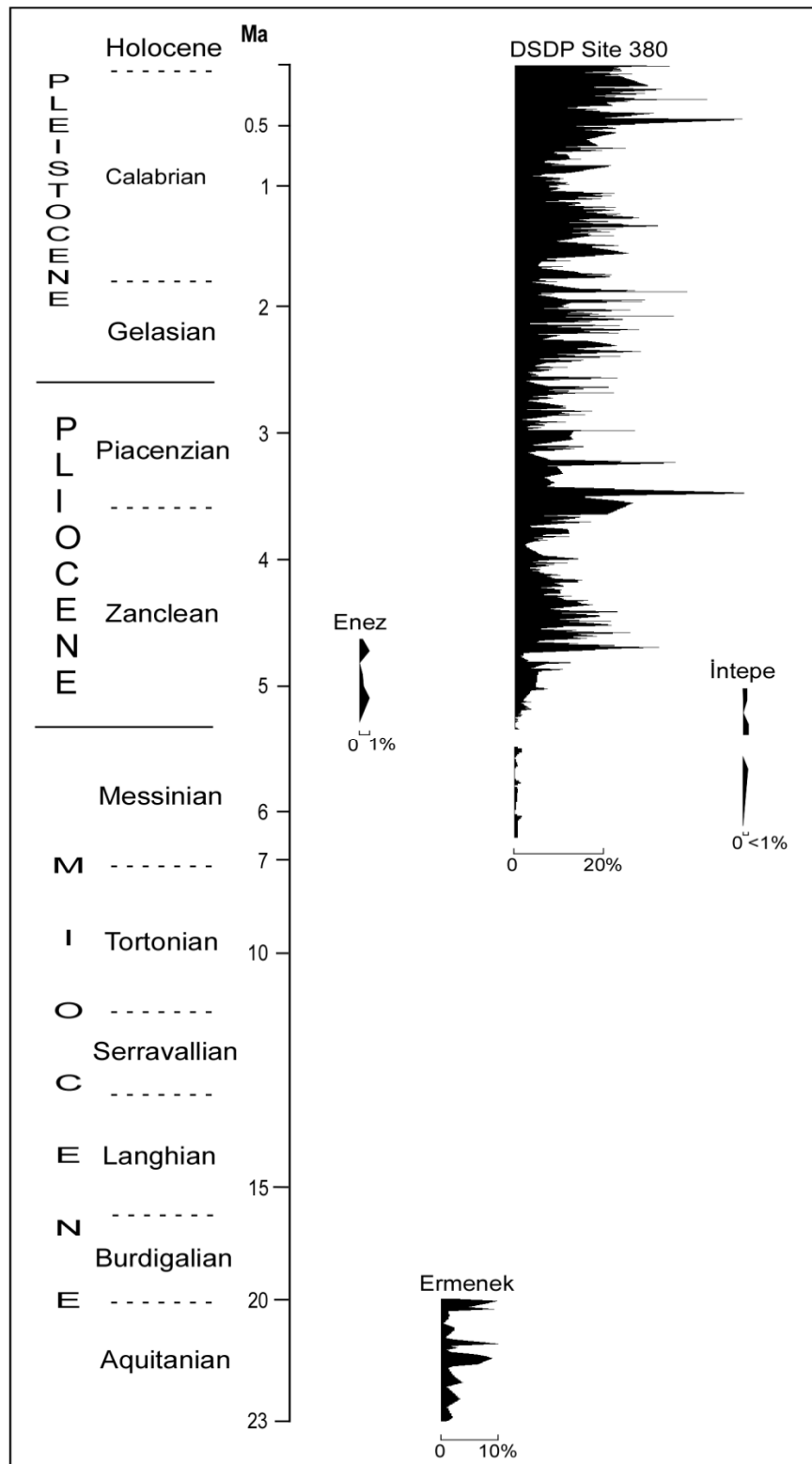


Figure 6.9 : Chronological distribution of *Artemisia* steppes since the Early Miocene until today in the studied region.

6.3 Climate

6.3.1 Global climate context during the Miocene and Pliocene

Neogene climate constitutes the transition from greenhouse conditions of Paleogene to the icehouse conditions of Quaternary. East Antarctic Ice Sheet (EAIS) expanded at the beginning of the Neogene (Pagani *et al.*, 1999; Zachos *et al.*, 2001) (Fig. 6.10). This situation is well-documented at worldwide-scale with decrease in temperature and positive oxygen isotope incursion (Miller *et al.*, 1991; Zachos *et al.*, 2001). The benthic foraminiferal oxygen isotope values give the evidence for at least nine glacial events during the Miocene, four of them occurred during the Early Miocene (Miller *et al.*, 1991; Pagani *et al.*, 1999).

Until the Middle Miocene (~15 Ma) global ice volume stayed low (with slightly bottom water temperatures) with several brief glaciations (i.e., Mi-events) (Zachos *et al.*, 2001). The low CO₂ values are in correspondence with major glaciations (Kürschner *et al.*, 2008). At the Late-Middle Miocene (Upper Burdigalian-Lower Langhian, ~17-15 Ma) a warm phase occurred known as the Miocene Climatic Optimum (Zachos *et al.*, 2001, 2008) (in Fig. 6.10). During this warm phase, CO₂ concentrations were 500 ppmv (Kürschner *et al.*, 2008). After this warm period, the Monterey cooling event occurred at 14 Ma ago. This event coincides with ice sheet expansion in Antarctica (Flower and Kennett, 1993, 1994; Miller *et al.*, 1991; Zachos *et al.*, 2001).

During the early Late Miocene, low-mid altitude surface waters of world oceans warmed up. This global climate variability was induced by two events: the closure of the Indonesian Seaway at 8-5.2 Ma and the onset of the Tibetan Plateau uplift (Zhisheng *et al.*, 2001; Zhang *et al.*, 2009; Yunfa *et al.*, 2010). During the Late Miocene (Tortonian), high seasonality existed in the Eastern Mediterranean (Eronen *et al.*, 2009). Summer drought increased from Tortonian to the Messinian. High evaporation and low rainfall occurred with lower seasonality due to the increased duration of summer aridity in the Eastern Mediterranean during the Messinian (Eronen *et al.*, 2009).

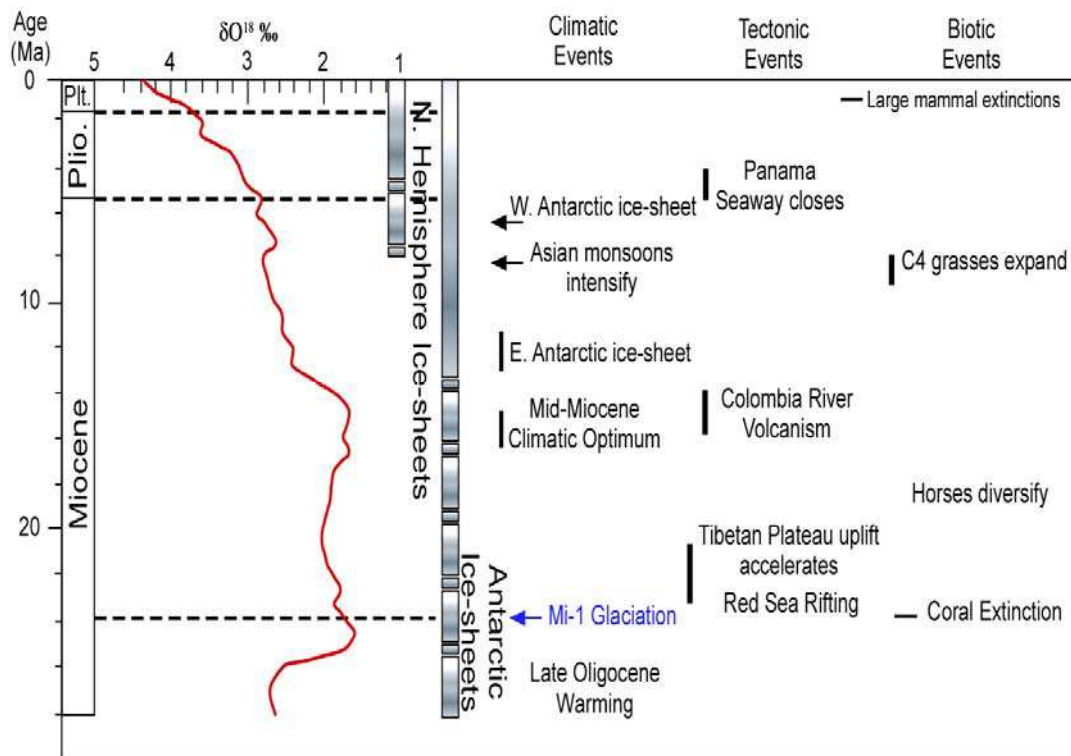


Figure 6.10 : Global deep-sea oxygen records with main events (taken from Zachos *et al.*, 2001).

The Pliocene constitutes the transition from relatively warm episodes to the cooler climates of the Pleistocene (Suc, 1984; Dowsett and Poore 1991; Lisiecki and Raymo 2007; Haywood *et al.*, 2009). The Pliocene epoch could be split into three phases: (1) the Early Pliocene warm period including three inner subdivisions, (2) a relatively short-lived ‘warm interval’ at ca. 3 Ma, known as the mid-Pliocene warm interval and (3) a climatic deterioration during the Late Pliocene leading to the high-magnitude climate variability associated with glacial/interglacial cycles of Pleistocene.

Although a progressive cooling existed during the Tertiary, the Pliocene seems to have been warmer than today (Jansen *et al.* 2007). The Early Pliocene was an interval of global warmth characterized by high CO₂ levels (Van der Burgh *et al.*, 1993; Raymo *et al.*, 1996; Kuerschner *et al.*, 1996; Billups *et al.*, 2008) and warm sea-surface temperatures (in upwelling regions and at high latitudes) (e.g., Dowsett *et al.*, 1992; Herbert and Schuffert, 1998; Dowsett *et al.*, 2005; Wara *et al.*, 2005; Lawrence *et al.*, 2006; Ravelo *et al.*, 2007). During the middle Pliocene (~3 Ma), the paleontological data, sea level, vegetation, land-ice distribution, sea-ice distribution and sea surface temperatures (SST) were reconstructed.

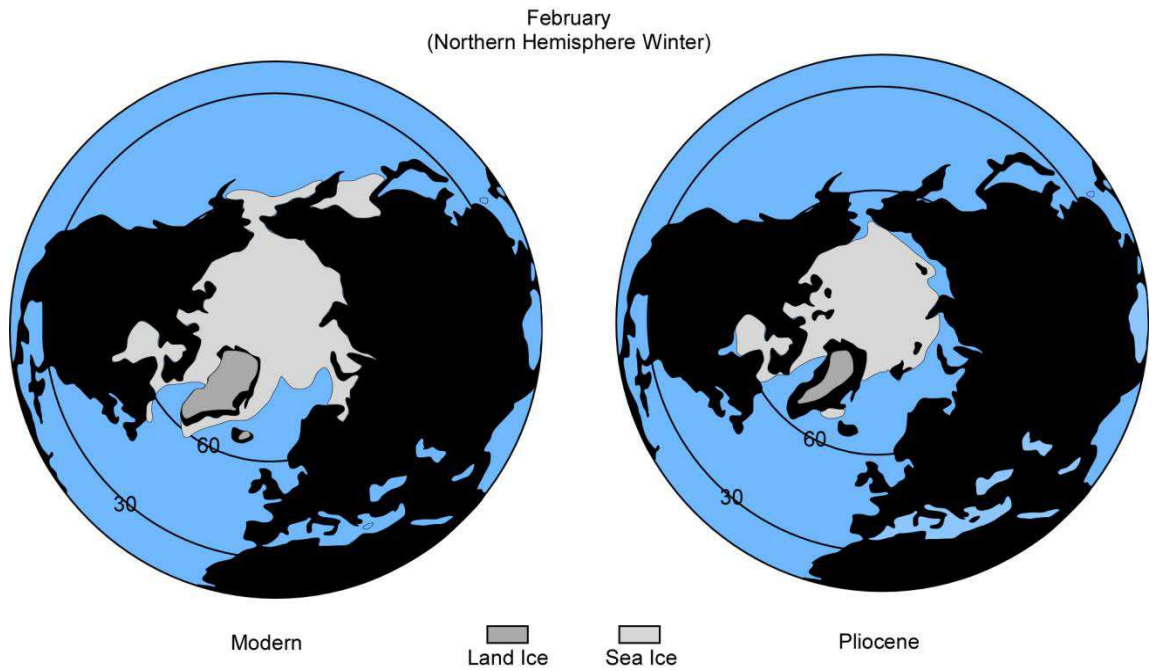


Figure 6.11 : Distribution of modern and mid-Pliocene land and sea ice in the Northern Hemisphere (from Dowsett *et al.*, 1994).

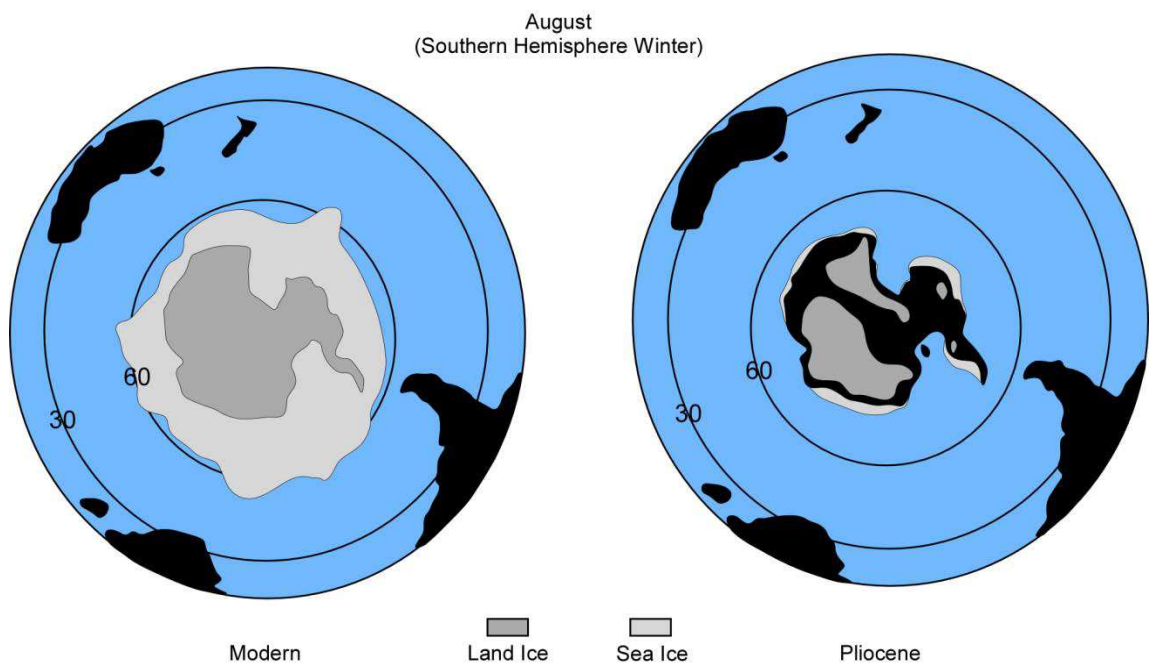


Figure 6.12 : Distribution of modern and mid-Pliocene land and sea ice in the Southern Hemisphere (from Dowsett *et al.*, 1994).

The middle Pliocene sea level was at least 25 m higher than present because of the reduction in size of the East Antarctic Ice Sheet (Dowsett *et al.*, 1994). The Pliocene winter reconstructions (Dowsett *et al.*, 1994) indicate that sea ice covered the north coast of Siberia and Greenland in the Northern Hemisphere, regions which are today completely covered by ice during the winter (Fig. 6.11). In the Southern Hemisphere, sea ice was then in the Weddell Sea, the coast of the Queen Maun Land, Wilkes Land and Marie Byrd Land (Fig. 6.12) (Dowsett *et al.*, 1994).

At the end of the Pliocene, with the onset of major Northern Hemisphere glaciations at approximately 2.6 Ma, climate got cooler and glacial–interglacial cycles appeared in the Northern Hemisphere (Lisiecki and Raymo, 2007). The mid-Pleistocene transition (MPT) was a crucial event when the dominant periodicity of glacial response changed from 41 to 100 kyrs. The “saw-tooth” asymmetry of glacial cycles first appears shortly after the onset of major Northern Hemisphere Glaciations and duration of interglacial phases decreased at 1.4 Ma (Lisiecki and Raymo, 2007).

6.3.2 Climatic evolution of the studied areas

Results of pollen data provide a climate synthesis of the studied areas during the Late Miocene-Early Pleistocene. Before the Messinian Salinity Crisis, at the early Messinian, abundance of mega-mesothermic and mesothermic trees in the Ponto-Euxinian region indicate that subtropical, i.e. warm climate conditions, existed during that time in the region (Popescu, 2006).

Climate also was humid according to the existence of thermophilous elements which require very humid conditions during all the year (Wang, 1961). In the Northern Aegean area, in the İntepe, Burhanlı and Eceabat regions (Melinte *et al.*, 2009), the high abundance of open vegetation elements (Poaceae, Asteraceae Asteroideae, Asteraceae Cichorioideae, and Amaranthaceae-Chenopodiaceae, etc.) indicate drier climate conditions.

However, abundance of mesothermic trees (deciduous *Quercus*, *Carya*, *Zelkova*, etc.) with few subtropical taxa (Taxodiaceae, *Engelhardia*) also suggests a coastal freshwater marsh (Fig. 6.13). At the Late Miocene (before the MSC), Prosilio pollen flora shows that the presence and high abundance of mid- (mainly *Tsuga*) and high-altitude (*Abies* and *Picea*) conifers and high abundance of Cupressaceae in the northern Greece during this time-interval.

The existence of mid- and high-altitude trees with Cupressaceae suggests that some elevated massifs existed in the region with a cool-temperate climate. During the Late Miocene (latest Messinian)-Early Pliocene (earliest Zanclean), after the MSC, in Enez, West Seddülbahir, İntepe, Ptolemais Notio, Ptolemais Base, Lion of Amphipoli and Trilophos, the vegetation mainly characterized by herbs (Poaceae, Asteraceae Asteroideae, Asteraceae Cichorioideae, and Amaranthaceae-Chenopodiaceae, etc.) while forest assemblages were composed of mesothermic elements such as deciduous *Quercus*, *Carya*, *Zelkova*, etc. (in Fig. 6.13). This points out warm and dry climate conditions at low altitude in the region.

The studies based on CO₂ trend during the Miocene indicates that the presence of C4 plants (grasslands) at the Middle-Late Miocene (Kürschner *et al.*, 2008). Another significant change observed in the pollen floras is the increase in conifer (mainly *Cedrus*, *Abies* and *Picea*) (Melinte *et al.*, 2009). Calculation of the mean annual temperature based on pollen records have been performed using the “climatic amplitude” transfer function (Fauquette *et al.*, 1998). For İntepe samples 22-26, calculated mean annual temperature is 16.5°C (range: 15-18°C) (Melinte *et al.*, 2009). The same trend, i.e. the increase in conifers, is also observed in areas (Ptolemais Notio, Ptolemais Base, Lion of Amphipoli and Trilophos). This could be caused by some uplift of the massifs of the region as considered in the İntepe region.

During the Late Miocene-Early-middle Pliocene, after the MSC, mega-mesothermic and mesothermic elements were abundant in the Ponto-Euxinian region, in contrast to herbs with some development of *Artemisia* steppes during cooler phases of Pollen zone 1 (Popescu, 2006; Popescu *et al.*, 2010). Warm and humid climate existed in the region during interglacials. While mesothermic plants increased during the Late Miocene-Early Pliocene, the impoverishment in thermophilous trees since the Miocene is regarded as the result of a continuous and progressive decrease in temperature since 14 Ma (Zachos *et al.*, 2001; Darby, 2008). During the Middle-Late Zanclean, according to pollen record from DSDP Site 380, the vegetation was characterized by dominant herbs with weakly developed *Artemisia* steppes. Subtropical trees are not abundant. Mesothermic trees are frequent. Cupressaceae and *Cathaya* were rare during that time which corresponds to Pollen zone 2 (702.80-624 m) of Popescu *et al.* (2010).

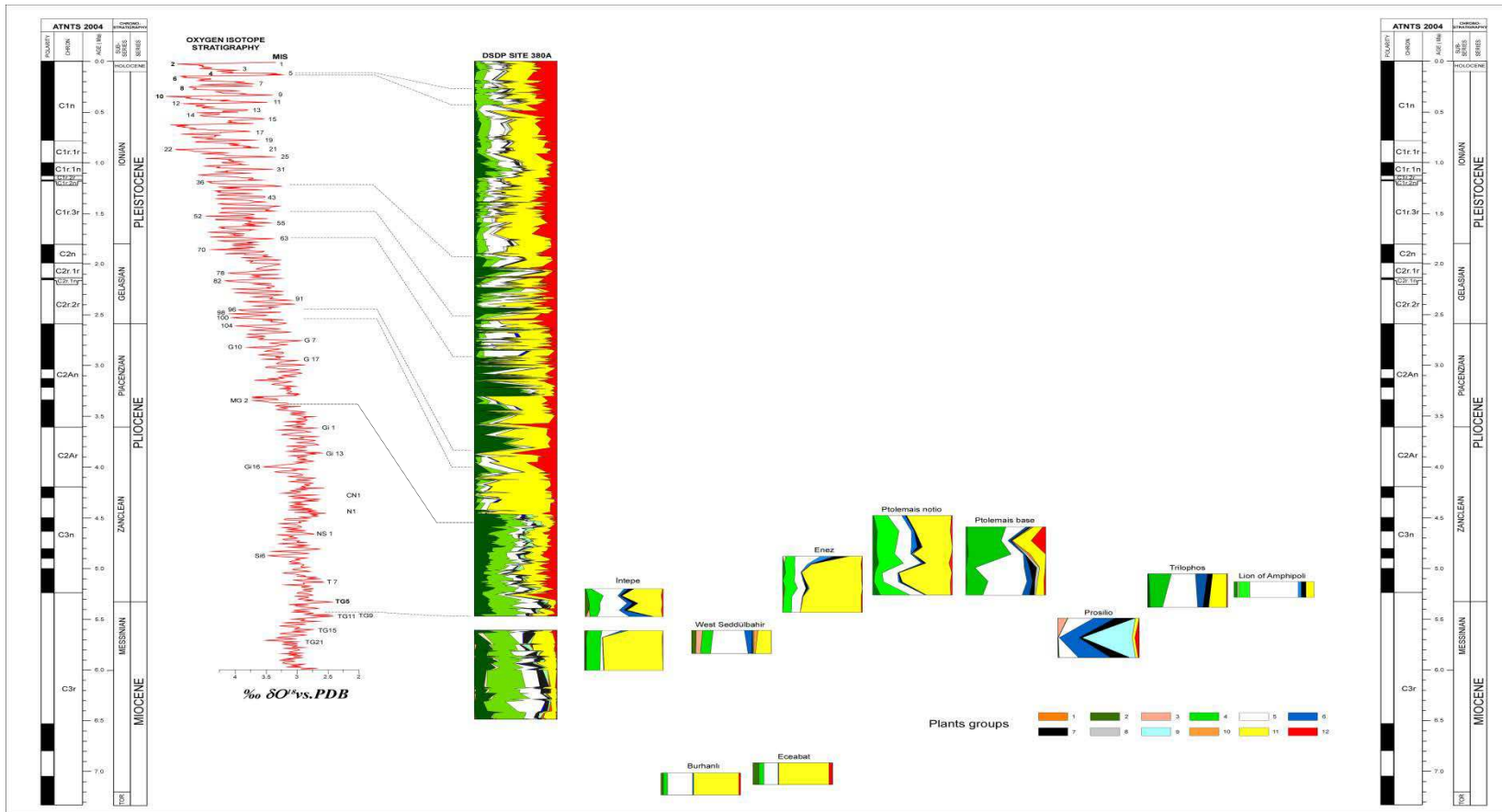


Figure 6.13 : Synthetic pollen diagrams of the studied localities. DSDP Site 380: S. Boroj, D. Biltekin and S.-M. Popescu, Grouping of plants follows Suc (1984): 1, Megathermic elements; 2, Mega-mesothermic elements; 3, *Cathaya*; 4, Mesothermic elements; 5, *Pinus*; 6, Meso-microthermic elements; 7, Microthermic elements; 8, Non-significant elements; 9, Cupressaceae; 10, Mediterranean xerophytes; 11, Herbs; 12, Steppe elements. The reference oxygen isotope curve is from Shackleton *et al.* (1990, 1995).

During that time climate was not very dry but cooler conditions existed. At the Latest Zanclean, vegetation is depicted by herbs with higher amounts of *Artemisia*. Mega-mesothermic and mesothermic trees are then not very important. The high presence of herbs and *Artemisia* steppes during this time suggests that climate was cooler and drier. Swamp forests (with *Glyptostrobus*, *Engelhardia*, Sapotaceae, *Nyssa*) seriously reduced at ca. 3.4 Ma but persisted during the Piacenzian (Late Pliocene) in contrast to significantly extending herbs with *Artemisia* steppes. Reduced deciduous mixed forests with mesothermic trees (deciduous *Quercus*, *Betula*, *Alnus*, *Liquidambar*, *Fagus*, *Carpinus orientalis*, *Carpinus betulus*, *Tilia*, *Acer*, *Ulmus*, *Zelkova*, *Carya*, *Pterocarya*) persisted too.

During this time, herbs composed of Amaranthaceae-Chenopodiaceae, Poaceae, Asteraceae Asteroideae, Asteraceae Cichorioideae, Caryophyllaceae, Brassicaceae, *Polygonum*, *Rumex*, etc. strongly strengthened. However, steppe elements are low during that time. This documents that cooler and drier climatic conditions existed since 3.4 Ma. There is some starting competition between moister-warmer phases to cooler-drier ones announcing the forthcoming interglacial-glacial phases. At ~3 Ma, paleoclimatic studies show that a warm event existed (Draut *et al.*, 2003).

Climate was warmer than today in the Arctic regions of North America, Iceland, Russia and western-central Europe (Dowsett *et al.*, 1994). In addition, diatom studies in the deep sea cores (DSDP 266, ODP 699A, ODP 747A and Eltanin Core 50-28) Southern Ocean also support that climate was warmer during that time, summer surface temperatures are more than 3-4°C warmer than present at latitudes between 55° and 60°S (Barron, 1996). This warmer period is also documented by pollen data of DSDP Site 380.

During this time, forest communities were somewhat more developed, especially represented by mega-mesothermic trees such as mainly Taxodiaceae, in contrast to lower representation of herbs and steppe elements. Results of the GISS General Circulation Model (GCM) indicate the following temperatures in southern Europe: 6°C warmer over the Iberian Peninsula, 2-4°C warmer over the rest of southern Europe. Precipitation and winter soil moisture were close to modern levels (Chandler *et al.*, 1994). At the beginning of Pleistocene (~2.6 Ma), when climate got cooler, glacial-interglacial cycles turned into a strong and rapid competition between forests and open vegetations.

At the earliest Gelasian (Early Pleistocene), mega-mesothermic elements continued to rarefy. Nevertheless within them, Taxodiaceae (probably *Glyptostrobus*), *Engelhardia*, Sapotaceae, and *Nyssa* survived. Mesothermic elements composed of deciduous *Quercus*, *Betula*, *Alnus*, *Liquidambar*, *Fagus*, *Carpinus orientalis*, *Carpinus betulus*, *Tilia*, *Acer*, *Ulmus*, *Zelkova*, *Carya*, *Pterocarya*, etc. also almost disappeared. Herb phases were long with a prevalence of glacials over interglacials. During the Earliest Ioanian (~1.8 Ma), mega-mesothermic elements were in lower amounts (except several short peaks in the diagram). From time to time, mesothermic trees were abundant despite a longer and intense development of herbs with high *Artemisia* at the end of the interval. This demonstrates shorter and warmer interglacials in opposition with longer, colder and drier glacials. In the Early-Middle Ioanian, thermophilous forest elements enlarged again with strong repeated fluctuations between forest and open environments. After this time, herbs (with *Artemisia* steppes) have continued to increase up to the present-day.

7. CONCLUSIONS

This study has been carried out on 11 sections (in the Black Sea: DSDP 380 Site; in Thrace: Enez; in the Northern Aegean: İntepe, Seddülbahir, Burhanlı, Eceabat; in Macedonia: Ptolemais Notio and Ptolemais Base, in Greece: Prosilio, Lion of Amphipoli, and Trilophos). Most of the sections are well-dated by nannofossils. Pollen grains are generally well preserved in these sediments. Totally, 436 samples have been analysed, 378 of these samples (Early Pliocene-Early Plesitocene) are from the Site 380 borehole and the remaining 58 samples come from outcrops in the other areas. In this study, 107 different taxa have been identified representative of various ecological environments. Pollen floras from these localities are rich and diversified and taxa have been arranged from the temperature requirement viewpoint according to Nix's classification (1982):

- (1) megathermic elements (tropical): *Avicennia alba*, Euphorbiaceae, Rubiaceae and Rutaceae;
- (2) mega-mesothermic elements (subtropical): Taxodiaceae including *Taxodium*-type, *Engelhardia*, *Platycarya*, Sapotaceae, *Distylium*, *Microtropis fallax*, *Ginkgo*, *Loropetalum*, Arecaceae and *Cathaya*;
- (3) mesothermic elements (warm-temperate): *Carpinus orientalis*, *Juglans*, *Juglans* cf. *cathayensis*, *Carya*, *Pterocarya*, *Liquidambar orientalis*, *Platanus*, *Nyssa*, *Ulmus*, *Zelkova*, *Celtis* and *Eucommia*;
- (4) meso-microthermic elements (cool-temperate): *Cedrus* and *Tsuga*.
- (5) microthermic elements (boreal): *Abies* and *Picea*.

Nevertheless, an important factor could be as today the altitude which controls temperature and precipitation. Hence, vegetation should be organized in altitudinal belts after comparison with the current plant ecosystems (see Discussion chapter). Pollen records of the studied localities indicate changes in vegetation and climate in time and space. The vegetation is depicted mainly by herbs in İntepe, Burhanlı and Eceabat during the Early Messinian.

Before the Messinian Salinity Crisis (MSC), trees are relatively abundant in the İtepe area and mainly composed of mesothermic elements (deciduous *Quercus*, *Carya*, *Zelkova*, etc.) while vegetation is dominated by herbs (Poaceae, Asteraceae, Asteroideae, Amaranthaceae-Chenopodiaceae, Caryophyllaceae, etc.) with *Artemisia*.

At the Late Miocene, mid- (mainly *Tsuga*) and high-altitude (*Abies* and *Picea*) coniferous trees were abundant in Prosilio (Northern Greece). Another significant result in the pollen spectra of Prosilio is the abundance of Cupressaceae, the curve of which is consistent with those of mid- and high-altitude trees. This suggests that cooler climate existed in the region. Moreover, the abundance of altitudinal conifers displays that some uplift of the surrounding massifs occurred before that time.

Just after the MSC, at the Latest Messinian-Earliest Zanclean, herbs are still abundant in İtepe, Enez, West Seddülbahir, Trilophos, Lion of Amphipoli, Ptolemais Notio and Ptolemais Base (Poaceae, Amaranthaceae-Chenopodiaceae, Asteraceae, etc.). Among arboreal trees, mesothermic elements are common at this time. Within subtropical trees, *Ginkgo* is recorded at Enez. Today, *Ginkgo biloba* is the only species of Ginkgoaceae, living in China. The other prominent result is a significant increase in altitudinal trees (*Cedrus*, *Tsuga*, *Abies* and *Picea*) which denotes some uplift in the Dardanelles area during the MSC.

Vegetation and climate of the Pliocene time is accurately documented by the high-resolution pollen record from DSDP Site 380 (SW Black Sea) characterized by various plant assemblages. Most of them were inherited from the Miocene. Several megathermic (tropical) trees suffered because of the progressive decrease in temperature since 14 Ma. Within megathermic (tropical) elements, it is appreciable to mention the last evidence for the Mediterranean region *s.l.* of *Avicennia alba*, a mangrove tree, in the Early Pleistocene from DSDP Site 380, at about 1.6 Ma.

As several records of *Avicennia* are known from the underlying sediments of DSDP Site 380, one may postulate that a residual *Avicennia* mangrove persisted on the coastal areas in the Ponto-Euxinian region. On the whole, according to Site 380 pollen record, it is established that a strong competition between arboreal trees and herbs with *Artemisia* steppes started in the Black Sea region at the Earliest Pliocene which became more pronounced after 2.6 Ma.

During the Early Pliocene (at the end of the Zanclean), herbs composed of mainly Amaranthaceae-Chenopodiaceae, Poaceae, Asteraceae Asteroideae, Asteraceae Cichorioideae developed with *Artemisia* steppes. During this time, Amaranthaceae-Chenopodiaceae reaches up ca. 88%. In addition, subtropical trees were not as abundant as mesothermic plants. This suggests cooler and probably drier climatic conditions in the region.

Swamp forests (with *Glyptostrobus*, *Engelhardia*, Sapotaceae, *Nyssa*) persisted during the Piacenzian (Late Pliocene) in contrast to extending herbs with *Artemisia* steppes. Reduced deciduous mixed forests with mesothermic trees (deciduous *Quercus*, *Betula*, *Alnus*, *Liquidambar*, *Fagus*, *Carpinus orientalis*, *Carpinus betulus*, *Tilia*, *Acer*, *Ulmus*, *Zelkova*, *Carya*, *Pterocarya*) persisted too. During this time, vegetation was depicted by herbs such as mainly Amaranthaceae-Chenopodiaceae, Poaceae, Asteraceae Asteroideae, Asteraceae Cichorioideae, Caryophyllaceae, Brassicaceae, *Polygonum*, *Rumex*, etc., containing some aquatic plants e.g., *Sparganium*, *Potamogeton*, *Typha*, etc. Steppe elements are composed of *Artemisia*, *Ephedra*, *Hippophae rhamnoides*). They are in small amounts during that time. This indicates that cooler and drier climatic conditions existed.

At the Earliest Gelasian (Early Pleistocene), mega-mesothermic elements strongly rarefied. Among them, Taxodiaceae (probably *Glyptostrobus*), *Engelhardia*, Sapotaceae, and *Nyssa* persisted. Deciduous mixed forest assemblages composed of mesothermic trees (warm-temperate) such as *Betula*, *Fagus*, *Tilia*, *Acer*, *Ulmus*, *Carya*, etc. almost disappeared too. Within this vegetation belt, a riparian forest also perpetuated with *Salix*, *Alnus*, *Carya*, *Carpinus orientalis*, *Zelkova*, *Ulmus*, *Liquidambar*, etc.

Very weak fluctuations are recorded opposing thermophilous trees and the highly dominant herbs. Herb phases were long with a prevalence of glacials over interglacials. During the Earliest Ioanian (Middle Pleistocene), vegetation is characterized by mega-mesothermic elements with low amounts (except some peaks in the diagram), high amounts of mesothermic trees and longer temporal development of herbs with high *Artemisia* at the end of the interval. This demonstrates shorter and warmer interglacials in opposition with longer, colder and drier glacials.

At the Early-Middle Ionian (394.50-302.40 m), is observed an increase in thermophilous forest elements with strong repeated fluctuations between forest and open (with higher *Artemisia* steppes) environments. This indicates prominent climatic fluctuations between interglacials and glacials. After this period, herbs mostly Amaranthaceae-Chenopodiaceae, Poaceae, Asteraceae Asteroideae, Asteraceae Cichorioideae, Brassicaceae, etc., with *Artemisia* steppes (with other steppe elements: *Ephedra* and *Hippophae rhamnoides*) have continued to increase until today.

An outstanding result is the development of *Artemisia* steppes in Anatolia. The earliest settlement of *Artemisia* steppes in Anatolia have reached to the Early Miocene (Aquitanian~23.0-20.4 Ma) in the Ermenek region, central Taurus (Biltekin, unpublished). *Artemisia* is common in this region during the Early Miocene (ca. 10%). The noticeable change is located between the Miocene and the Pliocene. The high-resolution pollen record of DSDP Site 380 clearly documents the development of *Artemisia* steppes in Anatolia. The main development of *Artemisia* with non-boreal (herbaceous) vegetation in Anatolia started during the Early Pliocene in the Ponto-Euxinian region. Indeed, at Eceabat, Burhanlı and İtepe localities, *Artemisia* is found in small amounts. The increase of *Artemisia* continued through the Pliocene (reaching up about 62%).

At the beginning of the Pleistocene (~2.6 Ma), with the start of the glacial-interglacial cycles, *Artemisia* steppes continued to develop through the Pleistocene until today. The development of *Artemisia* in Anatolia could both relate with the uplifting of the Tibetan Plateau, global cooling and reinforcement of the Asian monsoon.

At last, thermophilous elements such as *Pterocarya* and *Liquidambar* have persisted on coastal slopes of Anatolia. They have been observed in the pollen floras since the Early Miocene (Aquitanian). Some others, such as *Carya*, *Parrotia persica*, *Cathaya* and *Tsuga* persisted in the region. Their disappearance seems to have happened during the Middle Pleistocene. However, Taxodiaceae disappeared from the Euxinian-Hyrcanian region sub-recently. The persistence of relict plants in Anatolia can be explained by the significant influence of the Asian monsoon which takes place along a longitudinal gradient. This brought about the preservation of relict plants in Anatolia.

REFERENCES

- Adams, C. C., Benson, R. H., Kidd, R. B., Ryan, W. B. F. and Wright, R. C., 1977. The Messinian salinity crisis and evidence of Late Miocene eustatic changes in the world ocean. *Nature*, **269**, 383–6.
- Aguirre, J., 1998. El Plioceno del SE de la Península Ibérica (provincia de Almería). Síntesis estratigráfica, sedimentaria, bioestratigráfica y paleogeográfica. *Revista de la Sociedad Geológica de España* **11**, pp. 297–315.
- Akcar, N and Schlüchter, C., 2005. Paleoglaciations in Anatolia: A schematic review and first results, *Eiszeitalter und Gegenwart* **55**, 102-121, 8 Abb., Hannover.
- Akgün, F., Akyol, E., 1999. Palynostratigraphy of the coal-bearing Neogene deposits graben in Büyük Menderes Western Anatolia. *Geobios*, **32**, 3, 367–383.
- Akman, Y., Ketenöglu, O., 1986. The climate and vegetation of Turkey. In “Plant Life of SW Asia”, *Proceedings of the Royal Society of Edimburgh*, Section B, 113- 122.
- Akman, Y., Quézel, P., Ketenöglu, O., Kurt, F., 1993. Analyse syntaxonomique des forêts de *Liquidambar orientalis* en Turquie. *Ecologia Mediterranea*, **19**, 49–57.
- Akman, Y., and Quézel, P., 1996. La steppe centro-anatolienne: interpretation phytoécologique. Actes des 7èmes Rencontres de l’A.R.P.E. Provence Alpes-Côte d’Azur. Colloque scientifique international Bio’Mes, Digne, 127–131.
- Aksu, A. E., Hiscott, R. N. and Yafiar, D., 1999. Oscillating Quaternary water levels of the Marmara Sea and vigorous outflow into the Aegean Sea from the Marmara Sea-Black Sea drainage corridor. *Marine Geology* **153**, 275–302.
- Aldanmaz E., 2002. Mantle source characteristics of alkali basalts and basanites in an extensional intracontinental plate setting, western Anatolia, Turkey: Implications for multi-stage melting. *Int. Geol. Rev.*, **44**:440-457.
- Amigues, S., 2007. Le styrax et ses usages antiques. *Journal des Savants*, Juillet-Décembre, **2**, 263–318.
- An, Z. S., Song, Y. G., Zhang, P. Z., Wang, E. Q., Wang, S. M., Qiang, X. K., Li, L., Chang, H., Liu, X. D., Zhou, W. J., Liu, W. G., Cao, J. J., Li, X. Q., Shen, J., Liu, Y., Ai, L., 2006. Changes of the monsoon-arid environment in China and growth of the Tibetan Plateau since the Miocene. *Quaternary Science* **26**(5), 678–693.

- Armijo, R., Meyer, B., Hubert, A., Barka, A.,** 1999. Westward propagation of the North Anatolian fault into the northern Aegean: timing and kinematics. *Geology* **27**, 267–270.
- Axelrod, D. I., Al-Shehbaz, I., Raven, P.,** 1996. History of the modern flora of China. In: Zhang, Aoluo, Wu, Sugong (Eds.), *Floristic Characteristics and Diversity of East Asian Plants*. In Springer-Verlag, Berlin, pp. 43–55.
- Bachiri Taoufiq, N.,** 2000. Les environnements marins et continentaux du corridor rifain au Miocène supérieur d'après la palynologie. *Thesis*, Univ. Casablanca, 206 p.
- Bachiri Taoufiq, N., Barhoun, N., Suc, J.-P., Méon, H., Elaouad, Z., Benbouziane, A.,** 2001. Environnement, végétation et climat du Messinien au Maroc. *Paleontologia I Evolució*, **32-33**, 127-138.
- Barka, A. and Hancock, P. L.,** 1984. Neotectonic deformation patterns in the convex-northward arc of the North Anatolian fault zone: Dixon, J. E., and Robertson, A.H.F., eds. *The Geological Evolution of the Eastern Mediterranean*. Geological Society of London, Special Publication, **17**, 285-296.
- Barka, A.,** 1985. Kuzey Anadolu Fay Zonundaki bazı Neojen-Kuvaterner havzaların jeolojisi ve tektonik evrimi. *Ketin Sempozyumu Kitabı*, 209-227.
- Barka, A. A.,** 1992. The North Anatolian fault Zone. *Ann. Tectonicae*, **6**, 164-195.
- Barron, J. A.,** 1996. Diatom constraints on the position of the Antarctic Polar Front in the middle part of the Pliocene. *Marine Micropaleontology* **27** (1996) 195-213.
- Batten, D. J., and Grenfell, H. R.,** 1996. *Botryococcus*. In Jansonius, J., and McGregori, D.C. (Eds), *Palynology: principles and applications*. Am. Assoc. Stratigr. Palynol. Found., **1**:205–214.
- Beaudouin, C.,** 2003. Effets du dernier cycle climatique sur la végétation vall Rhône et sur la sédimentation de la plate-forme du golfe du Lion d'après la palynologie. *PhD thesis*, Université Claude Bernard Lyon-1, France, 403 p.
- Benda, L.,** 1971. Grundzüge einer pollenanalytischen Gliederung des Türkischen Jungtertiärs. *Beihefte zum Geologischen Jahrbuch*, **113**, 1–45.
- Benson, W. E., Sheridan, R. E., and Shipboard Scientific Party,** 1978. Site 391. Blake-Bahama Basin. In Benson, W. E., Sheridan, R. E., et al., *Init. Repts. DSDP, 44*: Washington (U.S. Govt. Printing Office), 153-336.
- Bertini, A., Corradini, D., Suc, J.-P.,** 1995. On *Galeacysta etrusca* and the connections between the Mediterranean and the Paratethys. *Rom. J. Stratigr.* **76** (suppl. 7), 141–142.
- Bertini, A.,** 2002. Palynological evidence of Upper Neogene environments in Italy. *Acta Univ. Carolinae, Geol.*, **46**(4), 15-25.
- Bessedik M.,** 1985. Reconstitution des environnements miocènes des régions nord-ouest méditerranéennes à partir de la palynologie. *Thèse*, Univ. Montpellier 2, 162 p.

- Billups, K., Kelly, C. and Pierce, E.,** 2008. The late Miocene to early Pliocene climate transition in the Southern Ocean. *Palaeogeography, Palaeoclimatology, Palaeoecology* **267** (2008) 31–40.
- Bornovas, J., Tsiambaou, Th.,** 1983. Geological map of Greece. Institute of geology and mineral exploration 1:500.000 scale.
- Bottema, S.,** 1986. Late Quaternary and modern distribution of forest and some taxa in Turkey. *Proceedings of the Royal Society of Edinburgh*, **89B**, 103–111.
- Boydak, M.,** 2006. Biology and silviculture of Turkish Red Pine (*Pinus brutia* Ten.). Lazer Ofset Matbaa Tesisleri San, Ankara, 253 p.
- Browicz, K.,** 1982-1994. Chorology of Trees and Shrubs in the S-W Asia and adjacent regions. Polish Academy of Sciences, Institute of Dendrology, **10** volumes.
- Bukry, D.,** 1973. Low Latitude Coccolith Biostratigraphic Zonation. In: Edgar, N.T., Saunders, J.B., et al. (Eds.), *Initial Reports DSDP*, vol. **15**. US Govt. Printing Office, Washington, pp. 685–703.
- Cambon, G., Suc, J.-P., Aloisic, J.-C., Giressec, P., Monacoc, A., Touzanic, A., Duzera, D., Ferriera, J.,** 1997. Modern pollen deposition in the Rhône delta area (lagoon and marine sediments) France. *Grana*, **36**, 105-113.
- Chandler, M., Rind, D. and Thompson, R.,** 1994. Joint investigations of the Middle Pliocene climate II: GISS GCM Northern Hemisphere results. *Glob. Planet. Change* **9**, 197–219.
- Chikhi, H.,** 1992. Une palynoflore méditerranéenne à subtropicale au Messinien préévaporitique en Algérie. *Géol. Médit.* **19** (1), 19-30.
- CIESM,** 2007. The Messinian Salinity Crisis from mega-deposits to microbiology-Consensus Report. *CIESM Workshop Monographs*, Almeria, 7-10 November, 2007.
- Cita, M. B., Wright, R. C., Ryan, W. B. F., Longinelli, A.,** 1978. Messinian palaeoenvironments. In: Hsu, K.J., Montadert, L. (Eds.), *Initial Reports of the Deep Sea Drilling Project*, vol. **42** part 1. US Government Printing Office, Washington, pp. 1003–1035.
- Cita, M. B. and Colombo, L.,** 1979. Sedimentation in the latest Messinian at Capo Rossello (Sicily). *Sedimentology* **26**, 497–522.
- Clauzon, G., Suc, J.-P., Gautier, F., Berger, A., Loutre, M.-F.,** 1996. Alternate interpretation of the Messinian salinity crisis: Controversy resolved? *Geology* **24** (4), 363-366.
- Clauzon, G., Rubino, J.-L., Casero, P.,** 2001. Regional modalities of the Messinian salinity crisis in the framework of a two phases model. Late Miocene to Early Pliocene environments and ecosystems. *2nd EEDEN Workshop*. Sabadell, Spain, pp. 17–18.

- Clauzon, G., Suc, J.-P., Popescu, S.-M., Marunteanu, M., Rubino, J.-L., Marinescu, F. and Melinte, M. C., 2005.** Influence of the Mediterranean sea-level changes over the Dacic Basin (Eastern Paratethys) in the Late Neogene. The Mediterranean Lago Mare facies deciphered. *Basin Research*, **17** : 437-562.
- Clauzon, G., Suc, J.-P., Popescu, S.-M., Melinte, M. C., Quillévéré, F., Warny, S. A., Fauquette, S., Armijo, R., Meyer, B., Rubino, J.-L., Lericolais, G., Gillet, H., Çağatay, M. N., Uçarkuş, G., Escarguel, G., Jouannic, G. and Dalesme, F., 2007.** Chronology of the Messinian events and paleogeography of the Mediterranean region *s.l.* The Messinian Salinity Crisis from mega-deposits to microbiology-Consensus Report. *CIESM Workshop Monographs*, Almeria, 7-10 November, 2007.
- Combourieu-Nebout, N., 1987.** Les premiers cycles glaciaires– interglaciaires en région méditerranéenne d’après l’analyse palynologique de la série Plio–Pléistocène de Crotona (Italie méridionale). *Thesis*, Univ. Montpellier II, 161 pp. (unpublished).
- Cour, P., 1974.** Nouvelles techniques de détection des flux et de retombées polliniques: étude de la sédimentation des pollens et des spores à la surface du sol. *Pollen et Spores* **16** (1), 103-141.
- Cullen, H. M. and deMenocal, P. B., 2000.** North Atlantic influence on Tigris-Euphrates streamflow. *Int. J. Climatology*, **20**: 853-863.
- Çağatay, N. M., Görür, N., Alpar, B., Saatçılar, R., Akkök, R., Sakınç, M., Yüce, H., Yaltrak, C., Kuşcu, I., 1998.** Geological evolution of the Gulf of Saros, NE Aegean Sea. *Geo Marine Letter* **18**, 1–9.
- Çağatay, M. N., Algan, O., Sakınç, M., Eastoe, C. J., Egesel, L., Balkis, N., Ongan, D., Caner, H., 1999.** A mid-late Holocene sapropelic sediment unit from the southern Marmara sea shelf and its palaeoceanographic significance. *Quaternary Science Reviews* **18** (1999) 531-540.
- Çağatay, N. M., Görür, N., Flecker, R., Sakınç, M., Tünoğlu, C., Ellam, R., Krijgsman, W., Vincent, S., Dikbaş, A., 2006.** Paratethyan–Mediterranean connectivity in the Sea of Marmara region (NW Turkey) during the Messinian. *Sedimentary Geology* **188–189**, 171–187.
- Çağatay, M. N., Suc, J.-P., Clauzon, G. and Melinte, M. C., 2007.** Messinian in Northwest Turkey: implications for paleogeographic evolution and water mass exchange between Paratethys and Mediterranean. The Messinian Salinity Crisis from mega-deposits to microbiology-Consensus Report. *CIESM Workshop Monographs*, Almeria, 7-10 November, 2007.
- Çağatay, M. N., Eris, K., Ryan, W. B. F., Sancar, U., Polonia, A., Akçer, S., Biltekin, D., Gasperini, L., Görür, N., Lericolais G., Bard, E., 2009.** Late Pleistocene-Holocene evolution of the northern shelf of the Sea of Marmara. *Marine Geology*, **265**: 87-100.

- Darby, D. A.**, 2008. Arctic perennial ice cover over the last 14 million years. *Paleoceanography* **23**, pp. 1–9.
- Davis, O. K. and Ellis, B.**, 2010. Early occurrence of sagebrush steppe, Miocene (12 Ma) on the Snake River Plain. *Review of Palaeobotany and Palynology* **160** (2010) 172–180.
- de Bruijn, H., Saraç, G., van den Hoek Ostende, L., Roussiakis, S.**, 1999. The status of the genus name *Parapodemus* Schaub, 1938; new data bearing on an old controversy. *Deinsea* **7**, 95–112.
- DeDeckker, P.**, 1988. Biological and sedimentary facies of Australian salt lakes. *Palaeogeog., Palaeoclimatol., Palaeoecol.*, **62**:237–270.
- Diniz, F.**, 1984. Etude palynologique du bassin pliocène de Rio Maior. *Paléobiologie Continentale* **14**, 259-267.
- Dowsett, H. J. and Poore, R. Z.**, 1991. Pliocene sea surface temperatures of the North Atlantic Ocean at 3.0 Ma. *Quat. Sci. Rev.*, **10**: 189-204.
- Dowsett, H. J., Cronin, T. M., Poore, R. Z., Thompson, R. S., Whatley, R. C. and Wood, A. M.**, 1992. Micropaleontological evidence for increased meridional heat transport in the North Atlantic Ocean during the Pliocene. *Science*, **258**:1133-1135.
- Dowsett, H. J., Thompson, R. S., Barron, J. A., Cronin, T. M., Fleming, R. F., Ishman, S. E., Poore, R. Z., Willard, D. A., Holtz, T. R.**, 1994. Joint investigations of the Middle Pliocene climate: I. PRISM paleoenvironmental reconstructions. *Global and Planetary Change* **9**, 169–195.
- Dowsett, H. J., Chandler, M. A., Cronin, T. M. and Dwyer, G. S.**, 2005. Middle Pliocene sea surface temperature variability. *Paleoceanography*, **20**. PA2014, 1-8.
- Draut, A. E., Raymo, M. E., McManus, J. F. and Oppo, D. W.**, 2003. Climate stability during the Pliocene warm period. *Paleoceanography* **18**, 1078.
- Drivaliari, A.**, 1993. Images polliniques et paléoenvironnements au Néogène supérieur en Méditerranée orientale. Aspects climatiques et paléogéographiques d'un transect latitudinal (de la Roumanie au delta du Nil). *PhD Thesis*, Univ. Montpellier 2, 333 p.
- Erinç, S.**, 1996. *Klimatoloji ve Metodları* (genişletilmiş 4.cü baskı).
- Erinç, S.**, 1959. Regional and seasonal distribution of climatic elements in Turkey and its Dynamic-Genetic Background, İstanbul Üniversitesi Coğrafya Enstitüsü, *International Edition*, No:5.
- Eronen, J., Ataabadia, M. M., Micheels A., Karne, A., Bernor, R. L. And Fortelius, M.**, 2009. Distribution history and climatic controls of the Late Miocene Pikermian chronofauna. *PNAS*, 2009, vol. **106**, no. 29, 11867–11871.

- Fauquette, S.**, 1998. Le climat du Pliocène : nouvelle méthode de quantification basée sur les données polliniques et application à la Méditerranée occidentale", spécialité Biologie des Populations et Ecologie, Université Aix-Marseille 3. *PhD thesis*.
- Fauquette, S., Guiot, J., Suc, J.-P.**, 1998a. A method for climatic reconstruction of the Mediterranean Pliocene using pollen data. *Palaeogeography, Palaeoclimatology, Palaeoecology* **144**, 183– 201.
- Fauquette, S., Suc, J.-P., Guiot, J., Diniz, F., Feddi, N., Zheng, Z., Bessais, E., Drivaliari, A.**, 1999. Climate and biomes in the west Mediterranean area during the Pliocene. *Palaeogeography, Palaeoclimatology, Palaeoecology* **152**, 15– 36.
- Favre, E.**, 2007. Evolution de la végétation de l'Europe et du pourtour méditerranéen au Néogène dans les contextes climatique global et géographique régional. Approches statistiques et élaboration de cartes de végétation à partir des données polliniques. *PhD Thesis*, Univ. Lyon 1, 262 p.
- Flower, B. and Kennett, J. P.**, 1993. Middle Miocene ocean-climate transition: high resolution oxygen and carbon isotopic records from Deep Sea Drilling Project Site 588A, Southwest Pacific. *Paleoceanography*, **8**:811-843.
- Flower, B. and Kennett, J. P.**, 1994. The middle Miocene climatic transition: East Antarctic ice sheet development, deep ocean circulation and global carbon cycling. *Palaeogeography, Palaeoclimatology, Palaeoecology*, **108**:537-555.
- Fornaciari, E., Iaccarino, S., Mazzei, R., Rio, D., Salvatorini, G., Bossio, A. and Monteforti, B.**, 1997. Calcareous plankton biostratigraphy of the Langhian historical stratotype. In: A. Montanari, G. S., Odin and R. Coccioni (eds), *Miocene Stratigraphy: an Integrated Approach. Elsevier Science*:89-106.
- Gheorghian, M.**, 1978. In D. A. Ross, N. P. , Neprochnov, and Micropaleontological investigations sediments from sites 377, 380 and 381 of Leg42B. *Initial reports of the Deep Sea Drilling*, v. **41**, p.783-788.
- Gillet, H.**, 2004. La stratigraphie tertiaire et la surface d'érosion messinienne sur les marges occidentales de la mer Noire: stratigraphie sismique haute résolution. *Thèse*, Univ. Bretagne occidentale, 259 p.
- Gillet, S., Gramann, F., Steffens, P.**, 1978. Neue biostratigraphische Ergebnisse aus dem brackischen Neogen an Dardanellen und Marmara-Meer (Türkei). *Newsletters of Stratigraphy* **7**, 53–64.
- Gibbard, P. L. and Head, M. J.**, 2009b. IUGS ratification of the Quaternary System/Period and the Pleistocene Series/Epoch with a base at 2.58 Ma. *Quaternaire* **20** (4): 411-412.
- Gong, W., Chen, C., Dobeš, C., Fu, C.-X., Koch, M.**, 2008. Phylogeography of a living fossil: Pleistocene glaciations forced *Ginkgo biloba* L. (Ginkgoaceae) into two refuge areas in China with limited subsequent postglacial expansion. *Molecular Phylogenetics and Evolution* **48** (2008) 1094–1105.

- Görür, N., Çağatay, M. N., Sakıncı, M., Sümengen, M., Şentürk, K., Yaltırak, C., Tchapylyga, A.,** 1997. Origin of the Sea of Marmara as deduced from neogene to Quaternary paleogeographic evolution of its frame. *Intern. Geol. Rev.*, **39** : 342-352.
- Görür, N., Çağatay, M. N., Sakıncı, M., Akkök, R., Tchapylyga, A., Natalin, B.,** 2000. Neogene Paratethyan succession in Turkey and its implications for the palaeogeography of the Eastern Paratethys. In "Tectonics and Magmatism in Turkey and the surrounding area", Bozkurt E., Winchester J.A., Piper J.D.A. éd., *Geol. Soc. London, spec. publ.*, **173**: 251-29.
- Graham, A.,** 1996. A contribution to the geological history of the Compositae. In: Hind D, Beentje H, eds. *Proceedings of the Kew International Compositae Conference 1994*, Vol. 1. London: Royal Botanic Gardens, Kew, pp. 123–140.
- Gray, J.,** 1960. Fossil chlorophycean algae from the Miocene of Oregon. *J. Paleontol.*, **34**:453–463.
- Guy-Ohlson, D.,** 1992. *Botryococcus* as an aid in the interpretation of palaeoenvironment and depositional processes. *Rev. Palaeobot. and Palynol.*, **71**:1–15.
- Hably, L. and Kvaček, Z.,** 1998. Pliocene mesophytic forests surrounding crater lakes in western Hungary. *Review of Palaeobotany and Palynology*, **101**: 257–269.
- Hajar, L., Francois, L., Khater, C., Jomaa, I., Deque, M., Cheddadi, R.,** 2010. *Cedrus libani* (A. Rich) distribution in Lebanon: Past, present and future. *C. R. Biologies* **333** (2010) 622–630.
- Haywood, A. M., Dowsett, H. J., Valdes, P. J., Lunt, D. J., Francis, E. J. and Sellwood, B. W.,** 2009. Introduction. Pliocene climate, processes and problems. *Phil. Trans. R. Soc. A* 2009 **367**, 3-17.
- Herbert, T. D., and Schuffert, J.,** 1998. Alkenone unsaturation estimates of late Miocene through late Pliocene sea surface temperature changes, ODP Site 958, *Proceedings of the Ocean Drilling Program*, Scientific Results, v. **159T**, p. 17-22.
- Heusser L.,** 1988. Pollen distribution in marine sediments on the continental margin of Northern California. *Marine Geology*, **80**, 131-147.
- Hristovski, K. D., Olson, L., Hild, N., Peterson, D. and Burge, S.,** 2007. The municipal solid waste system and solid waste characterization at the municipality of Veles, Macedonia. *Waste Management*. Volume **27**, Issue 11, 2007, Pages 1680-1689.
- Hsü, K. J.,** 1972. When the Mediterranean dried up: *Sci. Amer.*, v. **227**, p. 26-36.
- Hsü, K. J.,** 1974. The Miocene desiccation of the Mediterranean Sea and its climatic and Zoogeographic implications: *Naturwissenschaften*, v. **61**, p. 137-142.
- Hsü, K. J., and Bernoulli, D.,** 1978. Genesis of the Tethys and the Mediterranean: Init. Rep. Deep-Sea Drilling Project, v. **XLII**, no. 1, p. 943-950.

- Hsü, K.J. and Giovanoli, F.**, 1979. Messinian event in the Black Sea. *Palaeogeogr. Palaeoclimatol. Palaeoecol.*, **29**(1-2), 75-94.
- Ioakim, C., Rondoyanni, T. and Mettos, A.**, 2005. The Miocene Basins of Greece (Eastern Mediterranean) from a palaeoclimatic perspective, *Revue de Paléobiologie, Genève* (décembre 2005) **24** (2) : 735-748.
- Ivanov, D., Ashraf, A.R., Mosbrugger, V., Palmarev, E.**, 2002. Palynological evidence for Miocene climate change in the Forecarpathian Basin (central Paratethys, NW Bulgaria). *Palaeogeogr., Palaeoclimatol., Palaeoecol.*, **178**, 19– 37.
- Ivanov, D., Ashraf, R. A., Utescher, T., Mosbrugger, V. and Slavomirova, E.**, 2007. Late Miocene vegetation and climate of the Balkan region: palynology of the Beli Breg Coal Basin sediments, *Geologica Carpathica*, August 2007, **58**, 4, 367—381.
- Jansen, E., Overpeck, J., Briffa, K. R., Duplessy J.-C., Joos, F., Masson-Delmotte, V., Olago, D., Otto-Bliesner, B., Peltier, W. R., Rahmstorf, S., Ramesh, R., Raynaud, D., Rind, D., Solomina, O., Villalba, R., and Zhang, D.**, 2007. Palaeoclimate. In *Climate Change 2007: The Physical Science Basis. Contribution of Working Group I to the Fourth Assessment Report of the Intergovernmental Panel on Climate Change*. S. Solomon, D. Qin, M. Manning, Z. Chen, M. Marquis, K.B. Averyt, M. Tignor, and H.L. Miller, Eds. Cambridge University Press, pp. 433-497.
- Jiménez-Moreno, G.**, 2005. Utilización del análisis polínico para la reconstrucción de la vegetación, clima y estimación de paleoaltitudes a lo largo de arco alpino europeo durante el Mioceno (21-8 Ma). *Thèse, Univ. Grenoble et C. Bernard – Lyon 1*, 311 p.
- Jiménez-Moreno, G., Rodríguez-Tovar, F.-J., Pardo-Igúzquiza, E., Fauquette, S., Suc, J.-P., Müller, P.**, 2005. High-resolution palynological analysis in late early-middle Miocene core from the Pannonian Basin, Hungary: Climatic changes, astronomical forcing and eustatic fluctuations in the Central Paratethys. *Palaeogeogr., Palaeoclimatol., Palaeoecol.*, **216** (1-2), 73-97.
- Jiménez-Moreno G.**, 2006. Progressive substitution of a subtropical forest for a temperate one during the middle Miocene climate cooling in Central Europe according to palynological data from cores Tengelic-2 and Hidas-53 (Pannonian Basin, Hungary). *Review of Palaeobotany and Palynology* **142** (2006) 1–14.
- Jimenez-Moreno, G., and Suc, J.-P.**, 2007. Middle Miocene latitudinal climatic gradient in Western Europe: Evidence from pollen records. *Palaeogeography, Palaeoclimatology, Palaeoecology* **253** (2007) 224–241.
- Jiménez-Moreno, G., Fauquette, S., Suc, J.-P., Abdul-Aziz, H.**, 2007a. Early Miocene repetitive vegetation and climatic changes in the lacustrine deposits of the Rubielos de Mora Basin (Teruel, NE Spain). *Palaeogeography, Palaeoclimatology, Palaeoecology* **250**, 101–113.

- Jiménez-Moreno, G., Abdul-Aziz, H., Rodríguez-Tovar, F.J., Pardo-Igúzquiza, E., Suc, J.-P.,** 2007b. Palynological evidence for astronomical forcing in Early–Middle Miocene lacustrine deposits from Rubielos de Mora Basin (NE Spain). *Palaeogeography, Palaeoclimatology, Palaeoecology* **252**, 601–616.
- Jiménez-Moreno, G., Fauquette, S., Suc, J.-P.,** 2008. Vegetation, climate and paleoaltitude reconstructions of eastern alpine mountain ranges during the Miocene based on pollen records from Austria, Central Europe. *Journal of Biogeography* **35**, 1638–1649.
- Jiménez-Moreno, G., Mandic, O., Harzhauser, M., Pavelić, D., Vranjković, A.,** 2008. Vegetation and climate dynamics during the early Middle Miocene from Lake Sinj (Dinaride Lake System, SE Croatia). *Review of Palaeobotany and Palynology* **152** (2008) 237–245.
- Jiménez-Moreno, G., Fauquette, S., Suc, J.-P.,** 2010. Miocene to Pliocene vegetation reconstruction and climate estimates in the Iberian Peninsula from pollen data. *Review of Palaeobotany and Palynology* **162**, 403-415.
- Joannin, S.,** 2007. Changements climatiques en Méditerranée à la transition Pléistocène inférieur-moyen : pollens, isotopes stables et cyclostratigraphie. Université Claude Bernard Lyon 1, *PhD thesis*.
- Kahya, E., and Cengiz, T.,** 2007. North Atlantic Oscillation signals in the series of Beyşehir lake-levels (Turkey). Hydrology Days 2007, 19-21 March, Colorado State University, CO, USA
- Karabörk M. Ç., Kahya, E., and Karaca, M.,** 2005. The influences of the Southern and North Atlantic oscillations on climatic surface variables in Turkey. *Hydrological Processes*, **19**,1185-1211.
- Karaca M., Deniz, A.and Tayanç, M.,** 2000. Cyclone Track Variability over Turkey in Association with Region Climate. *International Journal of Climatology*. **20**, 1225-1236.
- Kasaplıgil, B.,** 1977. A Late-Tertiary conifer-hardwood forest from the vicinity of Güvem village, near Kızılcahamam, Ankara. *Bulletin of the Mineral Research and Exploration Institute of Turkey* **88**, 25-33.
- Kendrovski, V. T.,** 2006. The impact of ambient temperature on mortality among the urban population in Skopje, Macedonia during the period 1996-2000, *BMC Public Health* **6**: 44
- Kloosterboer-van Hoeve, M. L., Steenbrink, J., Brinkhuid, H.,** 2001. A short-term cooling event, 4.205 million years ago, in the Ptolemais Basin, northern Greece. *Palaeogeography, Palaeoclimatology, Palaeoecology* **173** (2001) 61-73.
- Kloosterboer-van Hoeve, M. L., Steenbrink, Visscher, H., J., Brinkhuis, H.,** 2006. Millennial-scale climatic cycles in the Early Pliocene pollen record of Ptolemais, northern Greece. *Palaeogeography, Palaeoclimatology, Palaeoecology* **229** (2006) 321– 334.

- Kovar-Eder, J., Kvacek, Z., Martinetto, E. and Roiron, P.,** 2006. Vegetation of southern Europe around the Miocene/Pliocene boundary (7–4 Ma—The High Resolution Interval I) as reflected in the macrofossil record, *in* Agusti, J., Oms, O., and Meulenkamp, J.E., eds., Late Miocene to Early Pliocene Environment and Climate Change in the Mediterranean Area: *Palaeogeography, Palaeoclimatology, Palaeoecology*, v. **238**, p. 321–339.
- Kovar-Eder, J., Henriette, Jechorek, H., Kvacek, Z. and Parashiv, V.,** 2008. The integrated plant record: an essential tool for reconstructing Neogene zonal vegetation in Europe. *Palaios*, 2008, v. **23**, p. 97–111.
- Krijgsman, W., Stoica, M., Vasiliev, I., Popov, V. V.,** 2010. Rise and fall of the Paratethys Sea during the Messinian Salinity Crisis. *Earth and Planetary Science Letters* **290** (2010) 183–191.
- Kürschner, W. M., Van der Burgh, J., Visscher, H. and Dilcher, D. L.,** 1996. Oak leaves as biosensors of Late Neogene and Early Pleistocene paleoatmospheric CO₂ concentrations. *Mar. Micropaleontol.* **27**, 299–312.
- Kürschner, W. M., Kvacek, Z. and Dilcher, D. L.,** 2008. The impact of Miocene atmospheric carbon dioxide fluctuations on climate and the evolution of terrestrial ecosystems. *Pnas*, vol. **105**, no. 2, 449-453.
- Lawrence, K. T., Liu, Z. H. and Herbert, T. D.,** 2006. Evolution of the eastern tropical Pacific through Plio-Pleistocene glaciation. *Science* **312**, 79–83.
- LePage, B. A.,** 2003. A new species of *Thuja* (Cupressaceae) from the Late Cretaceous of Alaska: implications of being evergreen in a polar environment *American Journal of Botany*. 2003; **90**:167-174.
- Li, J. J.,** 1991. The uplift of the Qinghai–Xizang Plateau and its effect on environment. In: Liu, T. (Ed.), Quaternary Geology and Environment in China. *Science Press*, Beijing, pp. 265– 272.
- Li, J. J., Fang, X. M.,** 1999. Uplift of the Tibetan Plateau and environmental changes. *Chinese Science Bulletin*, **44**, 2117–2124.
- Lisiecki, L. E., Raymo, M. E.,** 2007. Plio-Pleistocene climate evolution: trends and transitions in glacial cycle dynamics. *Quaternary Science Reviews*, **26**, 56-69.
- Lolis, C. J., Bartzokas, A., Metaxas, D. A.,** 1999. Spatial covariability of the climatic parameters in the Greek area. *Int. J. Climatol.* **19**:185–196.
- Loukas, L., Vasiliades, Dalezios, N. R. And Domenikiotis, C.,** 2001. Rainfall-Frequency Mapping for Greece, *Phys. Chem. Earth (B)*, Vol. **26**, No. 9, pp. 669-674.
- Lourens, L. J., Hilgen, F. J., Laskar, J., Shackleton, N. J., Wilson, D.,** 2004. The Neogene period. In: Gradstein, F.M., Ogg, J.G., Smith, A.G. (Eds.), A Geological Time Scale 2004. Cambridge University Press, Cambridge, pp. 409-440.
- Mariolopoulos, E. G.,** 1925. Etude sur le climat de la Grèce. Précipitation. Stabilité du climat depuis le temps historiques. Paris, 1925.

- Mariolopoulos, E. G.**, 1938. Climate of Greece. Athens, Greece.
- Marunteanu, M. and Papaianopol, I.**, 1998. Mediterranean calcareous nannoplankton in the Dacic Basin. *Romanian Journal of Stratigraphy*, **78**:115-121.
- McKenzie, D. P.**, 1972. Active tectonics of the Mediterranean region: *Geophys. Jour. Roy. Astr. Soc.*, v. **30**, p. 109.
- Melinte-Dobrinescu, M. C., Suc, J.-P., Clauzon, G., Popescu, S.-M., Armijo, R., Meyer, B., Biltekin, D., Çağatay, M. N., Uçarkuş, G., Jouannic, G., Fauquette, S., and Çakır, Z.**, 2009. The Messinian Salinity Crisis in the Dardanelles region: Chronostratigraphic constraints *Palaeogeography, Palaeoclimatology, Palaeoecology* **278** (2009) 24–39.
- Meulenkamp, J. E., Kovac, M., Cicha, I.**, 1996. On Late Oligocene to Pliocene depocentre migrations and the evolution of the Carpathian-Pannonian system. *Tectonophysics* **266**, 310-317.
- Meulenkamp, J. E., and Sissingh, W.**, 2003. Tertiary palaeogeography and tectonostratigraphic evolution of the Northern and Southern Peri-Tethys platforms and the intermediate domains of the African-Eurasian convergent plate boundary zone. *Palaeogeography, Palaeoclimatology, Palaeoecology* **196**, 209-228.
- Meulenkamp, J. E., Sissingh, W., Calvo, J. P., Daams, R., Londeix, L., Cahuzac, B., Kovac, M., Marunteanu, M., Ilynia, L. B., Khondkarian, S. O., Scherba, I. G., Roger, J., Platel, J.-P., Hirsch, F., Sadek, A., Abdel-Gawad, G. I., Yeddi, R. S., Yaich, C., Bouaziz, S.**, 2000b. Tertiary. In: Crasquin, S. (Coord.), Atlas Peri-Tethys, Palaeogeographical Maps-Explanatory Notes. CCGM/CGMW, Paris, pp.153-208.
- Miller, K. G., Feigenson, M., Wright, J. D. and Clement, B.**, 1991. Miocene isotope reference section, Deep Sea Drilling Project Site 608: an evaluation of isotope and biostratigraphic resolution. *Palaeoceanography*, **6**, 33–52.
- Müller, P., Geary, D. H., Magyar, I.**, 1999. The endemic molluscs of the Late Miocene Lake Pannon: their origin, evolution and family level taxonomy. *Lethaia* **32**, 47–60.
- Nakoman, E.**, 1967. Microflore des dépôts tertiaires du sud-ouest de l'Anatolie. *Pollen et Spores*, **9**, 1, 121–142.
- Neogene system**, 1986. Stratigraphy of the USSR. *Moscow Nedra.*, **1**:419p.
- Nix, H.**, 1982. Environmental determinants of biogeography and evolution in Terra Australis. In: Barker, W.R., Greenslade, P.J.M. (Eds.), Evolution of the Flora and fauna of Arid Australia. Peacock Publishing, Frewville, 47–66.
- Ogilvie, A. G.**, 1920. A contribution to the geography of Macedonia, *Geographical Journal* **55**, 1-34.

- Okay, A. I., Satır, M., Maluski, H., Siyako, M., Monie, P., Metzger, R. and Akyüz, S.,** 1996. Paleo- and Neo-Tethyan events in northwest Turkey: geological and geochronological constraints. In: A. Yin and M. Harrison (eds.), *Tectonics of Asia* (Cambridge University Press, 420-441).
- Okay, A., Tüysüz, O.,** 1999. Tethyan sutures of northern Turkey. In: Durand, B., Jolivet, L., Horvath, F., Seranne, M. (eds) *The Mediterranean Basins: Tertiary Extension within the Alpine Orogen*. *Geological Society London*, Special publications, **156**, 475-515.
- Olteanu, R.,** 1978. Ostracoda from DSDP Leg 42B. *Init. Rep. DSDP*, **42,2**: 1017-1038.
- Olteanu, R. and Jipa, D. C.,** 2006. Dacian Basin environmental evolution during Upper Neogene within the Paratethys domain. *GEO-ECO-MARINA* 12/2006.
- Pagani, M., Arthur, M. A. and Freeman, K. H.,** 1999. Miocene evolution of atmospheric carbon dioxide. *Paleoceanography*. Vol. **14**, No 3, Pages: 73-292.
- Percival, S. F.,** 1978. Indigenous and reworked coccoliths from the Black Sea. In: Ross, D.A., Neprochnov, Y.P., et al. (Eds.), Leg 42. *Initial Report of the Deep Sea Drilling Project* **42**, 2. U.S. Government Printing Office, 773-780.
- Popescu S.-M.,** 2001. Végétation, climat et cyclostratigraphie en Paratéthys centrale au Miocène supérieur et au Pliocène inférieur d'après la palynologie. *Thèse*, Univ. C. Bernard- Lyon 1, 223 p.
- Popescu S.-M.,** 2001. Repetitive changes in Early Pliocene vegetation revealed by high-resolution pollen analysis: revised cyclostratigraphy of southwestern Romania. *Review of Palaeobotany and Palynology* **120** (2001) 181-202.
- Popescu, S.-M.,** 2006. Upper Miocene and Lower Pliocene environments in the southwestern Black Sea region from high-resolution palynology of DSDP site 380A (Leg42B). *Palaeogeography, Palaeoclimatology, Palaeoecology* **238**, 64-77.
- Popescu, S.-M., Krijgsman, W., Suc, J.-P., Clauzon, G., Mărunțeanu, M., Nica, T.,** 2006. Pollen record and integrated high-resolution chronology of the early Pliocene Dacic Basin (southwestern Romania). *Palaeogeography, Palaeoclimatology, Palaeoecology* **238** (2006) 78-90.
- Popescu, S.-M., Biltekin, D., Winter, H., Suc, J.-P., Melinte-Dobrinescu, M. C., Klotz, S., Rabineau, M.,** 2010. Pliocene and Lower Pleistocene vegetation and climate changes at the European scale: Long pollen records and climatostratigraphy. *Quaternary International* **219** (2010) 152-167.
- Popov, S. V., Ilyina, L. B., Paramonova, N. P., Goncharova, I. A. et al.,** 2004. Lithological-paleogeographic maps of Paratethys. *Cour. Forsch. Inst. Senckenb.* **250**, 1-46 (10 maps).

- Popov, S. V., Shcherb, I. G., Ilyina, L. B., Nevesskaya, L. A., Paramonova, N. P., Khondkarian, S. O., Magyar, I.,** 2006. Late Miocene to Pliocene palaeogeography of the Paratethys and its relation to the Mediterranean. *Palaeogeography, Palaeoclimatology, Palaeoecology* **238** (2006) 91–106.
- Quézel, P.,** 1973. Contribution à l'étude phytosociologique du massif du Taurus. *Phytocoenologia*, **1**, 131–222.
- Quézel, P., Barbero, M., Akman, Y.,** 1980. Contribution à l'étude de la végétation forestière d'Anatolie septentrionale. *Phytocoenologia*, **8**, 365–519.
- Quézel, P., Barbero, M.,** 1985. Carte de la Végétation potentielle de la région Méditerranéenne. Feuille No 1: Méditerranée Orientale. Editions du Centre National de la Recherche Scientifique.
- Quézel, P.,** 1986. The forest vegetation of Turkey. In "Plant Life of S-W Asia", *Proceedings of the Royal Society of Edinburgh*, **89B**, 123–134.
- Quézel, P.,** 1995. La flore du bassin méditerranéen: origine, mise en place endémisme. *Ecologia Mediterranea*, **21**, 19–39.
- Quézel, P.,** 1998. Cèdres et cédraies du pourtour méditerranéen: signification bioclimatique et phytogéographique. *Forêt méditerranéenne*, **19**, 3, 243–260.
- Quézel, P., Médail, F.,** 2003. Ecologie et biogéographie des forêts du bassin méditerranéen. *Elsevier*, Paris, 8–570.
- Raffi, I., Backman, J., Fornaciari, E., Pälke, H., Rio, D., Lourens, L. J., Hilgen, F. J.,** 2006. A review of calcareous nannofossil astrobiochronology encompassing the past 25 million years. *Quaternary Science Review* **25**, 3113–3137.
- Ravelo, A. C., Billups K., Dekens, P. S., Herbert, T. D. and Lawrence, K. T.,** 2007. Onto the Ice Ages: Proxy Evidence for the onset of Northern Hemisphere Glaciation, From: M. Williams, A. M. Haywood, J. Gregory and D. Schmidt (eds), Deep-time perspectives on climate change: marrying the signal from computer models and biological proxies. The Micropaleontological Society, Special Publications. *The Geological Society, London*, 563-573, (2007).
- Raymo, M. E., Grant, B., Horowitz, M. and Rau, G. H.,** 1996. Mid-Pliocene warmth: stronger greenhouse and stronger conveyor. *Mar. Micropaleontol.* **27**, 313–326.
- Ross, D. A.,** 1978. Black Sea stratigraphy. Initial Report of the Deep Sea Drilling Project, **42**, 2, U.S. Gov. Print. Off.: 17-26.
- Ross, D. A. et al.,** 1978. Site 380. In "Initial Report of the Deep Sea Drilling Project", Ross, D.A., Neprochnov, Y.P. et al. eds., **42**, 2, U.S. Gov. Print. Off.: 119-291.
- Ross D. A. and Degens E. T.,** 1974. Recent sediments of Black Sea. In "The Black Sea –geology, chemistry and biology". Degens E.T. and Ross D. A. édit., *Amer. Ass. Petrol. Geol. Mem.*, **20**: 183-199.

- Rowley, D. B., Currie, B. S.,** 2006. Palaeoaltimetry of the late Eocene to Miocene Lunpola basin, central Tibet. *Nature* **439**, 677–681.
- Rögl, F., and Steininger, F. F.,** 1983. Vom Zerfall der Tethys zu Mediterran und paratethys. Die neogene Paläogeographie und Palinspastik des zirkum-mediterranean Raumes. *Ann. Naturhist. Mus. Wien*, **85**, A : 135-163.
- Ruggieri, G.,** 1967. The Miocene and later evolution of the Mediterranean Sea. In: Adams, C.G., Ager, D.V. (Eds.), Aspects of Tethyan Biogeography. *Syst. Assoc. Publ.*, vol. **7**, pp. 283–290.
- Ryan, W. B. E., and Cita, W. B.,** 1978. The nature and distribution of Messinian erosional surfaces. Indicators of several kilometers-deep Mediterranean in the Miocene. *Marine Geol.*, v. **27**, p. 193-230.
- Sabato, L., Bertini, A., Masini, F., Albianelli, A., Napoleone, G., Pieri, P.,** 2005. The lower and middle Pleistocene geological record of the San Lorenzo lacustrine succession in the Sant’Arcangelo Basin (Southern Apennines, Italy). *Quaternary International* **131** (2005) 59–69.
- Sakıncı, M., Yalıtırak, C., Oktay, F. Y.,** 1999. Palaeogeographical evolution of the Thrace Neogene Basin and the Tethys-Paratethys relations at northwestern Turkey (Thrace). *Palaeogeogr. Palaeoclimatol. Palaeoecol.* **153**, 17-40.
- Sakıncı, M., and Yalıtırak, C.,** 2005. Messinian crisis: what happened around the northeastern Aegean?. *Marine Geology* **221**, 423–436.
- Sakıncı, M.,** 2007. Trakya Tersiyer’inin silisleşmiş ağaçları. Proje no: 103Y137. İstanbul Technical University.
- Salzmann, U., Haywood, A. M., Lunt, D. J., Valdes, P. J., and Hill, D. J.,** 2008. A new global biome reconstruction and data-model comparison for the Middle Pliocene. *Global Ecology and Biogeography*, (2008) **17**, 432–447.
- Sayar, C.,** 1987. İstanbul ve çevresi Neojen çökelleri ve Paratetis içindeki konumu. *Maden fak. 40. yıl Bülteni*, pp. 250–266.
- Schrader, H.-J.,** 1978. Quaternary through Neogene history of the Black Sea, deduced from the paleoecology of diatoms, silicoflagellates, ebridians, and chrysomonads. In “Initial Report of the Deep Sea Drilling Project”, Ross, D.A., Neprochnov, Y.P. *et al.* eds., **42**, 2, U.S. Gov. Print. Off.: 789-901.
- Shackleton, N. J., Berger, A., Peltier, W. R.,** 1990. An alternative astronomical calibration of the lower Pleistocene time scale based on ODP Site 677. Transactions of the Royal Society of Edinburgh: *Earth Sciences* **81**, 251-261.
- Shackleton, N. J., Hall, M.A., Pate, D.,** 1995. Pliocene stable isotope stratigraphy of Site 846. In: Pisias, N.G., Mayer, L.A., Janecek, T.R., Palmer-Julson, A., van Andel, T.H. (Eds.), Leg 138. *Proceedings of the Ocean Drilling Program*, Scientific Results, **138**, pp. 337-355.

- Siyako, M., Bürkan, A. K., Okay, A. I.,** 1989. Biga ve Gelibolu yarımadaları'nın Tersiyer jeolojisi ve hidrokarbon olanakları. *TPJD Bülteni*, cilt **1** (3), 183–199.
- Smith, A. D., Taymaz, T., Oktay, E, Yuce, H., Alpar, B., Basaran, H., Jackson, A. J., Kara, S., and Simsek, M.,** 1995. High-resolution seismic profiling in the Sea of Marmara (northwest Turkey): Late Quaternary sedimentation and sea-level changes: *Geol. Soc. Amer. Bull.*, v. **107**, p. 923-936.
- Stanley, D. J., and Blanpied, C.,** 1980. Late Quaternary water exchange between the eastern Mediterranean and the Black Sea: *Nature*, v. **285**, p. 537-541.
- Steenbrink, J., Van Vugt, N., Hilgen, F. J., Wijbrans, J. R., Meulenkamp, J. E.,** 1999. Sedimentary cycles and volcanic ash beds in the lower Pliocene lacustrine succession of Ptolemais (NW Greece): discrepancy between $^{40}\text{Ar}/^{39}\text{Ar}$ and astronomical ages. *Palaeogeogr. Palaeoclimatol. Palaeoecol.* **152**, 283–303.
- Steenbrink, J., Van Vugt, N., Kloosterboer-van Hoeve, M. L., Hilgen, F. J.,** 2000. Refinement of the Messinian APTS from sedimentary cycle patterns in the lacustrine Lava section (Servia Basin, NW Greece). *Earth Planet. Sci. Lett.* **181** (3–4), 161–173.
- Steenbrink, J., Hilgen, F. J., Krijgsman, W., Wijbrans, J. R., Meulenkamp, J. E.,** 2006. Late Miocene to Early Pliocene depositional history of the intramontane Florina–Ptolemais–Servia Basin, NW Greece: Interplay between orbital forcing and tectonics. *Palaeogeography, Palaeoclimatology, Palaeoecology* **238** (2006) 151–178.
- Stoffers, P. and Müller, G.,** 1978. Mineralogy and lithofacies of Black Sea sediments DSDP Project, *Init. Rep. Deep Sea Drill. Proj.*, Ross D. A., Netrochnov Y.P. *et al.* édit., **42**, 2, U. S. Gov. Print. Off. : 373-413.
- Suc J.-P.,** 1980. Contribution à la connaissance du Pliocène et du Pléistocène inférieur des régions méditerranéennes d'Europe occidentale par l'analyse palynologique des dépôts du Languedoc-Roussillon (sud de la France) et de la Catalogne (nord-est de l'Espagne). *Thèse*, Univ. Montpellier 2 : 198 p.
- Suc J.-P.,** 1984. Origin and evolution of the Mediterranean vegetation and climate in Europe. *Nature*, **307**, 5950 : 429-432.
- Suc, J.-P. and Bessais, E.,** 1990. Pérennité d'un climat thermo-xérique en Sicile avant, pendant, après la crise de salinité messinienne. *Paleoclimatology*. C. R. Acad. Sci. Paris, t. 310, **Série II**, p. 1701-1707.
- Suc, J.-P. and Drivaliari, A.,** 1991. Transport of bisaccate coniferous fossil pollen grains to coastal sediments: an example from the earliest Pliocene Orb Ria (Languedoc, Southern France). *Review of Palaeobotany and Palynology*, **70**, 247-253.

- Suc, J.-P., Diniz, F., Leroy, S., Poumot, C., Bertini, A., Dupont, L., Clet, M., Bessais, E., Zheng, Z., Fauquette, S., Ferrier, J.,** 1995a. Zanclean (~Brunsumian) to early Piacenzian (~early-middle Reuverian) climate from 4° to 54° north latitude (West Africa, West Europe and West Mediterranean areas). *Mededelingen Rijks Geologische Dienst*, **52**, 43–56.
- Suc, J.-P., Bertini, A., Comborieu-Nebout, N., Diniz, F., Leroy, S., Russo-Eromolli, E., Zheng, Z., Bessais, E., Ferrier, J.,** 1995b. Structure of West Mediterranean vegetation and climate since 5.3 ma. *Acta zoologica Cracoviensia* **38** (1), 3–16.
- Suc, J.-P., Fauquette, S., Popescu, S.-M.,** 2004. L'investigation palynologique du Cénozoïque passe par les herbiers. Actes du Colloque “Les herbiers: un outil d'avenir. Tradition et modernité”, Villeurbanne. Edit. Association française pour la Conservation des Espèces Végétales, Nancy, pp. 67–87.
- Suc, J.-P., and Popescu, S.-M.,** 2005. Pollen records and climatic cycles in the North Mediterranean region since 2.7 Ma. In: Head, M.J., Gibbard, P.L. (Eds.), Early-Middle Pleistocene Transitions: The Land-Ocean Evidence, *Geological Society of London*, Special Publication **247**, 147–158.
- Sümengen, M., Terlemez, I., Şentürk, K., Karasöse, C., Erkan, E. N., Ünay, E., Gürbüz, M., Atalay, Z.,** 1987. Gelibolu Yarımadası ve Güneybatı Tersiyer havzasının stratigrafisi, sedimentolojisi ve Tektoniği. MTA Jeoloji Etüdüleri Dairesi Raporu 8128 (245 pp.).
- Szabo, C., Harangi, Sz., and Csontos, L.,** 1992. Review of Neogene and Quaternary volcanism of the Carpathian-Pannonian region. *Tectonophysics*, **208**:243-256.
- Şengör, A. M. C.,** 1979. The North Anatolian transform fault, its age, offset and tectonic significance: *Journal of the Geological Society London*, **136**, 269-282.
- Şengör, A. M. C., Görür, N., and Saroglu, F.,** 1985. Strike-slip faulting and related basin formation in zones of tectonic escape: Turkey as a case study, in Biddle, K. T., and Christie Blick, N., eds., Strike-slip deformation, basin formation, and sedimentation: Tulsa, OK, Soc. Econ. Paleontol. Mineral., Spec. Publ., v. **37**, p. 227-264.
- Tappan, H.,** 1980. *The Paleobiology of Plant Protists*: San Francisco (W.H. Freeman).
- Thompson, D. W. J. and Wallace, J. M.,** 2001. Regional climate impact on Northern Hemisphere annular mode. *Science*, **292**, 85-89.
- Türkecan, A. and Yurtsever, A.,** 2002. Türkiye Jeoloji Haritası, İstanbul Paftası, 1/500,000. MTA Genel Müdürlüğü, Ankara.
- Türkeş M.,** 1996. Meteorological drought in Turkey: a historical perspective, 1930-93. *Drought Network News* **8**: 17-21.

- Türkeş , M., and Erlat, E.,** 2003. Precipitation changes and variability in Turkey linked to the North Atlantic Oscillation during the period 1930-2000. *International Journal Climatology*, **23**, 1771–1796.
- Van de Weerd, A.,** 1979. Early Ruscinian rodents and lagomorphs (Mammalia) from the lignites near Ptolemais (Macedonia, Greece). *Proc. Kon. Akad. Wetensch. Amsterdam B82* (2), 127–170.
- Van der Burgh, J., Visscher, H., Dilcher, D. L. and Kürschner, W. M.,** 1993. Paleoatmospheric signatures in Neogene fossil leaves. *Science* **260**, 1788–1790.
- Van Vugt, N., Steenbrink, J., Langereis, C. G., Hilgen, F. J., Meulenkamp, J. E.,** 1998. Magnetostratigraphy-based astronomical tuning of the early Pliocene lacustrine sediments of Ptolemais (NW Greece) and bed-to-bed correlation with the marine record. *Earth Planet Sci. Lett.* **164** (3–4), 535–551.
- Vasiliev, I., Krijgsman, W., Langereis, C. G., Panaiotu, C. E., Matenco, L., Bertotti, G.,** 2004. Towards an astrochronological framework for the eastern Paratethys Mio-Pliocene sedimentary sequences of the Focsani basin (Romania). *Earth Planet Sci. Lett.* **227**, 231–247.
- Velitzelos, E and Gregor, H.-J.,** 1990. Some aspects of the Neogene floral history in Greece. *Review of Palaeobotany and Palynology* **62** (1990): 291–307.
- Wake, L. V., and Hillen, L. W.,** 1980. Study of a “bloom” of the oil-rich alga *Botryococcus braunii* in the Darwin River Reservoir. *Biotechnol. Bioeng.*, **22**:1637–1656.
- Wan, S. M., Li, A. C., Peter, D., Clift, J., Stuut, W.,** 2007. Development of the East Asian monsoon: Mineralogical and sedimentologic records in the northern South China Sea since 20 Ma. *Palaeogeography, Palaeoclimatology, Palaeoecology* **152**, 37–47.
- Wang, C.W.,** 1961. The forests of China with a survey of grassland and desert vegetation. Maria Moors Cabot Foundation, vol. **5**. Harvard University, Cambridge, Massachusetts.
- Wang, X. M., Zhang, X. L., Wang, M. Z., Li, C. S.,** 2003. The palynoflora from Paleogene of Fanshi, Shanxi and discussion on their geological age. *Journal of Shandong University of Science and Technology (Natural Science)* **22** (3), 26–31.
- Wara M. W., Ravelo A. C., Delaney M. L.,** 2005. Permanent El Niño-like conditions during the Pliocene warm period. *Science*, v. **309**, p. 758–761.
- Wigley, T. M. and Farmer, G.,** 1982. Climate of the Eastern Mediterranean and Near East. In: Paleoclimates, Paleoenvironments and Human Communities in the Eastern Mediterranean Region in Later Prehistory, J. L. Bintliff and W. Van Zeist (Ed.) B.A.R. *International Series*, **133**:3-37; Oxford.

- Xoplaki, E., Luterbacher, J., Burkard, R., Patrikas, I., Maheras, P.,** 2000. Connection between the large-scale 500 hPa geopotential height fields and precipitation over Greece during wintertime. *Clim. Res.* **14**:129–146.
- Yaltrak, C., Sakıncı, M., Oktay, F. Y.,** 2000. Westward propagation of North Anatolian fault into the northern Aegean: Timing and kinematics: Comment and Reply: Comment, *Geology*, February, 2000, v. **28**, p. 187-188.
- Yavuz Işık, N.,** 2007. Pollen analysis of coal-bearing Miocene sedimentary rocks from the Seyitömer Basin (Kütahya), Western Anatolia, *Geobios*, Volume **40**, Issue 5, September-October 2007, Pages 701-708.
- Yavuz Işık, N.,** 2008. Vegetational and climatic investigations in the Early Miocene lacustrine deposits of the Güvem Basin (Galatean Volcanic Province), NW Central Anatolia, Turkey, *Review of Palaeobotany and Palynology* **150** (2008) 130–139.
- Yavuz Işık, N. and Demirci, C.,** 2009. Miocene spores and pollen from Pelitçik Basin, Turkey—environmental and climatic implications. *C. R. Palevol* **8** (2009) 437–446.
- Yunfa, M., Qingquan, M., XiaominFan, X., Fuli, W., Chunhui, S.,** 2010. Origin and development of *Artemisia* (Asteraceae) in Asia and its implications for the uplift history of the Tibetan Plateau: a review *Quaternary International*, Article in Press.
- Zachos, J., Pagani, M., Sloan, L. and Billups, K.,** 2001. Trends, rhythms, and aberrations in global climate 65 Ma to present. *Science*, 292, 686–693.
- Zachos, J. C., Dickens, G. R., Zeebe, R. E.,** 2008. An early Cenozoic perspective on greenhouse warming and carbon-cycle dynamics. *Nature* **451**(17), 279–283.
- Zagwijn, W. H.,** 1960. Aspects of the Pliocene and early Pleistocene vegetation in the Netherlands. *Mededelingen Geologische Stichting Serie C* **3** (5), 78 pp.
- Zagwijn, W. H.,** 1963. Pollen-analytic investigations in the Tiglian of the Netherlands. *Mededelingen Geologische Stichting New Serie* **16**, 49-71.
- Zagwijn, W. H.,** 1975. Variations in climate as shown by pollen analysis, especially in the Lower Pleistocene of Europe. In: Wright, A.E. & Moseley, F. (Eds.), *Ice Ages: Ancient and Modern. Geological Journal special issue* **6**, pp. 137-152.
- Zagwijn, W. H., and Suc, J.-P.,** 1984. Palynostratigraphie du Plio-Pléistocène d'Europe et de Méditerranée nord-occidentales: correlations chronostratigraphiques, histoire de la végétation et du climat. *Paléobiologie Continentale* **14** (2), 475-483.
- Zagwijn, W. H.,** 1998. Borders and boundaries: a century of stratigraphical research in the Tegelen e Reuver area of Limburg (The Netherlands). In: van Kolfschoten, Th., Gibbard, P. L. (Eds.), *The Dawn of the Quaternary. Proceedings.*

- Zhang, Y. G., Ji, J., Balsam, W., Liu, L. and Chen, J.,** 2009. Mid-Pliocene Asian monsoon intensification and the onset of Northern Hemisphere glaciations. *Geology*, July 2009, v. **37** no. **7** p. 599-602.
- Zheng, Z.,** 1986. Contribution palynologique à la connaissance du Néogène du Sud-Est français et de Ligurie. *Thesis*, Montpellier II, 142 pp.
- Zhisheng, A., Kutzbach, J. E., Prell, W. L, Porter, C.,** 2001. Evolution of Asia Monsoon and phased uplift of the Himalaya-Tibetan plateau since Late Miocene times. *Nature*, vol. **411**, 62-66.
- Zohary, M.,** 1973. Geobotanical foundations of the Middle East. Fischer éd., Stuttgart, **2** vol., 739 p.

LIST OF TABLES

	<u>Page</u>
Table 3.1: Study locations and number of samples.....	32
Table 3.2: Taxa identified in the study.....	34
Table 3.3: Groups used in synthetic pollen diagrams according to classification of Nix (1982).....	35
Table 4.1: Age control of the study areas.	43

LIST OF FIGURES

	<u>Page</u>
Figure 1A : Distribution of <i>Liquidambar</i> , <i>Pterocarya</i> and <i>Zelkova</i>	2
Figure 1B : Distribution of <i>Cedrus libani</i>	3
Figure 1.2 : Map showing the studied pollen localities (black dots).....	6
Figure 1.3 : Map showing the main tectonic elements of eastern Mediterranean regions (modified from McKenzie, 1972; Şengör <i>et al.</i> , 1985; Okay <i>et al.</i> , 1999).....	7
Figure 2.1 : The present-day vegetation map of Turkey and Greece (Quézel and Barbero, 1985).....	12
Figure 2.2 : Atmospheric air masses affecting the Eastern Mediterranean region (cP: Continental Polar Air Mass; mP: Marine Polar Air Mass; cT: Continental Tropical Air Mass; mT: Marine Tropical Air Mass, PJF: Polar Front Jet; STJ: Subtropical Jet; ITCZ: Intertropical Convergence Zone (modified from Wigley and Farmer, 1982).....	15
Figure 2.3 : Macroclimate types of Turkey. Ia: Anatolian steppe climate; Ib: Southeastern Anatolian steppe climate; IIb: Central Black Sea climate; IIc: Western Black Sea climate; IIIa: Mediterranean climate; IIIb: Marmara climate; IVa: All seasons with precipitation type; IVb: Arid summer type (modified from Erinç, 1996).....	17
Figure 2.4 : Distribution of Neogene rocks in the Marmara regions and North Aegean (simplified from Türkecan and Yurtsever, 2002; Okay <i>et al.</i> , 1996 and Aldanmaz, 2002; Bornovas <i>et al.</i> , 1983) and numbers: 1; DSDP Site 380, 2; Enez, 3; Burhanlı, 4; Eceabat, 5; west Seddülbahir, 6; İntepe, 7; Trilophos, 8; Lion of Amphipoli, 9; Prosilio, 10; Ptolemais (Notio and Base).....	21
Figure 2.5 : Stratigraphy of studied sedimentary sections in DSDP Site 380, İntepe, Enez and Ptolemais.....	22
Figure 2.6 : Paleogeographic map of the Late Tortonian (8-7 Ma), indicating position of continental, shallow and deep basins. Thick black lines show fault zones (modified from Meulenkamp <i>et al.</i> , 2000b; Meulenkamp and Sissingh, 2003).....	24
Figure 2.7 : Palinspastic paleogeographic map for Late Miocene (Late Messinian, Late Pannonian-Early Pontian) showing shallow and deep basins (modified from Popov <i>et al.</i> , 2006; Olteanu and Jipa, 2006).....	25
Figure 2.8 : The Paleogeographic map of Marmara region and Greece and Macedonia before the Messinian Salinity Crisis (Early Messinian) (modified from Görür <i>et al.</i> , 1997; Sakıncı <i>et al.</i> , 1999; Vasiliev <i>et al.</i> , 2004; Çağatay <i>et al.</i> , 2006; Melinte <i>et al.</i> , 2009; Krijgsman <i>et al.</i> , 2010).....	27
Figure 2.9 : The Paleogeographic map of Marmara region	

	and Greece and Macedonia after the Messinian Salinity Crisis (Latest Messinian-Earliest Zanclean) (modified from Sakıncı and Yaltrak, 2005; Rögl and Steininger, 1983; Meulenkamp and Sissingh, 2003; Suc, J.-P., personal data).....	27
Figure 2.10	: Paleogeographic map of the Piacenzian-Gelasian (3.4-1.8 Ma), indicating position of continental, shallow and deep basins. Thick black lines show fault zones (modified from Meulenkamp <i>et al</i> , 2000b; Meulenkamp and Sissingh, 2003).....	29
Figure 3.1	: Some pollen photos from the studied regions.....	38
Figure 3.2	: Continued.....	40
Figure 4.1	: The chronostratigraphic position of the studied sections from the Late Miocene to the Early Pleistocene.....	42
Figure 5.1	: Lithology of DSDP 380 Site Black Sea core (Ross, 1978). Climate zones in the diagram: γ (Glacial), B (Interglacial), β (Glacial), A (Interglacial), α (Glacial). Studied intervals cover 319.03 to 702.4.....	48
Figure 5.2	: Detailed pollen diagram of DSDP Site 380 between 319.03-460 m.....	52
Figure 5.3	: Detailed pollen diagram of DSDP Site 380 between 460.54-702.4 m.....	53
Figure 5.4	: The synthetic pollen diagram of DSDP Site 380 obtained in this study. Pollen groups in the diagram: 1; Megathermic elements, 2; Mega-mesothermic elements, 3; <i>Cathaya</i> , 4; Mesothermic elements, 5; <i>Pinus</i> , 6; Meso-microthermic elements, 7; Microthermic elements, 8; Cupressaceae, 9; Herbs, 10; Steppe elements (see for explanation in the next page). The synthetic pollen diagram with oxygen isotope curve showing Marine Isotope Stages (Shackleton <i>et al.</i> , 1990, 1995), pollen zones, NW European climatostratigraphy (Zagwijn, 1960, 1998) and nannofossil biohorizons (Raffi <i>et al.</i> , 2006). Chronostratigraphy, Lourens <i>et al.</i> (2004).....	55
Figure 5.5	: The distribution of thermophilous trees during the Pliocene-Pleistocene in the DSDP Site 380.....	57
Figure 5.6	: The synthetic pollen diagram of Enez section. Note that only the samples with statistically significant pollen (minimum 150) numbers were analysed The numbers in the diagram show the pollen groups: 1; megathermic elements (Arecaceae, Sapotaceae), 2; mega-mesothermic elements (Taxodiaceae, <i>Engelhardia</i> , Ginkgoaceae, <i>Loropetalum</i> and <i>Distylium</i>), 3; <i>Cathaya</i> , 4; mesothermic elements (<i>Quercus</i> , <i>Carya</i> , <i>Pterocarya</i> , <i>Zelkova</i> , <i>Carpinus orientalis</i> , <i>Alnus</i> , <i>Ulmus</i> , <i>Corylus</i> , etc.), 5; <i>Pinus</i> , 6; meso-microthermic elements (<i>Cedrus</i> , <i>Tsuga</i>), 7; microthermic elements (<i>Abies</i> , <i>Picea</i>), 8; Cupressaceae, 9; herbs (Asteraceae Asteroideae, Asteraceae Cichorioideae,	

	Poaceae, Amaranthaceae-Chenopodiaceae, Brassicaceae, Plumbaginaceae, etc. and include some water plants (<i>Sparganium</i> , <i>Potamogeton</i>), 10; steppe elements (<i>Artemisia</i>).	58
Figure 5.7	: The distribution of thermophilous trees in Enez section during the end of the Messinian (after MSC)-the earliest Zanclean.	59
Figure 5.8	: The detailed pollen diagram of Enez section.	60
Figure 5.9	: The synthetic pollen diagram of İntepe section with a lithological log. Note that only the samples with statistically significant pollen (minimum 150) numbers were analysed.. The numbers in the diagram show the pollen groups: 1; mega-mesothermic elements (<i>Taxodiaceae</i> , <i>Engelhardia</i>), 2; <i>Cathaya</i> , 3; mesothermic elements (<i>Quercus</i> , <i>Carya</i> , <i>Pterocarya</i> , <i>Zelkova</i> , <i>Carpinus orientalis</i> , <i>Alnus</i> , etc.), 4; <i>Pinus</i> , 5; meso-microthermic elements (<i>Cedrus</i>), 6; microthermic elements (<i>Abies</i> and <i>Picea</i>), 7; mediterranean xerophytes 8; herbs (<i>Asteraceae Asteroideae</i> , <i>Asteraceae Cichorioideae</i> , <i>Poaceae</i> , <i>Amaranthaceae-Chenopodiaceae</i> , <i>Apiaceae</i> , etc., and include some fresh water plants (<i>Sparganium</i> , <i>Potamogeton</i> , <i>Typha</i> , etc), 9; steppe elements (<i>Artemisia</i> , <i>Ephedra</i>).	62
Figure 5.10	: The detailed pollen diagram of İntepe section.	63
Figure 5.11	: The distribution of thermophilous plants in İntepe section before and after the Messinian Salinity Crisis (MSC).	64
Figure 5.12	: The synthetic pollen diagram of west of Seddülbahir section with a lithological log. Note that only the samples with statistically significant pollen (minimum 150) numbers were analysed. The numbers in the diagram show the pollen groups: 1; mega-mesothermic elements (<i>Taxodiaceae</i> , <i>Distylium</i> , <i>Microtropis fallax</i> and <i>Engelhardia</i>), 2; <i>Cathaya</i> , 3; mesothermic elements (<i>Quercus</i> , <i>Carya</i> , <i>Pterocarya</i> , <i>Zelkova</i> , <i>Carpinus orientalis</i> , <i>Alnus</i> , etc.), 4; <i>Pinus</i> , 5; meso-microthermic elements (<i>Cedrus</i> and <i>Tsuga</i>), 6; microthermic elements (<i>Abies</i> and <i>Picea</i>), 7; Cupressaceae, 8; mediterranean xerophytes 9; herbs (<i>Asteraceae Asteroideae</i> , <i>Asteraceae Cichorioideae</i> , <i>Poaceae</i> , <i>Amaranthaceae-Chenopodiaceae</i> , <i>Apiaceae</i> , etc., and include some fresh water plant (<i>Typha</i>).	66
Figure 5.13	: The detailed pollen diagram of west of Seddülbahir.	67
Figure 5.14	: The synthetic pollen diagram of Eceabat section with a lithological log. Note that only the samples with statistically significant pollen (minimum 150) numbers were analysed. The numbers in the diagram show the pollen groups: 1; mega-mesothermic elements (<i>Taxodiaceae</i> and <i>Engelhardia</i>), 2; mesothermic elements (<i>Quercus</i> , <i>Carya</i> , <i>Zelkova</i> , <i>Alnus</i> , etc.), 3; <i>Pinus</i> , 4; meso-microthermic elements (<i>Tsuga</i>), 5; herbs (<i>Asteraceae Asteroideae</i> , <i>Asteraceae Cichorioideae</i> , <i>Poaceae</i> , <i>Amaranthaceae Chenopodiaceae</i> etc., and include fresh water plant <i>Sparganium</i>	68

Figure 5.15 : The synthetic pollen diagram of Burhanlı section with a lithological log. Note that only the samples with statistically significant pollen (minimum 150) numbers were analysed. The numbers in the diagram show the pollen groups: 1; mega-mesothermic elements (<i>Taxodiaceae</i> and <i>Engelhardia</i>), 2; mesothermic elements (<i>Carya</i> , <i>Zelkova</i> , <i>Carpinus orientalis</i> , <i>Liquidambar orientalis</i> , etc.), 3; <i>Pinus</i> , 4; meso-microthermic elements (<i>Cedrus</i>), 5; herbs (<i>Asteraceae Asteroideae</i> , <i>Asteraceae Cichorioideae</i> , <i>Poaceae</i> , <i>Amaranthaceae-Chenopodiaceae</i> etc., and include fresh water plant <i>Potamogeton</i> , 6; steppe elements (<i>Artemisia</i> and <i>Hippophae rhamnoides</i>).....	69
Figure 5.16 : The synthetic pollen diagram of Ptolemais Notio. Note that only the samples with statistically significant pollen (minimum 150) numbers were analysed. The numbers in the diagram show the pollen groups: 1; mega-mesothermic elements (<i>Taxodiaceae</i> , <i>Engelhardia</i>), 2; mesothermic elements (<i>Quercus</i> , <i>Carya</i> , <i>Pterocarya</i> , <i>Zelkova</i> , <i>Carpinus orientalis</i> , <i>Fraxinus</i> , <i>Alnus</i> , etc.), 3; <i>Pinus</i> , 4; meso-microthermic elements (<i>Cedrus</i> and <i>Tsuga</i>), 5; microthermic elements (<i>Abies</i> and <i>Picea</i>), 6; non-significant (<i>Ranunculaceae</i>), 7; <i>Cupressaceae</i> , 8; herbs (<i>Asteraceae Asteroideae</i> , <i>Asteraceae Cichorioideae</i> , <i>Poaceae</i> , <i>Amaranthaceae Chenopodiaceae</i> , <i>Apiaceae</i> , <i>Polygonum</i> , etc. and include some water plants (<i>Sparganium</i> , <i>Potamogeton</i> , <i>Typha</i>), 9; steppe elements (<i>Artemisia</i> , <i>Hippophae rhamnoides</i>).	71
Figure 5.17 : Detailed pollen diagram of Ptolemais Notio.	70
Figure 5.18 : The distribution of thermophilous plants during the Early Pliocene in Ptolemais Notio.	71
Figure 5.19 : The synthetic pollen diagram of Ptolemais Base. The numbers in the diagram show the pollen groups: 1; mega-mesothermic elements (<i>Taxodiaceae</i> , <i>Engelhardia</i>), 2; mesothermic elements (<i>Quercus</i> , <i>Carya</i> , <i>Pterocarya</i> , <i>Zelkova</i> , <i>Carpinus orientalis</i> , <i>Liquidambar</i> , <i>Fraxinus</i> , <i>Alnus</i> , etc.), 3; <i>Pinus</i> , 4; meso-microthermic elements (<i>Cedrus</i> and <i>Tsuga</i>), 5; microthermic elements (<i>Abies</i> and <i>Picea</i>), 6; non-significant (<i>Ranunculaceae</i> and <i>Rosaceae</i>), 7; mediterranean xerophytes (<i>Olea</i> , <i>Quercus ilex</i> type), 8; herbs (<i>Asteraceae Asteroideae</i> , <i>Asteraceae Cichorioideae</i> , <i>Poaceae</i> , <i>Amaranthaceae-Chenopodiaceae</i> , <i>Cistus</i> , etc. and include some water plants (<i>Sparganium</i> , <i>Potamogeton</i> , <i>Typha</i>), 9; steppe elements (<i>Artemisia</i> , <i>Ephedra</i>).....	73
Figure 5.20 : The distribution of thermophilous trees during the Early Pliocene in Ptolemais Base section.	73
Figure 5.21 : Detailed pollen diagram of Ptolemais Base.....	74
Figure 5.22 : The synthetic pollen diagram of Trilophos. Note that only the two samples of five with statistically significant pollen (minimum 150) numbers were	

	analysed. The numbers in the diagram show the pollen groups: 1; mega-mesothermic elements (<i>Taxodiaceae</i> , <i>Engelhardia</i>), 2; mesothermic elements (<i>Quercus</i> , <i>Carya</i> , <i>Pterocarya</i> , <i>Zelkova</i> , <i>Carpinus orientalis</i> , <i>Betula</i> , <i>Alnus</i> , etc.), 3; <i>Pinus</i> , 4; meso-microthermic elements (<i>Cedrus</i> and <i>Tsuga</i>), 5; microthermic elements (<i>Abies</i>), 6; herbs (<i>Asteraceae</i> <i>Asteroideae</i> , <i>Asteraceae</i> <i>Cichorioideae</i> , <i>Poaceae</i> , <i>Amaranthaceae-Chenopodiaceae</i> , <i>Geranium</i> , etc. and include some water plants (<i>Sparganium</i> , <i>Potamogeton</i> , <i>Typha</i>), 7; steppe element (<i>Artemisia</i>).....	75
Figure 5.23 :	Detailed pollen diagram of Trilophos.....	76
Figure 5.24 :	The synthetic pollen diagram of Prosilio. Note that only the three samples of six with statistically significant pollen (minimum 150) numbers were analysed. The numbers in the diagram show the pollen groups: 1; <i>Cathaya</i> , 2; mesothermic elements (<i>Quercus</i> , <i>Alnus</i> and <i>Ulmus</i>), 3; <i>Pinus</i> , 4; meso-microthermic elements (mainly <i>Tsuga</i>), 5; microthermic elements (<i>Abies</i> and <i>Picea</i>), 6; <i>Cupressaceae</i> , 7; herbs (<i>Asteraceae</i> <i>Asteroideae</i> , <i>Asteraceae</i> <i>Cichorioideae</i> , <i>Poaceae</i> , <i>Amaranthaceae-Chenopodiaceae</i> and include water plant <i>Sparganium</i> , 8; steppe element (<i>Artemisia</i> and <i>Hippophae rhamnoides</i>).	77
Figure 5.25 :	The detailed pollen diagram of Prosilio.	78
Figure 5.26 :	The synthetic pollen diagram of Lion of Amphipoli. Note that only the samples with statistically significant pollen (minimum 150) numbers were analysed. The numbers in the diagram show the pollen groups: 1; mega-mesothermic elements (<i>Taxodiaceae</i> , <i>Engelhardia</i> , <i>Taxodium</i> type), 2; <i>Cathaya</i> , 3; mesothermic elements (<i>Quercus</i> , <i>Carya</i> , <i>Pterocarya</i> , <i>Zelkova</i> , <i>Ulmus</i> , etc.), 4; <i>Pinus</i> , 5; meso-microthermic elements (<i>Cedrus</i>), 6; microthermic elements (<i>Abies</i> and <i>Picea</i>), 7; herbs (<i>Asteraceae</i> <i>Asteroideae</i> , <i>Asteraceae</i> <i>Cichorioideae</i> , <i>Poaceae</i> , <i>Amaranthaceae-Chenopodiaceae</i> , etc. and include water plant <i>Potamogeton</i>	79
Figure 6.1 :	Latest records of <i>Taxodiaceae</i> swamps in the Mediterranean region.	85
Figure 6.2 :	Latest records of <i>Avicennia</i> mangrove in the Mediterranean region.	86
Figure 6.3 :	Latest records of some thermophilous warm-temperate trees in the Mediterranean region. Dark blue circles indicate refuge areas.	88
Figure 6.4 :	The vegetation organization in altitude in the southeast China (ca. 25-30° of latitude) (from Wang, 1961).....	90
Figure 6.5 :	Late Neogene synthetic pollen diagrams in the study region. Numbers show the plants groups in synthetic pollen diagrams: 1, Megathermic elements;	

	2, Mega-mesothermic elements; 3, <i>Cathaya</i> ; 4, Mesothermic elements; 5, <i>Pinus</i> ; 6, Meso-microthermic elements; 7, Microthermic elements; 8, Non-significant elements; 9, Cupressaceae; 10, Mediterranean xerophytes; 11, Herbs; 12, Steppe elements.	93
Figure 6.6	: Interpolated vegetation map for herbs during the Zanclean (Favre, 2007).	94
Figure 6.7	: Interpolated vegetation map for mesothermic trees during the Zanclean (Favre, 2007).	94
Figure 6.8	: Diagram indicating the origin and development of <i>Artemisia</i> (from Yunfa <i>et al.</i> , 2010), with global climate (Zachos <i>et al.</i> , 2008), capital letters in the diagram: A, B, C, D are adapted from Li, 1991; Li and Fang, 1999; An <i>et al.</i> , 2006; Rowley and Currie, 2006; d. Wan <i>et al.</i> , 2007) and the Asian monsoon intensity (Wan <i>et al.</i> , 2007).	96
Figure 6.9	: Chronological distribution of <i>Artemisia</i> steppes since the Early Miocene until today in the studied region.	98
Figure 6.10	: Global deep-sea oxygen records with main events (taken from Zachos <i>et al.</i> , 2001).	100
Figure 6.11	: Distribution of modern and mid-Pliocene land and sea ice in the Northern Hemisphere (from Dowsett <i>et al.</i> , 1994).	101
Figure 6.12	: Distribution of modern and mid-Pliocene land and sea ice in the Southern Hemisphere (from Dowsett <i>et al.</i> , 1994).	101
Figure 6.13	: Synthetic pollen diagrams of the studied localities. DSDP Site 380: S. Boroi, D. Biltekin and S.-M. Popescu, Grouping of plants follows Suc (1984): 1, Megathermic elements; 2, Mega-mesothermic elements; 3, <i>Cathaya</i> ; 4, Mesothermic elements; 5, <i>Pinus</i> ; 6, Meso-microthermic elements; 7, Microthermic elements; 8, Non-significant elements; 9, Cupressaceae; 10, Mediterranean xerophytes; 11, Herbs; 12, Steppe elements. The reference oxygen isotope curve is from Shackleton <i>et al.</i> (1990, 1995).	104

ABSTRACT

This study concerns a long marine section (DSDP Site 380: Late Miocene to Present) and onshore exposed sections from the Late Miocene and/or Early Pliocene. The main target of this study is to reconstruct vegetation and climate in the North Anatolia and North Aegean region for the last 7 Ma. Two vegetation types were alternately dominant: thermophilous forests and open vegetations including *Artemisia* steppes. During the Late Miocene, most of the tropical and subtropical plants declined because of the climatic deterioration. However, some of them survived during the Late Pliocene, such as those which constituted coastal swamp forests (*Glyptostrobus*, *Engelhardia*, Sapotaceae, *Nyssa*) or composed deciduous mixed forests with mesothermic trees. Simultaneously, herbaceous assemblages became a prevalent vegetation component despite steppe elements (*Artemisia*, *Ephedra*, *Hippophae rhamnoides*) did not significantly develop. At 2.6 Ma, as a response to the onset of Arctic glaciations, subtropical elements rarefied despite some taxa persisted (*Glyptostrobus*, *Engelhardia*, Sapotaceae, *Nyssa*). In parallel, deciduous mixed forest assemblages composed of mesothermic trees (deciduous *Quercus*, *Betula*, *Alnus*, *Liquidambar*, *Fagus*, *Carpinus*, *Tilia*, *Acer*, *Ulmus*, *Zelkova*, *Carya*, *Pterocarya*) almost disappeared too while steppe environments strongly enlarged. Then, *Artemisia* steppic phases developed during longer temporal intervals than mesophilous tree phases all along the glacial-interglacial cycles (first with a period of 41 kyrs, then 100 kyrs). Since 1.8 Ma, herbaceous ecosystems including *Artemisia* steppes still continuously enlarged up today. Such an expansion of *Artemisia* steppes in the Ponto-Euxinian region was observed at the earliest Pliocene but their earliest settlement in Anatolia seems to have occurred in the Early Miocene. The development of the *Artemisa* steppes in Anatolia might result from the uplift of the Tibetan Plateau. Relictuous plants such as *Carpinus orientalis*, *Pterocarya*, *Liquidambar orientalis*, *Zelkova* persisted up today. This story can be explained by some influence of the Asian monsoon which reinforced as a result from the uplifted Tibetan Plateau.

TITRE

Végétation et climat des régions nord-anatolienne et nord-égéenne depuis 7 Ma d'après l'analyse pollinique

RESUME

Cette étude concerne un long enregistrement sédimentaire marin (Site DSDP 380 : Miocène supérieur à Présent) et des affleurements à terre de dépôts marins ou lacustres du Miocène supérieur et(ou) du Pliocène inférieur. L'objectif principal de cette recherche est de reconstruire la végétation et le climat des régions nord-anatolienne et nord-égéenne des 7 derniers Ma. Deux types de végétation y furent alternativement : les forêts de plantes thermophiles et les formations ouvertes incluant les steppes à *Artemisia*. A la fin du Miocène, la plupart des éléments mégathermes (tropicaux) et mégamésothermies (subtropicaux) avaient régressé en raison des détériorations climatiques. Cependant, certains d'entre eux ont survécu pendant le Pliocène supérieur, notamment ceux qui constituaient des forêts littorales marécageuses (*Glyptostrobus*, *Engelhardia*, Sapotaceae, *Nyssa*) ou participaient à des forêts mixtes avec des arbres décidus mésothermes. Pendant ce temps, les formations ouvertes à herbes sont devenues prédominantes dans la végétation sans que les éléments steppiques (*Artemisia*, *Ephedra*, *Hippophae rhamnoides*) soient très abondants. A 2,6 Ma, sous l'effet des premières glaciations arctiques, les éléments méga-mésothermes se sont très raréfiés malgré la persistance de quelques reliques (Taxodiaceae : probablement *Glyptostrobus*, *Engelhardia*, Sapotaceae, *Nyssa*). Simultanément, les forêts mixtes à éléments mésothermes (*Quercus* décidus, *Betula*, *Alnus*, *Liquidambar*, *Fagus*, *Carpinus*, *Tilia*, *Acer*, *Ulmus*, *Zelkova*, *Carya*, *Pterocarya*, etc) ont aussi quasiment disparu tandis que les environnements steppiques se développaient fortement. Désormais, tout au long des cycles glaciaire-interglaciaire (d'abord de 41 ka de périodicité puis de 100 ka), les steppes à *Artemisia* occuperont plus d'espace temporel que les phases arborées. Depuis 1,8 Ma, les environnements à herbes et les steppes à *Artemisia* n'ont cessé de s'étendre jusqu'à aujourd'hui. Cette expansion des steppes à *Artemisia* dans la région du Pont-Euxin a été observée au tout début du Pliocène mais leur premier enregistrement en Anatolie date du Miocène inférieur. Le développement de la steppe à *Artemisa* en Anatolie pourrait résulter du soulèvement du Plateau tibétain. Le maintien dans cette région de plantes thermophiles reliques en situation de refuges (*Carpinus orientalis*, *Pterocarya*, *Liquidambar orientalis*, *Zelkova*) peut être expliqué par l'influence grandissante de la mousson asiatique dont le renforcement aurait aussi résulté du soulèvement du Plateau tibétain.

DISCIPLINE Palynologie, Géologie

MOTS-CLES Anatolie, Nord Egée, Néogène supérieur, Quaternaire, Palynologie, Végétation, Climat

INTITULE ET ADRESSE DES LABORATOIRES :

Laboratoire PaléoEnvironnements et PaléobioSphère, UMR CNRS 5125, Université Claude Bernard – Lyon 1, 27-43 boulevard du 11 Novembre, 69622 Villeurbanne, France

School of Mines and Eurasia Institute of Earth Sciences, Istanbul Technical University, Maslak, 34469, Istanbul, Turkey